THE ROLE OF INFLAMMATION AND AMYLOID BETA IN ALZHEIMER DISEASE PATHOLOGY

by

Dara L. Dickstein

B.Sc., York University, 1997

A THESIS SUBMITTED IN PARTIAL FULFILMENT OF
THE REQUIREMENTS FOR THE DEGREE OF

DOCTOR OF PHILOSOPHY

in

THE FACULTY OF GRADUATE STUDIES

(Genetics)

We accept this thesis as conforming
to the required standard

.....

.....

.....

.....

THE UNIVERSITY OF BRITISH COLUMBIA

November 2004

Abstract

Alzheimer disease (AD) is the most common form of dementia. Due to longer life-spans the number of affected individuals is expected to triple over the next few decades. As a consequence, a great deal of research is focused on determining the many processes by which the disease manifests as well as in discovering biomarkers and therapeutics to aid in diagnosis and disease prevention. The neuropathological hallmarks of AD include extracellular deposits of amyloid into senile plaques, accumulation of abnormal Tau filaments into neurofibrillary tangles, extensive neurodegeneration and inflammation. Although significant advances have been made in AD neurodegeneration, there still remain many unanswered and unforeseen aspects to the disease.

It has been established that microglia, the immune cells of the brain, become activated in response to amyloid; however, the precise intracellular responses of microglia to amyloid and the relationship between microglia and amyloid deposition or clearance is unresolved. There have been many genes identified whose expression is upregulated in activated microglia and many of them have been proposed to be used as markers for inflammation. It has been demonstrated in humans that serum levels of melanotransferrin (p97), an iron binding molecule, is elevated in individuals affected with AD and that it is the activated, plaque-associated microglia that are responsible for this upregulation. This thesis further investigated the association between microglial activation and p97 gene expression and found that the levels of p97, both mRNA and protein, are increased in activated microglia in culture. The change in gene expression occurred largely in response to amyloid treatment possibly by the regulation of the AP-1 transcription factor downstream of the p38 mitogen-activated protein kinase pathway.

Moreover, p97 expression was altered by the treatment of activated microglia with anti-inflammatory drugs indicating that p97 may be used as a marker specific for amyloid-induced inflammation.

The production and degradation of amyloid in the brain appears to be in a strict equilibrium. In AD, it is thought that the production of amyloid occurs at a faster rate than its removal and degradation and it is this shift in equilibrium that leads to plaque development. This study addressed the role of microglia in amyloid plaque formation using an AD transgenic model mouse that exhibits dysfunctional microglia. These mice accumulated amyloid deposits at the same rate as AD model mice however, limited numbers of mice did not allow for definite conclusions. Interestingly, these mice also displayed a shift in amyloid distribution, as indicated by increased vascular deposits, whereas normal AD model mice did not.

Microglial activation and subsequent removal of amyloid deposits is one of the mechanisms suggested to explain the success of the amyloid beta vaccination treatment protocols. Immunization with amyloid and anti-human amyloid antibodies has resulted in the decrease in amyloid plaque burden, neurodegeneration, gliosis, early Tau pathology and cognitive and memory deficits. One aspect of AD not previously investigated was the effect of immunization on the integrity of the blood-brain barrier (BBB). The studies performed in this thesis show that there was a decrease in BBB permeability after amyloid immunization. These data further support amyloid immunization as a treatment for AD as well as provide an explanation of the mechanism by which immunization effectively reduces AD pathology.

Table of Contents

List of Figures

List of Tables

List of Abbreviations

Aβ	Amyloid beta
$A\beta_{1-40}$	40-residue C-terminal variant of amyloid beta
$A\beta_{1-42}$	42-residue C-terminal variant of amyloid beta
AD	Alzheimer disease
ADAMs	A disintegrin and metalloproteinase
ApoE	Apolipoprotein E
APP	Amyloid precursor protein
Aph-1	Anterior pharynx-defective-1
BACE	β-site APP cleavage enzyme
BBB	Blood-brain barrier
bp	Base pair
BSA	Bovine serum albumin
CAA	Cerebral amyloid angiopathy
Caspases	Cysteine aspartyl proteases
CC	Cerebral cortex
C-terminal	Carboxy-terminal
CFA	Complete Freund's adjuvant
CNS	Central nervous system
COX	Cyclo-oxygenase
CREB	cAMP responsive element binding protein
CSF-1	Colony stimulating factor 1
Cu(II)	Copper II
DMEM	Dulbecco's modified Eagle's medium
DMSO	dimethylsulfoxide
cDNA	Complementary deoxyribonucleic acid
dNTP	Deoxyribonucleotide triphosphate
DTT	dithiothreitol
ELISA	Enzyme linked immuno-absorbant assay
EOFAD	Early onset familial Alzheimer disease

ER	Endoplasmic reticulum
ERK	extracellular signal-regulated kinases
FBS	Fetal bovine serum
FcR	Fc receptor
Fe(III)	Iron III
FPRL1	formyl peptide receptor-like 1
GFP	Green fluorescent protein
hAPP	Human amyloid precursor protein
HI	hippocampus
HRP	Horse radish peroxidase
Ibu	Ibuprofen
ICFA	Incomplete Freund's adjuvant
IL	Interleukin
IFN-γ	Interferon gamma
i.p.	intraperitoneal
i.v.	Intravenous
JNK	c-jun N-terminal kinases
LOAD	Late-onset Alzheimer disease
LPS	Lipopolysaccharide
LRP-1	Low-density lipoprotein receptor related protein
MAPK	Mitogen-activated protein kinase
mRNA	Messenger ribonucleic acid
N.D.	Not determined
N-terminal	Amino terminal
Nim	Nimesulide
NFκB	Nuclear factor κB
NFTs	Neurofibrillary tangles
NSAIDs	Non-steroidal anti-inflammatory drugs
OD	Optical density
op/op	CSF-1 deficient mouse
PBS	Phosphate buffered saline

PCR	Polymerase chain reaction
PD	Parkinson's disease
Pen2	Presenilin enhancer 2
PFA	Paraformaldehyde
PPARγ	Peroxisome proliferators-activated receptor gamma
PS	Permeability coefficient x surface area
PS1	Presenilin 1
PS2	Presenilin 2
RAGE	Receptor for advanced glycation end product
ROS	Reactive oxygen species
sAPPα	Secreted amyloid precursor protein alpha
sAPPβ	Secreted amyloid precursor protein beta
SDS page	Sodium dodecyl sulfate-polyacrylamide gel electrophoresis
SR	Scavenger receptor
Smac	Second-mitochondria derived activator of caspase
TfR	Transferrin receptor
TGF-β	Transforming growth factor beta
Tg/+	Tg2576 AD model mouse
TNF-α	Tumor necrosis factor alpha
VEGF	Vascular endothelial growth factor
VLDL-R	Very low-density lipoprotein receptor
XIAP	X chromosome linked inhibitor of apoptosis protein
Zn(II)	Zinc II
ZO	Zonula occudens proteins
+/+	Wild-type mouse

Acknowledgements and Dedication

This thesis could not have been completed without the help of many people. First and foremost I would like to thank my supervisor, Dr. Wilfred Jefferies, for bringing me into his lab and giving me the opportunity to work on this exciting project. His encouragement and enthusiasm in this project, through the good times and the bad, have propelled me to excel and have taught me how to face things head on, to not give up and to think beyond the obvious. He has taught me how to be a successful scientist and for that I am eternally thankful. I am grateful to my committee members, Dr. Keith Humphries, Dr. Peter Reiner, Dr. Gerry Krystal and Dr. Elizabeth Simpson for their invaluable guidance and assistance, to the Genetics Graduate Program, the Biotechnology Laboratory and the Biomedical Research Centre. I would like to thank all of my lab members, past and present. In particular, Dr. Maya Kotturi, Dr. Cheryl Pfeifer, Dr. Maki Ujiie, and Jason Grant for their technical advice, their help with proof reading my thesis and most importantly for their friendship. A special thanks to Andy Jeffries and Ray Gopaul, for their assistance in experimental procedures, and their exceptional care of my animals, Brian Chung and Janet Lee for their help with many experiments and Dr. Aruna Somasiri, Arthur Legg, and Kenny To of Wax-it Histology for all their hard work and technical assistance. I also acknowledge the Alzheimer Society of Canada who granted me a Doctoral research scholarship for 4 years of my Ph.D.

Finally I would like to recognize my family and friends for all their love and support and constant encouragement throughout the years. In particular I would like to express my gratitude to my parents, who have always inspired me to strive for what I believe in and to attain each goal I put before myself.

This work is dedicated to the memory of my grandmother,

Ruth Arbuck,

1914-2003

Chapter 1: Introduction

1.1 Alzheimer disease

Alzheimer disease (AD) was first described in 1907 by Alios Alzheimer as a neuropathological syndrome characterized by progressive dementia and deterioration of cognitive function along with neurological lesions identified as dark staining plaques and fiber-like tangles [1]. AD accounts for approximately 65% of all dementia cases in the elderly [2]. It is estimated that there are approximately 20 million people affected worldwide with either AD or mild cognitive impairment. The prevalence of AD, in the general population, increases with age as the rate is 3% in those between 65 and 74 years compared with 47% among those over 85 years of age [3]. Progressive memory and cognitive decline as well as difficulty in language, praxis and visual perception are the clinical manifestations which characterize the disease. The decline in intellectual function progresses at a slow but inexorable rate and leads to severe debilitation and death within 12 years after onset [4].

Pathologically, AD selectively damages brain regions and neural circuits critical for cognition and memory and is distinguished by the presence of proteinaceous deposits in the brain, comprised of extracellular amyloid plaques and accumulated paired helical filaments of hyper-phosphorylated Tau in intracellular neurofibrillary tangles (NFTs), dystrophic neuritis and neuropil threads [5,6]. Inflammation also plays a key role in AD and appears to be facilitated by activated microglia, the immune cells of the central nervous system (CNS). It took 75 more years to determine that the main constituent of the plaques was a 40-42 amino acid peptide referred to as amyloid β (Aβ) [7]. Aβ is a

metabolic product resulting from the proteolytic cleavage of the amyloid precursor protein (APP) and its aggregation into fibrils is thought to be the central event of AD. The "amyloid cascade hypothesis" proposes that Aβ precipitation into fibrils initiates the formation of amyloid plaques which in turn contribute to the formation of neurofibrillary tangles, initiate complement cascades and inflammatory processes and ultimately culminate in cell death [8]. However, this hypothesis is not consistent with recent advances that implicate inflammation, NFTs and oxidative stress as independent processes that may even be upstream of Aβ aggregation.

1.2 Genetics of Alzheimer disease

The inheritance of predisposing genetic factors appears to play an important role in AD. After age, family history is the second greatest risk factor for AD. There are two classes of AD: early-onset familial AD (EOFAD), where the age of onset is less than 60 years of age; and late-onset AD (LOAD), where age of onset is greater than 60 years. The genetics of AD are complex since AD is a heterogeneous genetic disorder in which numerous genetic factors, with both minor and major effects, play independent, simultaneous and interdependent roles. Further complexity arises since mutations and polymorphisms in multiple genes are acting together with many environmental factors. Moreover, AD represents a dichotomous situation where genes which cause EOFAD are rare in prevalence but 100% penetrant, while genes which confer increased risk for LOAD are highly prevalent with low penetrance [9]. Present research is focused on elucidating the genes responsible for the various aspects of AD. This will make it

possible to create and estimate a person's genetic susceptibility profile that will aid in both early diagnosis and the development of preventative treatment.

1.2.1 Early onset gene candidates

The first candidate gene for AD was discovered in the early 1980's. Linkage analysis and subsequent positional cloning techniques were performed on multigenerational families who all had EOFAD. The inheritance pattern in all these families appeared to be autosomal dominant and highly penetrant. The findings from these families showed linkage to chromosome 21 and focused on a candidate gene encoding the APP [10]. Although association was later found to be a false positive, it did lead investigators to a compelling candidate gene. More persuasive evidence for the involvement of APP in AD was the fact that Down's Syndrome patients, who have trisomy 21, had strikingly similar brain pathology to those suffering from AD [11]. In addition, Down's patients had increased APP messenger ribonucleic acid (mRNA) expression along with elevated APP and Aβ in the serum and brain [12,13]. Finally, mice overexpressing mutant forms of APP developed AD-like pathology, further implicating APP as a genetic determinant for AD.

The first APP mutation was found in 1990 in a Dutch family where individuals were affected with cerebral hemorrhage with significant amyloid deposits in accordance with an autosomal dominance inheritance pattern [9]. Since then 20 mutations in the APP gene have been found, all of which are missense mutations located close to or within the coding region of the Aβ fragment in the β and γ-secretase cleavage sites (Figure 1.1) [10]. Overall, mutations in the APP gene result in an increase in the production of $A\beta_{1-42}$ peptide, the more amyloidogenic and toxic species of Aβ. Other mutations, such as the

London mutation (V7171), cause an increase in the ratio of $A\beta_{1-42}$ peptide to $A\beta_{1-40}$ peptide [14], whereas the Swedish mutation (K670N/M671L) causes an increase in the production of both species of $A\beta_{1-40}$ and $A\beta_{1-42}$ [15]. Individuals with APP mutations have an average year of onset of 49 ± 8 years and disease duration of approximately 12 years [5]. Mutations in the APP gene account for 5-7% of all EOFAD cases which account for less than 2% of all AD cases.

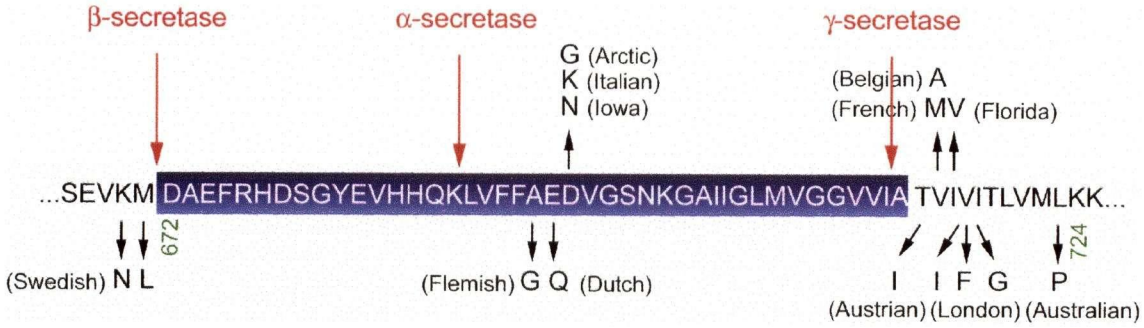

Figure 1.1. Mutations in APP genetically linked to EOFAD
The Aβ coding region within the APP is expanded and shown by amino acid code. The arrows indicate residues with known missense mutations which have been identified in EOFAD and/or hereditary cerebral hemorrhage with amyloidosis. Mutations of APP near the positions 670, 693 and 715 have been found to increase the risk of AD. A double mutation at K670 and M671 increases the production of both $A\beta_{1-40}$ and $A\beta_{42}$, while mutations near the γ-secretase cleavage site favors the production of $A\beta_{1-42}$. Three-digit numbers refer to the residue number of APP (Adapted from Selkoe [16]).

A year after the discovery of mutations in the APP gene, another FAD locus was found to be linked to chromosome 14 and later identified as the presenilin 1 (PS1) gene [9]. Shortly after, another gene encoding a second member of the presenilin family called presenilin 2 (PS2) located on chromosome 1 was also identified [5]. To date there are

approximately 140 mutations in PS1 and 10 mutations in PS2, and together presenilin mutations account for the majority of EOFAD cases [10,16]. PS1 encodes a 7 transmembrane spanning protein that functions as an aspartyl protease and is required for γ-secretase activity [17]. At first it was thought that PS1 was the γ-secretase. However, many studies have demonstrated that PS1 is part of a protease complex consisting of at least three other proteins including, nicastrin, APH-1, and Pen-2 [18,19,20]. Mutations in presenilin genes result in the over production of $A\beta_{1-42}$, presumably by altering γ-secretase activity [21]. Individuals with PS1 mutations have an earlier age of disease onset (43.5 ± 0.7 years) and have shorter disease duration (4.5 ± 0.7 years), while PS2 mutations have a later age of onset and longer duration [5,22]. Interestingly, PS2 mutations are not highly penetrant compared to PS1 mutations which are completely penetrant. Overall, mutations in PS genes account for greater than 55% of all EOFAD mutations.

1.2.2 Late onset gene candidates

LOAD accounts for approximately 95% of AD cases and is classified as sporadic AD. The genetic contributions to LOAD are more difficult to address due to the lack of complete family histories and fewer living subjects from which to obtain blood samples. There are a few gene candidates for LOAD which have been identified by association or linkage disequilibrium studies. Co-segregation of particular allele(s) and disease phenotype was one of the strategies employed to identify an allele of the gene encoding apolipoprotein E (ApoE) as a risk factor for AD [23]. There are three alleles of the ApoE gene; ε2, ε3, and ε4. Individuals who have the ε4 allele, either heterozygous or homozygous, have a greater risk of developing AD; however, there are many individuals who are homozygous for the ε4 allele and do not develop dementia. Therefore, the ε4

allele is neither necessary nor sufficient for the development of AD. ApoE is a 299 amino acid glycoprotein that normally functions in cholesterol and lipid metabolism [24]. It is thought that the ε4 allele acts as a modifying gene by decreasing the age of onset in a dose dependent manner [10]. The ε4 isoform has also been reported to promote Aβ aggregation by mechanisms not yet elucidated. It is thought that ε4 is less capable of clearing Aβ from the neuropil and that ε4 binds to Aβ with a lower affinity than the other isoforms [25].

Genetic linkage studies have also given rise to many more candidate genes including α_2-macroglobulin, low-density lipoprotein receptor related protein (LRP-1), insulin degrading enzyme, urokinase plasminogen activator and the very low-density lipoprotein receptor (VLDL-R). α_2-Macroglobulin and LRP-1, both located on chromosome 12, appear to play a role in Aβ clearance and degradation. LRP-1 can also serve as a receptor for ApoE, α_2-macroglobulin and secreted forms of APP and polymorphisms in exon 3 and 6 have been linked to AD [9,26]. Insulin degrading enzyme and urokinase plasminogen activator, located on chromosome 10, have also been suggested to play a role in Aβ degradation [27]. Finally, VLDL-R, located on the short arm of chromosome 9, may be a receptor for lipoproteins such as ApoE [9]. There are also many inflammatory factors that are deemed to have high risk alleles. Polymorphisms in interleukin (IL)-1α, IL-1β, IL-6, tumor necrosis factor α (TNF-α) and α_1-antichymotrypsin have all been shown to influence AD risk [28]. There are approximately 10 polymorphisms that have been found in the general population and individuals carrying one or more of these alleles are hypersensitive to oddities resulting in inflammatory processes that can cause increased degeneration [28]. Since the genes

identified to date are believed to only account for approximately 30% of the genetic variance in AD, the search for genetic factors associated with AD is an ongoing research effort.

1.3 The amyloid precursor protein and amyloid beta

1.3.1 The amyloid precursor protein

With the identification of APP being a genetic determinant for EOFAD, research began into clarifying the biological role of APP and its proteolytic cleavage products. APP is a type 1 transmembrane glycoprotein that is localized to chromosome 21 (21q21.2-3), contains 18 exons and spans 170 kilobases [29]. APP is expressed ubiquitously throughout the body and can exist in at least three isoforms: APP_{770}, APP_{751}, and APP_{695}, arising from alternative splicing with different isoforms expressed in specific tissues [30]. The full length protein contains zinc and copper binding sites, a cysteine rich subdomain and an acidic region at the amino terminus. There is also a kunitz protease inhibitor domain, although the functional significance of this domain is unclear [4]. In the brain the APP_{695} isoform is the predominant form and is expressed in glial, endothelial and neuronal cells. APP has been observed to be localized to many membranous structures including the endoplasmic reticulum (ER), Golgi compartments, plasma membrane, postsynaptic densities, axons, and dendrites. In addition, APP has been found in cholesterol and GM1 ganglioside rich membrane microdomains [30].

The exact function of APP is not clear and many studies have focused on the role of APP and its fragments. It had been demonstrated that APP and its fragments, such as

secreted APPα (sAPPα), secreted APPβ (sAPPβ) and Aβ, are powerful regulators of neuronal functions including synaptic plasticity and transmission, neuritic outgrowth, cell excitability, cholesterol metabolism, cell adhesion, cell death and gene transcription [1]. One possible function of full length APP is as a cell surface G-protein-coupled receptor. Binding of G-proteins to APP causes the G-protein to dissociate into its dimeric form resulting in the activation of multiple signal transduction molecules such as phospholipase C, voltage dependant calcium channels, adenylyn cyclase and many enzymes involved in apoptotic signaling cascades. However, the role of APP mediated G-protein activation is not fully understood. APP has also been implicated in cell adhesion. Immunohistochemical studies have demonstrated that cell surface APP co-localizes with adhesion proteins such as β-1 integrin [31] and telencephalin [32]. Moreover, APP contains several domains that facilitate the binding of heparin, collagen and laminin [1]. Other possible functions include synaptic transmission and plasticity and more recently memory and cognition. Nerve process outgrowth is thought to be regulated, in part, by APP. Studies focusing on embryonic development and APP expression have shown that APP expression is at its highest between embryonic day 6-9, when neuritic outgrowth is at its maximum [4]. Moreover, *in vitro* experiments with synthetic APP demonstrate that APP is able to stimulate neuritic outgrowth in PC12 neuronal cells [4]. Research on APP function is conflicting since most AD animal models are transgenic for the human form of the protein that may interfere in the evaluation of the endogenous mouse protein function.

1.3.2 APP processing

The processing of APP into its metabolites involves three different enzymes: β-, α-, and γ-secretases and two cleavage pathways (Figure 1.2). In APP, there are two main cleavage sites on the extracellular side of the membrane and one site within the transmembrane domain. β- and α-secretase cleavage appears to be mutually exclusive events, each generating soluble carboxyl-terminal (C-terminal) fragments. The remaining amino-terminal (N-terminal) fragment of APP is then cleaved by γ-secretase [4]. In the non-amyloidogenic pathway, APP is cleaved by α-secretase at a cleavage site located within the Aβ peptide. This cleavage precludes the production of Aβ producing a 612 amino acid soluble protein, sAPPα, which has been shown to have neuroprotective and memory enhancing effects [33]. Cleavage at this site is dependent on secondary structure and on the location of the cleavage site from the membrane. In addition, α-secretase activity can be regulated by protein kinase C activity as well as by other molecules such as estrogen, testosterone, various neurotransmitters and growth factors [34]. Although the exact identity of α-secretase is still unknown, three proteins have been described that appear to have α-secretase-like activities. Studies with protease inhibitors have shown that α-secretase is a zinc metalloproteinase and belongs to the family of a disintegrin and metalloproteinase (ADAMs). The three candidate proteins are ADAM17 (also known as TNF-α convertase), ADAM10 and ADAM9 (also known as MDC9) [33]. ADAMs are type 1 integral membrane proteins with a multi-domain structure and function in cell adhesion, cell fusion, intracellular signaling and proteolysis [34]. The expression and localization of each these proteins in AD are altered and gives rise to the potential role of each in APP processing. ADAM17 has been found to localize to

neurons as well as to senile plaques and tangles, although there is no change in its expression in AD. In contrast, ADAM10 protein levels are significantly reduced in AD, as are levels of sAPPα and α-secretase activity [33]. The emerging hypothesis, as suggested by studies involving knock out mice and enzymatic inhibition, is that all three ADAM enzymes are involved to a similar extent in APP processing acting together at the α-secretase cleavage site to varying degrees depending on cell type. It is possible that ADAM10 is involved in both constitutive and regulative pathways of α-secretase, whereas ADMA17 may be involved solely in the regulatory pathway and ADAM9 in the actual cleavage event [33].

In the amyloidogenic pathway of APP processing, APP is first cleaved by β-secretase followed by cleavage with γ-secretase. These events generate two metabolites, sAPPβ and the Aβ peptide. Two enzymes capable of cleavage at the β-secretase cleavage site are the β-site APP cleavage enzymes (BACE1) and BACE2 [6]. BACE1, also referred to as Asp2 or memapsin2, is a transmembrane aspartyl protease and exists in three isoforms. BACE1 is expressed at high levels in the pancreas, moderate levels in the brain and at low levels in most peripheral tissue. However, BACE1 activity is highest in neuronal tissue and is increased in AD [35]. Intracellularly, BACE1 can be found primarily in the trans-Golgi network, and the endosomal compartments, although it can also be found in the endoplasmic reticulum and on the cell surface [34]. Cleavage by BACE1 is the rate limiting step in the generation of Aβ. BACE1 cleaves at two positions depending on intracellular localization, either at the Asp1 (β-site) or at Glu11 (β'-site) of Aβ, generating an $A\beta_{1\text{-}40/42}$ fragment or an $A\beta_{11\text{-}40/42}$ fragment, respectively. β-site cleavage predominantly occurs in the ER while β'-site cleavage occurs in the Golgi [34]. Further

evidence to support the role of BACE1 as β-secretase comes from studies on various AD animal models. In APP transgenic mice expressing the Swedish mutation, there is a 10 fold increase in BACE cleavage activity. Moreover, mice which overexpress human BACE have a significant increase in $A\beta_{1-40/42}$ levels and knock out of this gene perturbs APP processing and prevents Aβ generation [36]. Finally, in $BACE1^{-/-}$/APP mice there is a lack of Aβ compared to other APP transgenics [36].

BACE2, another aspartyl protease, is 55% identical to BACE1 and shows similar substrate specificity to BACE1. BACE2 is widely expressed in peripheral tissues but is not highly expressed in the brain. It cleaves Aβ at position Asp1 and at position Phe19 or Phe-20 of the Aβ peptide [34]. The precise role of BACE2 in APP processing is unclear. There is no direct evidence for the role of BACE2 in AD however, cleavage at positions 19 and 20 located within Aβ is affected by the FAD Flemish mutation [34] and BACE2 maps to chromosome region 21q22.2-22.3 [37].

The final event in APP processing is the cleavage of the C83 or C99 APP fragments by γ-secretase. Cleavage occurs at a site located within the APP transmembrane domain. It was first thought that PS1 and PS2 were γ-secretases since mutations in PS1 and PS2 cause an increase in the production of $A\beta_{1-42}$ [38]. In addition, PS1 and PS2 contain aspartic acid residues in transmembrane domain 6 and 7, sites necessary for aspartyl protease activity and hence γ-secretase activity [17]. PS1 is expressed in its full length form as an integral membrane protein with 8 membrane spanning regions. In this form, PS1 is thought to be inactive. To form an active presenilin complex, the presenilin protein is cleaved between membrane domains 6 and 7. This yields C- and N-terminal fragments, which remain coupled and form a

heterodimeric active complex [1]. If one or both of the aspartic residues in presenilin are mutated or knocked out, the production of Aβ and the P3 peptide is greatly reduced along with an associated increase in the amount of C-terminal fragments, sAPPα and sAPPβ [17]. This theory was questioned and an alternative hypothesis proposed that states that γ-secretase is multifaceted and is made up of several proteins. The role of presenilins in this complex would be in APP trafficking to sites where cleavage by the complete γ-secretase complex can take place. This viewpoint was corroborated by biochemical and genetic studies which have identified four membrane proteins as components of γ-secretase: heterodimeric presenilin, (composed of its N- and C-terminal fragments); anterior pharynx-defective-1 (Aph-1); nicastrin, (glycosylated); and presenilin enhancer 2 (Pen-2) [20].

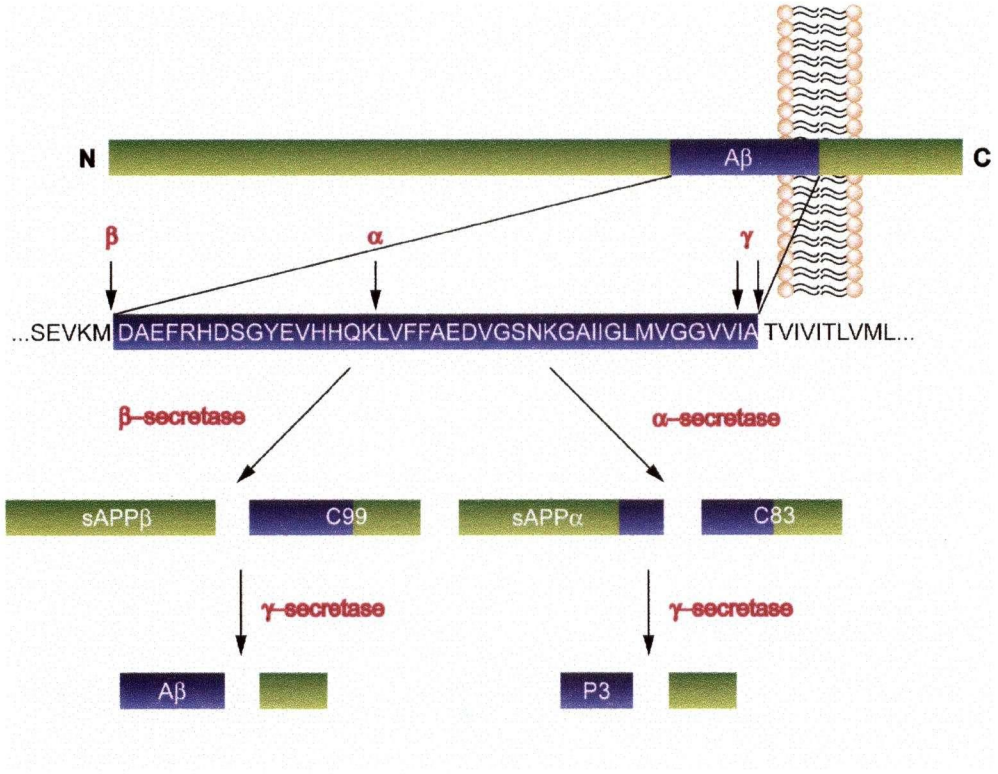

Figure 1.2. Schematic diagram of APP and its metabolic derivatives
APP is a type 1 membrane protein and exists in three major isoforms, $A\beta_{770}$, $A\beta_{751}$, and $A\beta_{695}$. Enlargement of the Aβ peptide region shows the amino acid sequence and primary sites of cleavage by the various secretases. Cleavage of APP by either β- or α-secretase results in soluble N-terminal fragments, sAPPβ and sAPPα and two membrane-bound C-terminal fragments, C99 and C83, respectively. Subsequent cleavage by γ-secretase gives rise to a non-pathogenic Aβ peptide and P3 (Adapted from Small, [4]).

Nicastrin is a type 1 transmembrane glycoprotein that is 709 amino acids long and contains 4 conserved cysteine residues at the N-terminus. It is encoded on chromosome 1q23, a region previously identified as a susceptibility locus for LOAD [34]. Nicastrin has been shown to interact with PS1 and PS2 as well as with the C-terminal APP fragments, C83 and C99. Mutations in either PS1/2 directly effect nicastrin trafficking and post-translational modifications thereby preventing its maturation and function. In this state, the γ-secretase complex cannot form and Aβ production is abolished [34]. Aph-1 and Pen-2 were two proteins discovered through a genetic screen of *Caenorhabditis elegans*. These

genes both encode multi-pass transmembrane proteins that have the capability of binding to PS1, PS2, and nicastrin with high affinity. The specific role of Aph-1 and Pen-2 and the protein-protein interactions responsible for assembling Aph-1 and Pen-2 into the multimeric protease complex remains unknown. Recently, it was revealed that Aph-1 binds to nicastrin in its immature, non-glycosylated form and remains bound after glycosylation and maturation [39]. In regards to how this complex forms, it is thought that Aph-1 and nicastrin initially form a subcomplex. Once nicastrin is modified and matured the Aph-1/nicastrin complex binds to and stabilizes presenilin. Pen-2 then binds, confers the γ-secretase activity and facilitates endoproteolysis of presenilin which serves as the catalytically active core of the γ-secretase complex [39]. There are many details about the active γ-secretase complex that remain to be uncovered These include determining which γ-secretase co-factors physically interact with one another and identifying the protein-protein binding domains that govern these interactions.

1.3.3 Amyloid beta, structure and function

Aβ is a 4 kiloDalton peptide and is a normal cellular product and exists in two predominant forms with different C-termini, $A\beta_{1-40}$ and $A\beta_{1-42}$. Aβ contains seven positively and seven negatively charged residues at the N-terminal region and a hydrophobic domain at residues 17-21 and 29-40/42 (Figure 1.2) [21]. The Aβ protein exists as monomers, dimers, and oligomers and can undergo further aggregation to yield full fibrils. The conformation of Aβ appears to be in a dynamic flux and is dependant upon environmental conditions, metal binding and interactions with various other proteins. In its monomeric state Aβ exists as a random coil containing two α-helices between residues 15-23 and 31-35 [40]. Transition of these α-helical coils into β-pleated

sheets facilitates fertilization where the β-pleated sheets are anti-parallel to one another. It is these full fibrils that are found to make up the bulk of the senile plaques and are thought to have neurotoxic properties [41]. However, pools of soluble Aβ have been found in the brains of AD patients indicating that monomeric, dimeric and oligomeric forms of Aβ may facilitate the pathology of AD [41]. The proportion of soluble $A\beta_{1-42}$ in these pools is significantly higher than soluble $A\beta_{1-40}$ levels. Soluble $A\beta_{1-42}$ dimers have also been shown to have a higher magnitude of neurotoxicity than $A\beta_{1-40}$ [41].

The deposition of amyloid is not found in all regions of the brain. Aβ plaques exhibit a spatio-temporal distribution pattern where regions such as the cortex and hippocampus contain many plaques and regions such as the cerebellum exhibit little to no Aβ. One possible explanation for the distribution pattern of Aβ has been proposed stating that the presence of Aβ in the neuropil of neurons sets in motion a cascade of reactions including inflammation, neuritic sprouting and the upregulation of APP expression [4]. This model is based on a positive feedback loop which relies on neuritic sprouting and APP expression. It is known that as the brain ages, certain areas become myelinated and mechanisms which facilitate neuritic outgrowth are suppressed. However, regions of the brain responsible for memory have ongoing synaptic remodeling, continuation of neuritic outgrowth and are thus the most vulnerable. These include the cortex, hippocampus and olfactory system all of which are affected in AD [4]. In addition, regions of the brain that are the last to undergo myelination, such as the temporal cortex, are the first regions to be affected. Therefore, myelin proteins may prevent neuritic sprouting and subsequent APP expression thereby protecting a given brain region from degeneration [42].

The aggregation of Aβ into fibrils and toxicity can occur in response to a variety of actions, including a shortage in the supply of energy in the cell, oxidative stresses, calcium dysregulation and apoptosis. Studies have shown that a disruption in mitochondrial energy metabolism and dysregulation of calcium homeostasis can up regulate the expression of APP as well as promote the pro-amyloidigenic processing of APP to Aβ and subsequent plaque formation [43,44]. Oxidative stresses like hydrogen peroxide, ultraviolet light, and superoxide radicals have been shown to increase the production of neuronal Aβ. Moreover, high concentrations of extracellular Aβ had been shown to induce oxidative stress and in turn render cells vulnerable to exocitoxicity and apoptosis through the dysregulation of calcium homeostasis. Metal ions have also been shown to cause Aβ aggregation and promote the formation of diffuse plaques. In the AD brain, there are significant amounts of transition metals, such as copper II (Cu(II)), zinc II (Zn(II)) and iron III (Fe(III)), in both Aβ plaques and neuropil [45]. Histidine residues located in the Aβ peptide bind to Cu(II), Zn(II) and Fe(III) as sequester it in the brain during times of oxidative stress and inflammation, since the interaction of these metals with hydrogen peroxide, which is generated in both processes, would cause the production or reactive oxygen species [45]. Treatment of post-mortem AD brains with metal-chelators confirmed this finding since the chelators were able to enhance the solubilization of Aβ [46]. The generation of reactive oxygen species has many harmful consequences including disruption of calcium homeostasis by impairing ATPase activity, increase lipid peroxidation and altering the activity of the anti-oxidant enzyme, superoxide dismutase [41].

It was originally demonstrated in non-neuronal cells, that APP metabolism can elevate intracellular calcium levels which enhances Aβ production. This creates a feed back loop since an increase in Aβ results in the increase of intracellular calcium [47]. Soon after studies in neuronal cells, other studies reported that exposure to fibrillar Aβ causes a disruption in calcium homeostasis generally leading to an increase in cytosolic calcium [47,48,49]. The influx of calcium is thought to be mediated by L-type voltage-gated calcium channels and is regulated by the mitogen-activated protein kinase (MAPK) pathways [48]. Under normal physiological conditions, calcium influx in neuronal cells has been implicated in promoting synaptic plasticity and thus beneficial. However, if too much calcium enters the cell or if the entry of calcium occurs at a dramatic rate, it could cause down-regulation of neuronal plasticity mechanisms due to the self-inhibitory mechanisms of calcium [1]. Pierrot *et al.* have recently established that high cytosolic calcium concentrations favour the amyloidogenic pathway of APP by preventing the cleavage of APP by α-secretase possibly through modifications of APP by phosphorylation [49]. In addition, high calcium levels resulted in the increase in $A\beta_{1-42}$, with no change in $A\beta_{1-40}$, suggesting that calcium may also regulate γ-secretase activity. Nonetheless, alterations in calcium homeostasis are detrimental to neuronal survival due to their high polarized nature.

Recent advances in AD research suggest that in addition to extracellular Aβ, intracellular neuronal Aβ plays a significant role in neurodegeneration. Increasing evidence indicates that Aβ is more toxic to cells in its protofibrillar state rather than in its β-pleated conformation [16]. Initial studies by Wertkin *et al.* demonstrated that NT2N neuronal cells produced Aβ and either stored it in the cell or secreted it into the medium

[50]. Examination of brain sections from young and old animal models illustrated an anterior to posterior gradient of intra-neuronal Aβ immunoreactivity in the hippocampus which increased with age in distal processes and synaptic compartments [51]. What effect intraneuronal Aβ exerts on neurons is unclear. Current studies in hAPP and PS transgenic rats propose that physiological levels of Aβ play a role in synaptic plasticity via activation of cAMP Responsive Element Binding Protein (CREB) directed gene expression [52]. A pathological increase in intraneuronal Aβ would cause abnormal phosphorylation patterns that end up dysregulating these pathways. This is noteworthy since CREB-driven gene expression has been found to be important for learning and memory. It was also found that Aβ caused an upregulation of extracellular signal-regulated kinases (ERK), and ERK then phosphorylates a number of proteins, including Tau, inferring a further link between Aβ and Tau pathways [52]. In addition, both aged animal models and humans exhibit high levels of Aβ immunoreactivity in the cholinergic neuron of the basal forebrain. The accumulation of intracellular Aβ in neuronal processes and synapses is suggested to be associated with the manifestation of cognitive decline seen in AD, since accumulation of Aβ is concordant with abnormal cytoskeletal architecture and synaptic dysfunction [53]. Synaptic dysfunction is one of the proposed causes of cognitive decline. Moreover, oligomer Aβ neuronal accumulation and cognitive decline occur before plaque deposition. These findings proposed the "Synaptic Aβ Hypothesis" that proposes Aβ accumulates in neuronal synapses in the brain. Once the Aβ load in the neuron becomes too cumbersome, the cell dies and releases the amyloid into the extracellular space. The released amyloid can then act as a seed and attract soluble $A\beta_{1-40/42}$ thereby forming a plaque [53].

Apoptotic processes are viewed to play a major role in AD pathology. Evidence suggests that selective neuronal loss seen in AD involves the activation of cysteine aspartyl proteases (caspases), which initiate and execute apoptosis [54]. Both extracellular Aβ oligomers and intracellular Aβ may activate caspases. Extracellular Aβ initiates caspase activity via activation of cell surface death receptors. This pathway involves signaling through cell surface death receptors, such as the TNF receptor, which are regulated by decoy receptors and Fas-associated death domain proteins, however, direct binding of Aβ or Aβ oligomers to death receptors remains to be shown [55]. It is speculated that the binding of Aβ to these receptors causes downstream activation of various caspases such as caspases 2 and 8, leading to the activation of caspases 3, 6 and 7, all of which are important initiators of the apoptotic signaling cascade [54]. Alternatively, intracellular Aβ may activate caspases through a process that involves ER stress or mitochondrial stress. This leads to the downstream activation of caspase 9 and caspases 3, 6 and 7 [56]. Caspase activation is thought to facilitate the cleavage of Tau thereby favouring conformational changes of the protein into paired helical filaments. The accumulation of the altered Tau proteins causes cytoskeletal disruption and the consequent failure of axoplasmic and dendritic transport that culminates in neuronal death [54].

Aβ has also been shown to elicit its toxic effects by the initiation of host immune responses. The action of Aβ on glial cells results in an inflammatory reaction and progressive amyloid deposition promotes the chemotaxis and subsequent activation of microglia [26]. Studies by McDonald *et al.* have established that exposure of fibrillar Aβ to microglia or monocytes activates MAPK pathways involving p38 and the ERK, as well

as tyrosine kinase-dependent signaling pathways, involving Lyn, Syk and FAK [57,58]. The activation of these pathways leads to changes in the expression of various cytokine and pro-inflammatory genes and generates reactive oxygen intermediates, respectively, leading to further neurotoxicity and degeneration. The extensive effect of Aβ on the inflammatory response elicited by glial cells will be discussed in greater detail later.

1.3.4 Putative amyloid beta receptors

The binding of amyloid to plasma membranes has been implicated in many of the pathological features of AD. Binding of Aβ to various receptors elicits neurotoxicity in neurons and cerebral vascular endothelia and activation of inflammation in microglia. Due to its structure, Aβ can bind to a variety of molecules including proteins, proteoglycans, and lipids [59]. On microglia, scavenger receptor A (SR-A) and BI (SR-BI), CD36, heparin sulfate proteoglycan, formyl peptide receptor-like 1 (FPRL1) and a complex of CD36, α6β1-integrin, and CD47 have been shown to bind to Aβ. Neuronal receptors include the N-methyl-D-aspartate receptor, the α7-nicotinic acetylcholine receptor, the p75 neurotrophin receptor and the CLAC-P/collagen type XXV receptor [59]. Receptors common to glial cells, neurons and cerebral endothelia include the receptor for advanced glycation end product (RAGE), LRP, the insulin receptor, integrins and the serpine-enzyme complex receptor [59]. These receptors vary in their ability to bind monomeric or fibrillar Aβ. A few of these receptors will be discussed below.

SR-A and SR-BI receptors are expressed on microglia, bind fibrillar Aβ and mediate the clearance of amyloid aggregates [60]. These receptors have also been implicated in inflammatory responses and the production of reactive oxygen species;

however they are not needed for microglial activation. Expression of SR-A and SR-BI are developmentally regulated and are not expressed normally in adult mouse brain [61]; however, expression of SR-A and SR-B1 mRNA and protein are both upregulated *in-vitro* and *in-vivo* upon exposure to lipopolysaccharide (LPS), interferon gamma (IFN-γ) and IL-1α [62]. Another microglial receptor for Aβ is CD36. CD36 is a class B scavenger receptor that has been shown to bind to fibrillar Aβ and contribute to microglial activation. Aβ binding to CD36 elicits many signaling cascades involving Src family kinases Lyn and Fyn, and the mitogen-activated protein kinases (MAPK) as well as the production of reactive oxygen species. CD36 is also involved in a multi-receptor complex with α6β1-integrin and CD47, and this complex mediates the binding of microglia to fibrillar Aβ and the subsequent activation of pro-inflammatory pathways, respiratory bursts, adhesion and cell migration [63]. Both SR-A and CD36 are elevated in microglia in brains of AD patients compared to controls [64]. FPRL1 is a seven transmembrane, G-protein coupled protein and is thought to initiate pro-inflammatory effects in response to both soluble and fibrillar Aβ [65]. Activation of FPRL1 can lead to the production of reactive oxygen species and pro-inflammatory cytokines. In addition, FPRL1 is involved in mediating the chemotactic activity of Aβ on microglia. Other studies have shown that FPRL1 can form a complex with Aβ and can be internalized into cytoplasmic compartments resulting in the accumulation of intracellular amyloid aggregates [66]. Under normal condition FPRL1 is expressed at low levels. In AD, FPRL1 expression is increased and is seen at high levels in plaque infiltrating microglia [65].

The RAGE receptor is a multi-ligand receptor in the immunoglobulin superfamily found in neurons, microglia and cerebral endothelial cells. It binds many ligands such as

Aβ, the S100/calgranulin family of pro-inflammatory cytokine-like mediators and the high mobility group 1 DNA binding protein amphoterin [67,67]. The interaction of Aβ with RAGE initiates signaling cascades that result in oxidative stress via the production of reactive oxygen species and lipid peroxides as well as the enhanced expression of macrophage colony stimulating factor, which stimulates microglial proliferation and receptor expression. It has also been implicated in Aβ internalization on microglia [68]. Its expression is ligand dependent and is up-regulated in AD, particularly in the vasculature. RAGE expression is also increased in neurons and microglia, but not as much as in cerebral endothelia. Many *in vitro* and *in vivo* studies have demonstrated that RAGE mediates Aβ transport, therefore, RAGE is thought to be the major influx receptor for peripheral Aβ at the BBB [69,70,67].

LRP is a member of the LDL receptor family and is a multifunctional scavenger receptor and signaling receptor. Its ligands include biomolecules such as ApoE and α_2-macroglobulin, tissue plasminogen activator, APP and lactoferrin [71]. LRP has been genetically linked to LOAD, but the exact mechanism by which LRP affects disease onset in not known [9]. Expression of LRP in AD is decreased and many animal studies involving LRP deficient mice and AD mice results in increased cerebral amyloid load and increase in parenchymal amyloid plaques [72,73]. As a result, LRP is thought to regulate Aβ clearance by controlling its efflux from brain to blood [70].

1.3.5 Animal models

With the multiple genetic mutations associated with the APP gene, many transgenic mouse models have been created to mimic the diverse pathological features of AD. To date, there are approximately 20 APP transgenic mice made, some of which are

described in detail below (Table 1). The first generation of AD model mice involved expression of the wild-type human APP (hAPP) complementary deoxyribonucleic acid (cDNA) [74]. These mice, with the exception of the NSEAPP mouse, did not develop amyloid deposits. In the NSEAPP mouse the $hAPP_{751}$ isoform is expressed under control of the neuron-specific enolase promoter. These mice develop amyloid pathology; however, the deposits in the brain were diffuse and did not resemble the compact plaques seen in the brains of AD patients [75]. The next generation of mice focused on overexpressing the mutated hAPP protein at levels well above the endogenous gene level. This required vectors that provide transgene expression specific to the CNS. Examples of these promoters include the Thy-1 promoter, which exhibits neuron specific gene expression [76], and the hamster prion promoter, which is largely CNS specific with expression in peripheral organs such as the heart [77]. More recently, transgenic mice have been generated expressing the complete hAPP by using a yeast artificial chromosome [78].

Second generation AD mice include PDAPP, Tg2576 and APP23. The PDAPP transgenic mouse expresses all isoforms of the hAPP gene and contains the Indiana mutation, V717F, under control of the platelet-derived growth factor β-chain mini-promoter [79]. These mice exhibit many of the pathological features of AD including neuritic plaques in the hippocampus and neocortical regions, dystrophic neurites, astro- and microgliosis and synaptic degeneration. However, NFTs and clear neurodegeneration have not been identified in these animals [79,80]. Radial arm maze testing and Morris water maze testing showed that these mice also exhibit memory impairment as early as 3 months of age, in the pre-plaque stage, and that these

impairments were correlated with increased age and plaque load [81,82]. The pathological features observed in these animals are evident as early as 8 months of age [83].

A second transgenic model, which is one of the most widely used AD model, is the Tg2576 mouse. The Tg2576 mouse expresses the $hAPP_{695}$ transgene containing the Swedish double mutation K670N/M671L under control of the prion promoter at levels approximately 5 fold higher than the endogenous gene [84,85]. These mice develop amyloid plaques at approximately 9 months of age, with the first deposition in the entorhinal and piriform cortices [86]; exhibit increased gliosis, as well as a decrease in synaptic activity in the hippocampal CA1 region, dentate gyrus; and exhibit a reduction in long term potentiation [87] (see Appendix II for diagram of brain regions) . Cognitive deficits, as determined by Y-maze alternation and water maze learning, occur at 9-10 months of age [85]. The one shortfall of these animals is that there is a lack of neurodegeneration [83]. This may be due to genetic background since genetics influences susceptibility to excitotoxic cell death [88].

Another mouse model which expresses the Swedish mutation APP_{751} gene is the APP23 mouse. This mouse differs from the Tg2576 by expression of the gene under control of the Thy-1 promoter, resulting in a 7 fold increase in gene expression. As early as 6 months of age, these mice develop plaques and have astro- and microgliosis, memory deficits as well as hyperphosphorylated Tau [89,90,91]. In contrast to other mouse models, APP23 mice exhibit a 14% decrease in the number of CA1 neurons compared to control mice and have deposits of cerebral Aβ, preferentially in capillaries and arterioles, and develop cerebral amyloid angiopathy (CAA) [92,93].

In addition to transgenic mice expressing mutated hAPP, mice expressing PS1 mutations or PS-1 knock out mice have been generated. Expression of the presenilin gene did not result in the formation of plaques, but did result in an increase in the production of $A\beta_{1-42}$ [38]. These mice were then crossed with the aforementioned mouse models to develop mouse strains that would better represent human pathology. In PS1/hAPP mice there is an elevation in the levels of Aβ and most interestingly, acceleration in the rate of amyloid plaque depositions with plaque formation occurring at 6 months of age [94]. In addition, other transgenic mice, for example ApoE knock out, ApoE4, BACE overexpressing, BACE knockout mice and Tau mice have been crossed to APP mice in the hope to provide models which accurately mimic AD and help aid in future diagnosis, treatment and prevention. To date no single mouse model faithfully demonstrates the classic triad of human AD pathology; Aβ containing plaques, NFTs and wide spread neuronal loss in the hippocampus and cortical areas, and as such none can be considered a complete model of the disease.

Tg line (background)	Transgene promoter	Mutation	Age at onset of Aβ deposits	Plaque location	Micro- and Astrogliosis	Neuronal loss	Cognitive deficits	NFTs	Ref
Tg2576 (C57BL/6 x SJL)	Hamster PrP	(HuAPP$_{695}$) APP$_{K670M/N671L}$	9-12 months (Congo red Positive)	HI, CC, amygdala	yes	Not detectable	yes	AT8 positive	84, 85, 95, 83
PDAPP (C57BL/6 x DBA/2 x Swiss Webster)	PDGF-β	APP$_{V717F}$	6 months (diffuse and compact)	HI, corp call, CC	yes	Not detectable	Yes	AT8 positive	79, 80, 82
TgAPP23 (C57BL/6 x DBA/2)	Murine Thy-1	APP$_{K670M/N671L}$	6 months (congophilic and diffuse)	HI, neocortex	yes	Yes, ~25% in CA1 at 14-18 months	N.D.	AT8 positive	89, 92
TgAPP22 (C57BL/6)	Human Thy-1	APP$_{K670M/N671L}$ and $_{V717I}$	18 months	HI	yes	N.D.	N.D.	AT8 positive around Congo red plaques (no NFTs)	89
Tg2576/PS1 (PSAPP) (C57BL/6 x SJL)	Hamster PrP	APP$_{K670M/N671L}$ and PS1 P$_{M146L}$	6 months (Congo red Positive)	HI, CC, amygdala	yes	N.D.	Yes	AT8 positive	38,94
TgAPP/Ld/2 (FVB/N)	Murine Thy-1	APP$_{V717I}$	13-18 months (diffuse, mostly Aβ$_{1-42}$)	HI, CC	yes	No overt loss	yes	AT8 positive	96,97
TgAPP/Sw/1 (FVB/N)	Murine Thy-1	APP$_{K670M/N671L}$	18 months (diffuse, mostly Aβ$_{1-40}$)	HI, CC	yes	No over loss	N.D.	AT8 positive	98

Table 1. Summary of the primary APP-based transgenic mouse models of AD
Genetic parameters, onset of Aβ plaque formation and summary of inflammation and cognitive deficits are described above for some of the APP transgenic mice generated. Abbreviations: HI – hippocampus, CC – cerebral cortex, NFTs – Neurofibrillary tangles, N.D. – not determined (Adapted from Janus *et al.* [99, 100], Gotz *et al.* [101]).

1.4 Microglia, inflammation and Alzheimer disease

The involvement of inflammatory processes in AD pathology has been established by multiple lines of evidence. The upregulation of many inflammatory markers co-localize to regions of the brain affected by AD, in close proximity to Aβ deposits and NFTs [26]. There is also direct evidence of inflammatory mediated neurotoxicity as illustrated by the extensive amount of neuronal death in areas with dense microglia. Finally, many epidemiological studies have suggested that the use of non-steroidal anti-inflammatory drugs (NSAIDs) reduces the risk and delay the onset of AD [102,103]. The inflammatory processes seen in AD appear to be mediated by microglia [104].

1.4.1 Microglia as immune cells of the brain

Microglia were first functionally described by del Rio-Hortega in 1932 as mesodermal pial cells that invaded the brain during embryonic development. They have migratory and phagocytic properties and exist in different resting and activated states [105]. It is estimated that microglia make up 5-15% of the brain and are considered to be permanent residents that do not move like macrophages [106]. There is still much debate as to the ontogenic origin of microglia. Initially, microglia were thought to be of mesodermal origin. Further studies confirmed this and found that microglial precursor cells are found in the yolk sac and in the mesenchymal tissue associated with the neuroepithelium. These cells enter the brain, become amoeboid microglia and spread throughout the brain [107]. Alternatively, carbon particle tracing and immunohistochemical techniques showed that ramified microglia originated from circulating blood monocytes that entered the developing brain during development and assumed the form of amoeboid microglia that ultimately evolve to become the ramified microglia [107]. Lastly, others state

that microglia are not derived from monocytes, rather they are derived during fetal development from neuroectodermal cell precursors; glioblasts or cells of the germinal matrix [105]. Regardless of their origin, it is agreed that microglial cells constitute the immune system of the brain. They carry out the innate immune response observed in the central nervous system during injury and infection.

1.4.2 Morphological plasticity of microglia

It has been established that microglia can assume various morphological appearances that can correlate to a distinct functional state (Figure 1.3). Studies performed in the facial nerve system first demonstrated this phenomenon by showing that motor neuron regeneration occurred after injury as a result of a microglial response. Microglia appeared at the site of injury within minutes in response to neuronal signals, became activated and assumed a highly ramified morphology, proliferated and surrounded the injured neuron. During the degenerative phase of the response, microglia became rounded and phagocytosed the dying neuron [108]. In the normal adult brain, microglia exist in a resting state and also in a highly ramified state. Amoeboid microglia are also seen but these are present predominantly in the developing brain and can transform into ramified cells with age [107]. Resting microglia are small with flattened or angular nuclei and have been shown to be non-dividing. Once activated, microglia take on a different shape that is dependent on environment and brain architecture [105].

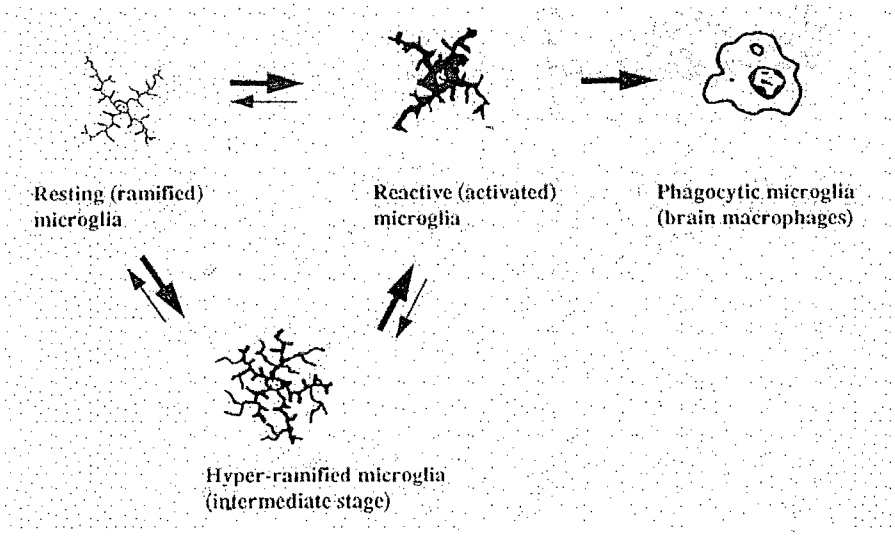

Figure 1.3. Morphological and functional plasticity of microglia
Microglia can assume different types of morphological shapes in response to environmental stimuli. Signals from damaged or dying neurons cause resting microglia to become active. The amount of signal dictates what conformational state the microglia adopt. In a resting state, microglia have small cell bodies and thin ramified processes with few branches. Intermediate signals from mildly injured neurons cause a hyper-ramified state but in most cases microglia become reactive in response to stimuli. This activation causes the cell to adopt a larger cell body and thicker more highly branched processes. In some instances microglia can become amoeboid in shape and take on a phagocytic role, removing dying cells from the brain (Adapted from Streit *et al.* [104]).

When activated, microglia adopt a reactive conformation with ramified thick processes and abundant cytoplasm. These microglia are usually found in the gray matter of the brain. The hyper-ramified state represents an intermediate stage between the resting and reactive form and signifies the beginning of microglial activation [104,105]. Microglia have also been seen as rod-shaped with elongated bodies and thin ramified processes. These can be found in the brain white matter as well as in the aged brains of normal individual. In this instance, aged microglia lose contact inhibition and fuse with one another to create rod cells [104,105]. Finally, upon neuronal cell death, microglia morph into brain macrophages, with even more cytoplasm than the reactive state and short thick

processes. It is this conformation that microglia are able to phagocytose and degrade cell debris [105].

1.4.3 The function of microglia in the central nervous system

Microglia are a highly responsive population of cells with the potential to engage in various functions. These include response to invading pathogens and injury, elimination of dying cells and debris, initiation in inflammatory processes as well as regulation of homeostatic mechanisms and neurodevelopment. When microglia respond to neuronal stress signals (ATP, neuropeptides and neurotransmitters) they become activated, release several secretory proteins such as complement (classical and alternative pathway proteins), proteinases, cytokines, chemokines, excitotoxins, reactive nitrogen and oxygen intermediates, and have altered gene expression [26,109]. Microglia can also function as antigen presenting cells, albeit not as well as peripheral macrophage. Microglia residing in the CNS rarely encounter T cells and as a result, may not need to present antigen efficiently [109]. Microglial activation in response to acute CNS injury is short lived and is a beneficial process. Within 24 hours of insult, microglia arrive to the area and upregulate surface protein expression. Proliferation occurs within 2-3 days and immunophenotypic changes are evident by day 7 [104]. Microglia maintains a very close physical association with injured neurons in order to facilitate targeted delivery of growth factors and to displace afferent synapses thereby aiding in neuronal regeneration. In non-reversible injury, such as ischemic damage, reactive microglia secrete neurotoxic factors that aid in killing the damaged neuron preparing it for removal and degradation by phagocytic microglia [104].

In circumstances that engage chronic activation, microglia may exert detrimental effects by transforming into autoaggressive effector cells that attack healthy cells, also known as bystander damage. Chronic CNS activation, as in AD, is primarily caused by bystander damage and is characterized by slow, progressive neurodegeneration that takes decades to develop. Exposure of cells to the various proteases and toxic molecules, produced by activated microglia for a long period of time causes extensive neuronal damage and death. Moreover, many of the pro-inflammatory cytokines and chemokines that are secreted contribute to a positive feedback mechanism, causing further attraction and activation of more microglia. These same factors have also been implicated in initiating signal transduction cascades on both microglia and neuronal cells that results in the transcription of IL-1β, transforming growth factor-β (TGF-β) and more cytotoxic agents via the nuclear factor κB (NFκB) transcription factor [105]. Finally, many of the inflammatory products secreted by microglia can alter the processing of APP in neurons to favour the production of $A\beta_{1-42}$, thereby resulting in more plaque formation, microglial activation and neuronal death [26].

1.4.4 The role of activated microglia in Alzheimer disease

Many reports imply that microglia may exacerbate the pathological states in neurodegenerative diseases. Persistent activation of microglia is an accepted hallmark of AD and a substantial amount of the neuronal damage observed in AD may be due to the inflammatory response mediated by microglia. Aβ, NFTs and degenerating neurons are most likely the stimulants for inflammation in AD. As in the periphery, there is not just one system of inflammation that is involved in a response. In the AD brain there is substantial evidence for the multiple interactions of complement pathways, cytokine and

chemokine pathways, cyclo-oxygenase (COX) and acute phase proteins. *In vitro* experiments with Aβ aggregates, *in vivo* experiments in AD mice and Aβ infused animals, and *in situ* studies on post-mortem AD brains have all demonstrated that Aβ can induce microglia to upregulate the expression of cytokines (IL-1β, TNF-α, IL-6), chemokines (IL-8, macrophage inflammatory protein-1α and macrophage chemoattractant peptide-1) chemokine receptors (CCR3 and CCR5), complement proteins (C1q and C3, C4) and major histocompatibility complex II [26] and other genes such as melanotransferrin (p97) [110,111] heme oxygenase 1 [112] and urokinase plasminogen-activating receptor [113]. Activated microglia also release the excitotoxins quinolinic acid [114] and glutamate [115]. Since endotoxins only cause limited damage to synapses and dendrites, it is thought that they may contribute to the neuronal dysfunction rather than complete neuronal death [26]. Together, all of these factors contribute to the inflammatory mechanisms observed in the disease.

It has been shown *in-situ* that microglia cluster around the sites of amyloid deposition both in humans and in APP transgenic mice [116,117,90,118]. The clustering of microglia around the senile plaques can be explained due to the chemotactic signaling of a number of molecules including Aβ, signals from damaged/dying neurons and also the many pro-inflammatory mediators which are found in the area of the plaque. Still under debate is the relationship between microglia and the development of Aβ plaques. One possibility is that microglia may directly contribute to amyloidosis by participating in the synthesis and processing of APP to Aβ fibrils. It has been demonstrated that cultured microglia are able to secrete Aβ; however, *in vivo*, microglia do not appear to express APP mRNA [26]. Therefore the likelihood that microglia secrete Aβ and contribute to Aβ plaque formation

is debatable and requires more research. Another possible mechanism relates to the potential of microglia to convert soluble Aβ into a more fibrillar and aggregative form. Many studies have stated that most activated microglia appear to associate around neuritic plaques rather than diffuse plaques in both mice and humans [119,118,90]; however, there are some microglia associated with diffuse plaques [120,121]. These data suggest that microglia play a role in transforming nonfibrillar amyloid into the more insoluble fibrillar form and aid in the transformation from diffuse plaques to neuritic plaques.

Finally, microglia may contribute to plaque formation by their ability to phagocytose and degrade Aβ. It is proposed that there is a dynamic balance between amyloid deposition and removal in the brain. It has been established in culture, that microglia migrate to and internalize microaggregates of $A\beta_{1-42}$, via a type A scavenger receptor, and deliver it to late endosomes and lysosomes, where it is degraded [122,60]. This uptake appears to occur rapidly; however, the degradation process occurs at a slow rate [123]. Furthermore, it has been reported that microglia found in the cortex of AD patients contain fragments of Aβ, most notably C-terminal fragments, inferring that the Aβ was phagocytosed [124,125]. This rapid internalization of Aβ microaggregates coupled with the slow degradation can lead to the accumulation of Aβ inside the cell. Therefore, in the case of AD, the overproduction and thus the persistence of Aβ may become too overwhelming for the microglia and thereby disrupting the dynamic balance between Aβ deposition and removal. This was demonstrated in a study by Rogers *et al.* where microglia cultured with Aβ were able to migrate to and phagocytose the Aβ; however, degradation of the fibrils took between 2-4 weeks [126]. Another study found that although some degradation of Aβ by microglia was observed over 3 days, no further degradation

was observed over the next 9 days. Instead, there was a slow release of intact Aβ [127]. Understanding the mechanism of Aβ clearance by microglia is important in determining the steps of Aβ plaque formation. It is possible that there is a fine balance between Aβ processing and deposition and degradation. Any disruption of the Aβ equilibrium can thereby lead to the accumulation of Aβ and the formation of amyloid plaques.

An alternative theory to the role of microglia in AD was offered by Streit [109] and states that microglia become senescent and/or dysfunctional with normal aging, therefore their ability to support neurons would be diminished resulting in neuronal degradation. The rate of deterioration can be affected by genetic and environmental risk factors thereby causing some individuals to develop AD. Some indication of dysfunction may be in the structural abnormalities seen in microglia as they age and in AD. Microglia which cluster around plaques have bulbous swellings in their cytoplasmic processes, called spheroids, as well as the formation of long stringy processes [109]. However, there is still little experimental evidence of microglial dysfunction in AD.

1.4.5 Signal transduction pathways and microglial activation

Many in vitro studies have demonstrated that the exposure of microglia to fibrillar Aβ results in the activation of complex kinase and phosphatase signal transduction pathways that lead to the activation of various transcription factors involved in inflammation. These include: the STAT family members, peroxisome proliferator-activated receptor γ (PPAR-γ), c-fos, and c-jun; NFκB; and members of the C/EBP family of transcription factors [58,128,129,130]. Subsequent immunohistochemistry studies in AD brains of both human and animal models have revealed the upregulation of many

signal transduction proteins in microglia and neurons that are in close proximity to the plaque [131].

One of the most important kinase families involved in the inflammatory response and consequent neuronal damage/death is the MAPK family. The complex molecular interactions between MAPKs and proteins associated with the evolution of AD form a cornerstone in the knowledge of a still burgeoning field. The MAPK family comprises four subfamilies: 1) ERK1/2 (p44/42 MAPK); 2) c-jun N-terminal kinases (JNK); 3) p38 MAPK; and 4) ERK5/big MAP kinase 1 [130]. Activation and subsequent phosphorylation of ERK1/2, JNK and p38 have been detected in AD. In the brain, the ERK1/2 kinase pathway has been implicated in eliciting stress responses, including oxidative stress, and in the regulation of intracellular calcium levels [130]. JNK pathways have also been shown to respond to cell stresses and in addition, evidence has confirmed that the phosphorylation of JNK leads to the activation of death domain receptors by TNF-α [132]. The p38 MAPK family is activated by inflammatory molecules and is involved in cell cycle, cell growth and cell differentiation [130]. In AD mice, phosphorylated p38 levels are increased approximately 3 fold in plaque-associated microglia. Many cell culture experiments have demonstrated that exposure of microglia and co-cultures of microglia and neurons to both oligomer and fibrillar Aβ leads to the activation of p38, ERK and JNK in microglia [57,133,128]. Moreover, MAPKs have been found to be integral to the induction of IL-1β, TNF-α and reactive nitrogen intermediates from LPS and Aβ treated cells [57,133]. The molecular mechanisms by which MAPK signaling contribute to glial mediated responses in AD are not fully elucidated. It is thought that the different MAPK pathways are activated in response to different mediators, leading to a differential

response by the microglia. Therefore, delineation of the downstream targets of these signaling cascades is also critical in order to further unravel their role in AD as well as in creating potential therapeutics.

1.5 The blood-brain barrier and Alzheimer disease

1.5.1 The blood-brain barrier, structure and function

The blood-brain barrier (BBB), found in all vertebrates, prevents the free diffusion of circulating molecules and cells into the brain interstitial space. The barrier is formed by the presence of epithelial-like, high resistance tight junctions that fuse brain capillary endothelia together into a continuous cellular layer separating blood and brain interstitial space. There are fine structural differences from the endothelium in the brain compared to that of other organs. These include tight junctions between adjacent endothelial cells, paucity of pinocytotic vesicles and lack of fenestrations [134]. The endothelial cells of the BBB have high mitochondrial content. It is thought that the energy generated in the mitochondria provide energy to the cell in order to create and sustain high-resistant tight junctions [134]. The junctions that comprise the BBB are made up of adherens junctions and tight junctions. Adherens junctions are made up of cadherins which form adhesive contacts between cells by binding to cadherins on the surface of neighboring cells. Inside the cell, cadherins bind to the actin cytoskeleton via proteins such as catenins [134]. Tight junctions consist of three integral membrane proteins, claudin, occludin and junction adhesion molecules. There are also many cytoplasmic accessory proteins that link tight junctions to the cytoskeleton of the cell. Claudins are

the major proteins found in tight junctions and bind to other claudins on adjacent cells to create the primary junction. The carboxy terminus of claudins also associates with cytoplasmic proteins, such as zonula occudens proteins (ZO) which, in turn, bind to actin. Occludins are also found with claudins in the cell membrane. These proteins also bind to ZO proteins and are implicated in the regulation of cell permeability [135]. The BBB is also comprised of a basement membrane, astrocyte foot processes that surround the vessel, and pericytes embedded within the basement membrane (Figure 1.4) [134]. The basement membrane is a heterogeneous mixture of proteins that are secreted from the endothelial cells and glial cells and include laminin, fibronectin, collagen type IV and proteoglycans. The presence of the basement membrane in the BBB is to provide elasticity to the vessels as well as to aid in the selective transport of highly charged molecules [136]. The contribution of astrocytes to the BBB appears to be that of influencing the morphogenesis and organization of the endothelial cells that make up the vessel wall. Studies involving the transplantation of cultured astrocytes into areas of the brain with leaky vessels have demonstrated that astrocytes induced the tightening of the junctions between the endothelial cells [137]. This is thought to be mediated by astrocyte derived soluble factors, such as TGF-β and IL-6, and may require direct contact between the astrocytes and the endothelium [138,134]. In contrast, it has been shown that upon glial cell activation, many cytokines and chemokines, such as TNF-α and IL-8, are produced resulting in an increase in vascular permeability and lymphocyte entry into the brain [136]. Pericytes wrap around endothelial cells and appear to play a role in structural integrity, formation of tight junctions and the differentiation of the intact vessel as well as in angiogenesis. Some studies have shown that pericyte loss can result in microaneurysm formation [139,140].

However, little is known how these processes are mediated since few studies on pericyte function have been conducted [134].

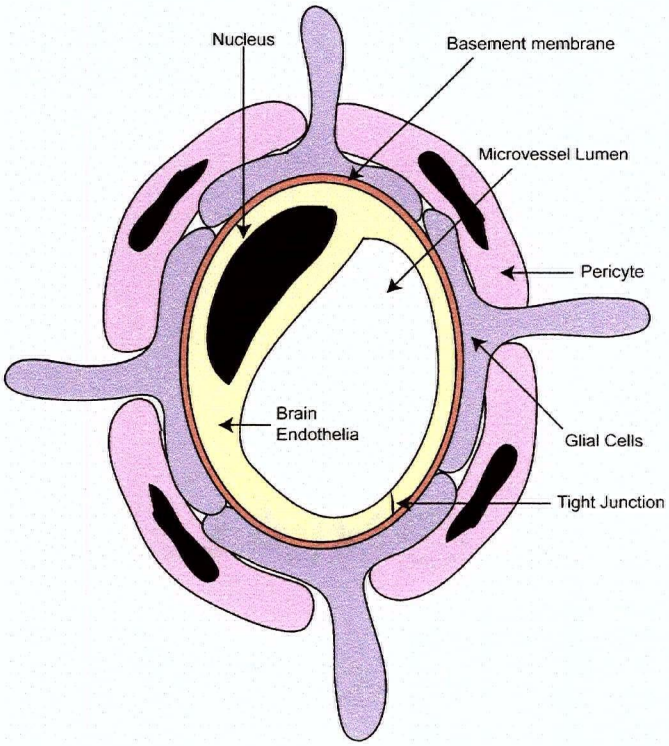

Figure 1.4. Schematic of the BBB.
The BBB is created by the tight apposition of endothelial cells lining blood vessels in the brain, forming a barrier between the circulation and the brain parenchyma. The BBB is permeable to small and lipophilic molecules. Larger and hydrophilic molecules can only be transported across via an active transport system. Blood-borne immune cells (lymphocytes, monocytes and neutrophils) cannot penetrate this barrier. A thin basement membrane, comprised of laminin, fibronectin and other proteins, surrounds the endothelial cells, associated astrocytes and pericytes, providing both mechanical support and a barrier function

The fluid of the central nervous system differs in composition from the non-neural extracellular fluid due to the selective permeability of the BBB [141]. The functional events that define the BBB occur at the capillary level. The BBB, under normal physiological conditions, regulates the passage of peptides, proteins and other molecules between the

periphery and the brain. The physiochemical properties of the penetrating substance or solute, determine whether it can be transported across the BBB. Hydrophobic solutes can penetrate across the BBB while hydrophilic substances are preferentially transported across the BBB by specific membrane carrier proteins for which they have a high affinity [142]. In contrast, most foreign substances cannot penetrate the BBB since they are not recognized by the carrier systems. The barrier works in both directions. In addition to keeping unwanted substances out, the BBB retains brain synthesized compounds, such as neurotransmitters, in the brain. The cerebral endothelia forms tighter junctions than other endothelia and contains specific proteins, which are specifically expressed in the brain. These include alkaline phosphatase, γ-glutamyl transpeptidase, the glucose transporter (Glut-1) [143], and the molecules involved in metal transport such as the transferrin receptor (TfR) and p97 [144].

1.5.2 BBB integrity and Alzheimer disease

The integrity of the BBB is an area of great contention in AD research. Studies comparing the vasculature of AD patients to controls have conflicting results. Upon analysis of vasculature from post-mortem AD brains there was a decreased mitochondrial content and increased pinocytotic vesicles as compared to values obtained previously in endothelium from multiple sclerosis patients and in AD animal models. Other findings such as accumulation of collagen in vascular basement membranes and focal necrotic changes in endothelial cells were present in AD patients indicating BBB disruption [145]. In contrast, Caserta *et al.* found that there was no difference in BBB integrity between AD cases and controls as indicated by blood-to-brain transport (KI) and tissue to blood

efflux (k2) of meglumine iothalamate, a radiopaque medium that binds to plasma proteins and is commonly used for angiography and venography [146].

In animals models the role of the BBB integrity in AD is also debated. Increased BBB permeability for some proteins, such as insulin, is evident and suggests some structural alterations at the BBB, however, these alterations do not support the concept of extensive BBB damage [147]. What's more, it appears that leukocytes are able to cross an intact BBB without causing concomitant BBB breakdown [148]. Alternatively, it has recently been established that the BBB integrity is compromised in hAPP overexpressing AD mice compared to controls and that the breach in BBB integrity precedes plaque formation [149]. Many studies have indicated that Aβ peptides promote pro-apoptotic and pro-angiogenic signals in endothelial cells [150,151,152], and that systemic-derived inflammation, either triggered by Aβ or neuronal signals, causes BBB tight junction disruption and increased paracellular permeability [153,154,155].

In addition to the neurodegeneration observed in AD, there are also considerable cerebrovascular abnormalities. It is becoming evident that the relationship between AD and CAA is growing more complex and it is harder to distinguish one disease being distinct from the other. It is estimated that the prevalence of CAA in AD patients varies from 70 to 100% [156,157,158,159]. CAA is characterized by the deposition of amyloid, primarily $A\beta_{1-39}$ and $A\beta_{1-40}$, in the cerebral vessel wall [160]. Since AD and vascular disease share common risk factors and since a history of strokes may be a risk factor for AD [161], it is important to understand the relationship between dementia, neurodegeneration and cerebrovascular abnormalities. It is possible that this relationship is attributed to alterations in the BBB. Furthermore, as evidenced by the first phase of

human clinical trials of the amyloid vaccine where cerebral complications ensued [162, 163], there is still much to learn about the relationship between neurodegeneration, dementia and cerebral abnormalities induced by Aβ.

1.6 Therapeutic strategies

The treatment of AD up until now has focused on the cholinergic system and symptoms thereof. Cholinergic therapeutics, such as Aricept, an acetylcholinesterase inhibitor, and psychotrophic drugs have had relative success in stabilizing the cognitive decline and behavioral deficits attributed to AD. Nevertheless, these therapies only treat the symptoms and do not delay or prevent disease progression. Based on the widely accepted "amyloid cascade hypothesis", research is now centered on the generation of anti-amyloid therapies. Therapeutic strategies directed at lowering Aβ levels and decreasing levels of toxic Aβ aggregates through: (1) inhibition of APP processing to Aβ, (2) inhibition, reversal or clearance of Aβ aggregation, (3) cholesterol reduction and (4) Aβ immunization are under development

As a target to alter Aβ metabolism, inhibition of both β- and γ-secretases are being pursued. Treatment of mice with γ-secretase inhibitors has resulted in a significant reduction in brain Aβ levels and an attenuation of Aβ deposition [164]. Inhibition of β-secretase is also under study and is thought to be a better target than γ-secretase inhibitors since γ-secretase cleavage is associated with the cleavage of other proteins, such as NOTCH, which is important for development. Studies on BACE1$^{-/-}$ mice demonstrate an absence in brain Aβ and no other obvious non-AD related pathologies [165]. Moreover, in BACE1$^{-/-}$/APP mice there is an absence of amyloid plaques, microgliosis and dystrophic

neuritis in the brain. At present, inhibitors for γ-secretase are in phase 1 clinical trials; however, more research is needed before such inhibitors are readily available for treatment.

In vivo, in vitro and epidemiological studies suggest that cholesterol may play a role in the generation of amyloid and its subsequent accumulation by its role in lipid metabolism. Retrospective analysis of people taking β-hydroxy-β-methylglutaryl-coenzyme A reductase inhibitors, or statins, show that there was up to a 70% reduced risk for developing AD, whereas individuals with high cholesterol levels had a higher risk for AD [166,167]. *In vitro* studies on primary neuronal cultures have shown that membrane cholesterol affects the cleavage sites for both β- and γ-secretase, favouring the production of $A\beta_{1-42}$, and that the removal of membrane cholesterol caused a decrease in Aβ production [168,169]. Other studies, in which APP mice were fed high cholesterol diets, found that there was a decrease in sAPPα and an increased the APP cytosolic fragment AICD and plaque burden in high cholesterol diet mice compared to mice on a control diet [170,171]. Furthermore, feeding mice with a statin called atorvostation, commercially known as Lipitor, resulted in a 50% decrease in plaque load and an increase in the formation of sAPPα in APP transgenic mice [172]. Similar results are seen in humans, where statin use resulted in an approximate 40% decrease in Aβ serum levels [173]. Taken together, these data suggest that cholesterol modulating drugs may have a significant clinical benefit to the treatment and prevention of AD.

Over the past few years the role of inflammatory mechanisms in AD pathogenesis is becoming more evident. NSAIDs, such as ibuprofen (Ibu), indomethacin and nimesulide (Nim), have been used as therapeutics for the treatment of AD. These drugs

have been shown to have anti-inflammatory properties by reducing the enzymatic activity of COX enzymes and thus the production of prostaglandins [26]. These drugs have also been demonstrated to have the capability of altering $A\beta_{1-42}$ production, presumably by acting on the γ-secretase complex and shifting cleavage towards the shorter less toxic forms of Aβ [174]. Treatment of neuroblastoma cells with the above NSAIDs resulted in the stimulation of α-secretase and secretion of sAPPα [33]. Recent clinical studies with NSAIDs are inconclusive due to small sample sizes and a large drop out rates. Thus, while the exact targets of anti-inflammatories remain to be clarified, new clinical studies, with larger cohorts and more extensive research into new drugs are ongoing and will hopefully illuminate the practice of anti-inflammatory therapeutics for AD.

The most recently developed anti-Aβ therapy is aimed at the reversal and/or clearance of Aβ aggregates and employs immunization with either Aβ peptides or anti-Aβ antibodies. Aβ immunization appears to be effective in reducing amyloid deposition and plaque formation, neuritic dystrophy, astro- and microgliosis, memory and cognitive deficits and early Tau pathology [175,176,177,178, 179,180,181]. How immunization reverses or attenuates disease pathology remains to be elucidated. It is thought that Aβ or anti-Aβ antibodies act by eliciting one or more of the following: 1) preventing fibril formation, 2) blocking the toxic effects of soluble and aggregated Aβ, 3) disrupting Aβ fibrils, and 4) enhancing the clearance of Aβ by microglia [164]. Clinical trials of active Aβ peptide immunization were undertaken but were suddenly halted in phase II when 5% of the patients exhibited meningio-encephalitis. New administration techniques, such as type of adjuvant and dose of Aβ peptide/anti-Aβ antibody, have been explored and currently new clinical trials, involving both active and passive immunization, are being pursued.

1.7 Project rationale and general approach

The focus of this thesis was to add to the basic understanding of the relationship between microglia and amyloid beta and to the various aspects of AD pathology. Both *in vitro* and *in vivo* experiments were performed in order to examine the role of microglial gene expression in response to Aβ stimulation as well as the role of microglia in plaque formation. It was hypothesized that in response to general activation, microglia upregulate the expression of specific genes, in particular, p97, and that these changes in gene/protein expression may be used as a means to determine anti-inflammatory drug efficacy. Moreover, it was hypothesized that activated microglia exacerbate the pathology of AD and contribute to plaque formation. Finally, it was hypothesized that the damage that activated microglia and Aβ incur on the BBB can be reversed by Aβ immunotherapy. Taken together, the studies presented here provide new ways by which AD progression and treatment can be monitored, as well as providing a new therapeutic target for AD treatments and disease prevention.

Chapter 2: Materials and Methods

2.1 Mice

2.1.1 Tg2576 AD model mice

The transgenic mice used in this study are the Tg2576 AD model mouse (Tg/+), which expresses the Swedish mutant of the amyloid precursor protein (K670N/M671L) [84] under control of the hamster prion protein promoter. Mice were maintained by mating Tg2576 males to C57B6/SJL F1 females. This strategy was undertaken since Tg2576 mice are heterozygous for the hAPP gene. Tg2576 mice were distinguished from control littermates by PCR at 2 weeks of age as previously described [84,85]. Briefly, primers specific to the Hamster prion promoter and human APP were used along with an internal control (1501, 1502, 1503; Table 2) to determine if mice contains the human APP gene. Animals were fed lab chow and water *ad libitum* and kept under a 12 hr light/dark cycle. Mice were group housed where possible, although the occasional male mouse had to be housed alone due to aggression. Wild type (+/+) littermates were used as controls. For the vaccination studies described below, 6 week and 11 month old mice were used.

2.1.2 Colony stimulating factor-1 deficient mice (op/op)

Colony stimulating factor -1 (CSF-1) deficient mice, referred to as op/op mice, are osteopetrotic model mice. These mice have a spontaneous mutation resulting in a base pair insertion approximately 280 base pairs into the coding region of the CSF-1 gene generating a stop codon and a nonfunctional CSF-1 [182,183,184]. CSF-1 is a major growth factor for macrophages in vivo controlling survival, proliferation and differentiation [185].

The osteopetrosis phenotype is characterized by the lack of osteoclasts, thus impairing bone remodeling accompanied by retarded skeletal growth, excessive accumulation of bone, and the absence of incisors. In addition there is an absence of monocyte derived macrophage. Mature macrophages are produced from other precursor cells by the influence of granulocytes and macrophage colony stimulating factor. There is also a reduction in the number and an alteration in the morphology and function of microglia in the brain [186,187]. These animals also have a reduced viability and poor breeding performance. op/op mice were fed with powdered chow in infant milk formula and water *ad libitum* and kept under a 12 hr light/dark cycle. Homozygous op/op mice were distinguished phenotypically from normal littermates by the absence of incisors and by a domed skull at day 10 [188].

2.1.3 Generation of Tg/+;op/op mice

Tg/+;op/op mice were first generated by crossing female Tg2576 AD model mouse, described above, to male op/op mice. The Tg/+;op/+ offspring were interbred to produce double mutant Tg/+;op/op mice. Littermates Tg/+;+/+, +/+;op/op, +/+;+/+ served as controls. All procedures were conducted with approval by the University of British Columbia Animal ethics committee.

2.2 Preparation of reagents

The amyloid beta peptides ($A\beta_{1-40}$ and $A\beta_{40-1}$) used in the present study were synthetic peptides of human Aβ (Bachem, Torrance, CA). The peptides were dissolved in double distilled water at 100 μM concentration and incubated at 37°C with 5% CO_2

for 5 days to allow for fibrils to form. The final concentration of Aβ for cell stimulation was 10 μM. This concentration was chosen as a result of a dose response experiment which showed optimal activation at 10 μM Aβ. Flourescent-labelled $A\beta_{1-40}$ (Calbiochem, La Jolla, CA), used for BBB studies, was resuspended in distilled water and used immediately after reconstitution. LPS from *Salmonella typhimurium* and mouse IFN-γ (Sigma-Aldrich Canada Ltd, Oakville, ON) was resuspended in sterile phosphate buffered saline (PBS) as 1 μg/ml stocks. For NSAID studies, Ibu and Nim (Sigma) were dissolved in dimethylsulfoxide (DMSO) at a 1mM concentration. Inhibitors of MAPK pathways, SB203580 (SB; p38 MAPK inhibitor) and PD98059 (PD; MEK1/2 inhibitor) (Calbiochem, La Jolla, CA) were made as 20 mM stocks in DMSO. All chemicals were of analytical grade.

All primers used in this study were synthesized by Sigma Genosis and are listed in Table 2.

Primer name	Primer sequence	Product size (bp)
1501(mouse APP)	5'-AAGCGGCCAAAGCCTGGAGGGTGGAACA-3'	~ 760
1502 (PrP promoter)	5'-GTGGATAACCCCTCCCCCAGCCTAGACCA-3'	
1503 (hAPP)	5'-CTGACCACTCGACCAGGTTCTGGGT-3'	~ 420
P97+1	5'-GAGGGTGACTTTTTGGCTACT-3'	~ 450
P97-1	5'-AACGGAAGGCTCCACTGAGC-3'	
S15 sense	5'-TTCCGCAAGTTCACCTACC-3'	~ 360
S15 antisense	5'-CGGGCCGGCCATGCTTTACG-3'	
P1800 FWD	5'-GGCACGGGTAGTAGTAGG GAA-3'	~ 1800
P1800 REV	5'-GGCAACGTTGGGTTGGCT-3'	

Table 2. List of primer sequences and product
Primers were custom synthesized by Sigma genosis, made up in distilled water at a concentration of 20 pM, aliquoted and kept at -20°C.

2.3 Cell culture

The murine microglial cell line, BV-2, provided by Dr. Michael McKinney (Mayo Clinic, Jacksonville, FL), was derived from vraf/v-myc-transfected primary murine microglia. These cells exhibit morphological and functional features similar to primary microglia, such as cytokine secretion and phagocytosis [189]. It has been reported that phenotype changes can occur in BV-2 cells after multiple passages [190]. To avoid this, all cells used were passaged no more than 3 times. BV-2 cells were cultured in Dulbecco's modified Eagle's medium (DMEM) (Invitrogen Life Technologies, Burlington, ON) supplemented with 10% (v/v) fetal bovine serum (FBS) (Medicrop, Montreal, PQ.), 2 mM L-glutamine (Sigma) and 20 mM Hepes (Sigma). JB/MS, a murine melanoma cell line which expresses high levels of p97, were provided by Dr. Vincent J. Hearing (National Institute of Health, Bathesda, MD) and bEnd.3, a murine brain endothelial cell line, obtained from American Tissue Type Culture Collection (ATCC), were maintained in DMEM supplemented with 10% (v/v) FBS, 2 mM glutamine and 20 mM Hepes. 3T3, a murine fibroblast cell line was obtained from ATCC and maintained in DMEM supplemented with 10 % (v/v) bovine calf serum, 4 mM L-glutamine and 20 mM Hepes. All cells were cultured at 37°C in a 5% CO_2 humidified incubator.

2.4 Cell stimulation

All cell lines described above were maintained and prepared the same way. Twenty-four hours before treatment, cells were washed with PBS, plated at a density of $5x10^5$ cells/ml in serum free DMEM and incubated overnight at 37°C. For determining

the effect of microglial activation on p97 expression, the cells were then washed twice with serum free DMEM and treated with either 10 μM $A\beta_{1-40}$, 50 ng/ml LPS, 5 ng/ml IFN-γ, 10 μM $A\beta_{40-1}$ or PBS for 24 hours. The supernatant was harvested and stored at -80°C for TNF-α ELISA. The cells were then washed with ice cold PBS and RNA was extracted for RT-PCR as described below. For NSAID studies, cells were treated with 10 μM $A\beta_{1-40}$ or 50 ng/ml LPS in the presence or absence of 10 μM drug or left untreated. The NSAIDs used in this study were Ibu, a non-selective inhibitor of the COX enzyme family, and Nim, a COX-2 specific inhibitor. After 24 hours of treatment, the supernatant was harvested and stored at -80°C for TNF-α ELISA and the cells were washed with ice cold PBS. mRNA was then extracted for RT-PCR or cell lysates were harvested for Western blot analysis.

2.5 Creation of stable BV-2 transfectant cell lines

The Balb/c mouse brain genomic DNA was used to clone the promoter region of mouse p97. The p97 promoter, spanning approximately 1800bp from nucleotides –1641 to +59 (nucleotides numbered according to GenBank accession NM_013900 from the National Centre for Biotechnology Information database), was cloned by PCR using the sense p1800 FWD primer and antisense p1800 REV primer (see Table 2 for primer sequences). The PCR product was subcloned into pCR2.1-TOPO vector (Invitrogen Life Technologies Burlington, ON) and sequenced using standard m13R (5'-CAGGAAACAGCTATGACC-3') and T7 primers (5'-TAATACGACTCACTATAGGG-3') at the NAPS Facility (Nucleic acid-Protein Service Unit, University of British

Columbia, Vancouver, BC). After digestion with ApaI and HindIII (New England BioLabs), the p97 promoter was subcloned in-frame into the pEGFP-1 expression vector (Figure 2.1) (Clonetech, Palo Alto, CA). pEGFP-1 was chosen as a reporter system, since it lacks its own promoter and produces green fluorescence upon EGFP gene expression initiated by a ligated promoter. The resulting p1800-GFP construct was sequenced with p1800 FWD and EGFP-N sequencing primer (5'-CGTCGCCGTCCAGCTCGACCAG-3') and digested with Apa I and Hind III to ensure correct DNA sequence and orientation (Figure 2.2).

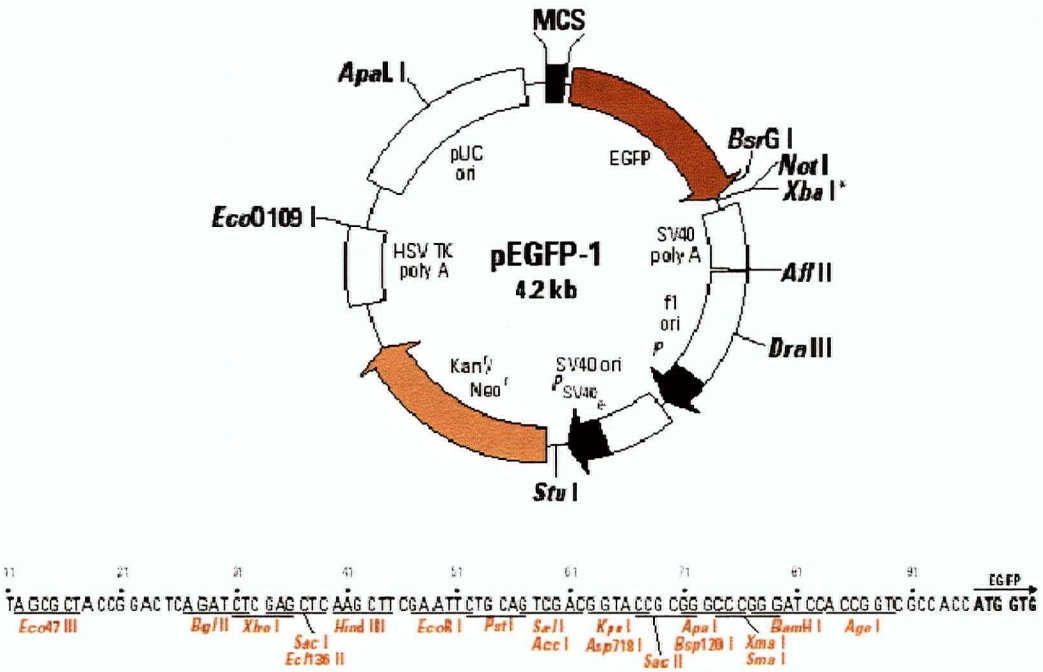

Figure 2.1. pEGFP-1 vector and multiple cloning site

This vector encodes a red-shifted variant of wild-type green fluorescent protein GFP which has been optimized for brighter fluorescence and higher expression in mammalian cells. pEGFP-1 encodes the GFPmut1 variant which contains the double-amino-acid substitution of Phe-64 to Leu and Ser-65 to Thr. pEGFP-1 is a promoterless EGFP vector which can be used to monitor transcription from different promoters and promoter/enhancer combinations inserted into the MCS located upstream of the EGFP coding sequence. The coding sequence of the EGFP gene contains more than 190 silent base changes which correspond to human codon-usage preferences. Sequences flanking EGFP have been converted to a Kozak consensus translation initiation site to further increase the translation efficiency in eukaryotic cells. SV40 polyadenylation signals downstream of the EGFP gene direct proper processing of the 3' end of the EGFP mRNA. A neomycin-resistance cassette (Neo^r) allows stably transfected cells to be selected using G418. A bacterial promoter upstream of this cassette confers kanamycin resistance in *E. coli*. (Adapted from Clontec).

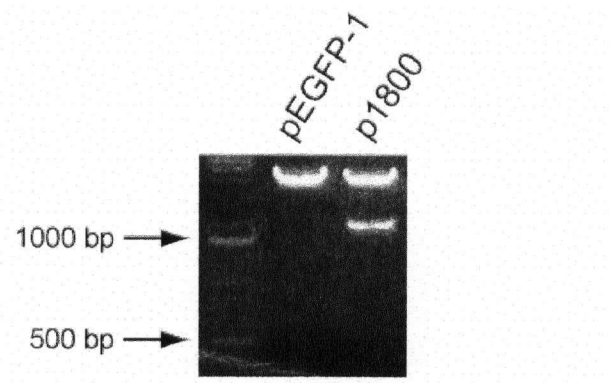

Figure 2.2. Gel of digested pEGFP and p97 promoter construct.
Each construct, pEGFP-p1800 and pEGPF, were digested with ApaI and HindIII for 3 hours at 37°C. The digested products were analyzed on a 1% agarose gel and visualized. The 4200 bp fragment indicates the pEGFP-1vector while the smaller 1800 bp product indicates the promoter region of p97.

BV-2 cells, at approximately 70% confluency, were transfected with the 5 μg of the p1800-GFP construct or the promoter-less pEGFP-1 vector by using Lipofectamine™ 2000 reagent (Life Technologies, Inc., Gaithersburg, MD) under serum free conditions. Cells containing either the p1800-GFP construct or the promoter-less pEGFP-1 vector were selected by adding 500 μg/ml G418 (Invitrogen). The transfectants continued to grow for approximately 3 weeks with 500 μg/ml G418, and then were sorted using the FACSDiva (BD Pharmingen, San Jose, CA) into single cell clones. Clonal cell lines continued to grow until confluency under selective conditions and were then analyzed for GFP expression. Since GFP expression is under control of the p97 promoter, cells were treated with 10 μM $A\beta_{1-40}$ for 24 hours and then sorted for high GFP expressing cells. Cells transfected with pEGFP-1 vector alone were sorted for low GFP expression. Three days later, cells were sorted again for low expressing GFP to isolate cells in an inactive,

resting state. These cell lines continued to grow for until confluency under selective conditions and were then used for experiments described.

2.6 RNA Isolation

mRNA from BV-2, JB/MS, 3T3 and b.End3 cells, as well as from mouse brain regions was extracted using the RNeasy mini Kit (Qiagen Inc., Mississauga, ON) according to the manufacturer's instructions. Cells were washed once in cold PBS, lysed with lysis buffer containing β-mercaptoethanol and spun down in a spin column. The cells were then washed with an appropriate buffer and RNA was isolated. RNA concentrations were determined using spectrophotometry at UV wavelengths of 260 and 280. Final RNA concentration was obtained form the following calculation

$$OD_{260} \text{ X } 40 = [\text{RNA}]\ \mu g/ml$$

2.7 Reverse transcriptase and Polymerase Chain Reaction

Reverse Transcriptase and Polymerase Chain Reaction (RT-PCR) was performed with oligonucleotide primers custom synthesized by Sigma Genosis listed in Table 2. The expression of p97 and S15 (loading control) was examined. To make the cDNA, 1 µg of RNA was used along with 1 µl of deoxyribonucleotide triphosphate (dNTPs) mix (10µl each of dATP, dCTP, dGTP and dTTP) (Invitrogen), 1µl of Oligo dT_{18} (Invitrogen) and Rnase free water to a total volume of 12 µl. The mixture was incubated at 65°C for 5 minutes followed by a quick chill on ice. Next, 4 µl of 5x first strand buffer, 2 µl of 0.1M dithiothreitol (DTT) and 1 µl of RNase OUT (Invitrogen) was added and incubated

at 42°C for 2 minutes followed by the addition of 1 µl of Superscript II (Invitrogen). The solution was mixed by gentle pipetting and incubated at 42°C for 50 minutes. After incubating, the reaction was then inactivated by heating the solution at 70°C for 15 minutes, followed by the addition of 1 µl of Rnase H (Invitrogen) and incubation at 37°C for 20 minutes. PCR amplification was performed through 35 cycles at 94°C for 30 sec, 56°C for 30 sec, and 72°C for 45 sec. The PCR was stopped with a final extension for 10 min at 72°C. Samples were then loaded into a 1% agarose gel and images were digitally captured and analyzed.

2.8 Real-time Polymerase Chain Reaction

RT-PCR results were confirmed by semi-quantitative real-time PCR for p97 and for S15 mRNA (used as internal control). RNA (1µg) from each sample was reverse transcribed using Superscript™ II Reverse Transcriptase (Invitrogen). Real-time PCR was performed using the Roche Light Cycler. In brief, 1 µl of cDNA and gene specific primers were added to SYBR® Green Taq ReadyMix™ (SYBR Green dye, Taq DNA polymerase, JumpStart Taq antibody, dNTP mix and optimal buffer components; SIGMA) and subjected to PCR amplification. The following protocol was used: denaturation (95°C for 5 minutes), amplification and quantification (40 cycles at 95°C for 5 seconds, 56°C for 5 seconds and 72°C for 30 seconds), melting curve program (65-95°C with a heating rate of 0.2°C per second and a continuous fluorescent measurement) and a final cooling step to 40°C. The primers used for p97 and S15 were synthesized by Sigma Genosis and are shown in Table 2. The amplified transcripts were quantified using

the comparative C_T method. Briefly, fold increase was calculated by determining the cycle at which the fluorescence passes the fixed threshold (C_T) for each sample. Below are formulas used to calculate the fold induction for each sample (as presented by Applied Biosystems).

$$\Delta C_T = C_T \text{ (gene of interest)} - C_T \text{ (endogenous control)}$$

$$\Delta \Delta C_T = \Delta C_T \text{ (sample X)} - \Delta C_T \text{ (control sample)}$$

$$\text{Fold Induction} = 2^{-\Delta \Delta C_T}$$

2.9 TNF-α ELISA assay

TNF-α produced by BV-2 microglial cells was determined in culture supernatants using a specific murine TNF-α ELISA kit capable of detecting levels as low as 5.1 pg/ml (R&D Systems, Inc., Minneapolis, MN) according to the manufacturer's protocol. TNF-α was chosen as a measurement of microglial activation since it has been established that microglia upregulate the production and secretion of TNF-α upon activation [26]. After 24 hours of treatment the cell culture supernatant was removed and stored at -80°C until assayed for TNF-α. ELISA measurements were performed using the Spectra Max 190; (Molecular Devices) using the standard and instructions supplied by the manufacturer.

2.10 Western blot analysis

Antibodies The phosphorylated forms of ERK and p38 MAPK were visualized using rabbit polyclonal primary antibodies raised against phosphor-(Thr202/Tyr204) ERK (1:1000) and phosphor-(Thr180/Thr182) p38 MAPK (1:1000), (Cell Signaling,

Beverly, MA). GFP was visualized using a mouse monoclonal raised against GFP (1:1000) (Santa Cruz Biotechnology, Santa Cruz, CA). Loading controls for ERK, p38 MAPK and GFP were determined by using extracellular regulated kinase1/2 (Erk1/2) (1:1000) polyclonal antibody, extracellular regulated p38 antibody (1:1000) and GAPDH (1:10000) (Santa Cruz Biotechnology) respectively. Secondary goat anti-rabbit (1:10000) and goat anti-mouse (1:10000) antibodies conjugated to horse radish peroxidase (Jackson ImmunoResearch Laboratories, West Grove, PA) were used.

BV-2 cells transfected with the p1800 promoter region of p97 fused to GFP were washed, resuspended at 5 x 10^5 cells/ml in DMEM containing G418 and incubated overnight at 37 °C. Cells were then washes 3 times in serum free media and incubated with 10 μM $A\beta_{1-40}$ or 50 ng/ml LPS for 24 hrs. For signal transduction studies, cells were treated with 20 μM SB or 50 μM PD for 30 min and then with either 10 μM $A\beta_{1-40}$ or 50 ng/ml LPS for 6 hrs. Following treatment, cells were lysed in 50 μl of lysis buffer containing 50 mM Tris-HCl (pH 7.5), 150 mM NaCl, 10% glycerol, 1% Nonidet P-40, 5 mM EDTA, 1 mM sodium vandadate, 5 mM sodium fluoride, 1 mM sodium molybdate, 5 mM β-glycerol phosphate, in the presence of 10 μg/ml soybean trypsin inhibitor, pepstatin, and 40 μg/ml phenylmethylsulfonyl fluoride. Protein concentrations were determined using the BCA protein assay (Pierce, Rockford, IL). Equal amounts of proteins were denatured by boiling in SDS sample buffer (0.16% (w/v) SDS, 0.002% (w/v) bromophenol blue and 1% (w/v) DTT.) run on 12% SDS-PAGE gel along prestained broad range standard (Bio-rad, Hercules, CA) and transferred to nitrocellulose membrane. Membranes were blocked for non-specific binding in 5% non-fat dry skim milk in PBS and 0.1% (v/v) Tween 20 detergent (Bio-rad). Primary antibodies to

phospho-p38 and phosphor-p44/42 were incubated in PBS/0.1% Tween 20 and the GFP primary antibody was incubated in blocking buffer. Primary antibodies were incubated with membranes overnight at 4°C. After incubation with HRP-linked secondary antibodies, proteins were detected using ECL detection reagent (Amersham Biosciences, Piscataway, NJ). After development, the blots were stripped in 62.5 mM Tris-HCl (pH 7.5), 0.2% SDS, and 100 mM 2-mercaptoethanol for 30 min at 50 °C and then reprobed with either a monoclonal antibody to GAPDH, extracellular regulated kinase1/2 (Erk1/2) (K-23) polyclonal antibody and extracellular regulated p38 (C-20) (Santa Cruz Biotechnology) as a protein-loading control.

2.11 Immunohistochemistry

Adjacent tissue sections were immunostained for the detection of amyloid deposits (4G8) and activated microglia (F4/80). Brains were fixed in 4% paraformaldehyde, paraffin embedded and cut into 8 μM sections. Sections were then deparaffinized, hydrated and incubated in DAKO Target retrieval Solution (DakoCytomatiom) in a steamer for 20 minutes to ensure proper unmasking of the antigen. The samples were then cooled at room temperature for 30 minutes and washed in water 3 times for 5 minutes each. Slides were then incubated in 3% H_2O_2 for 30 minutes, rinsed 3 times in water and blocked in the appropriate blocking solution for 40 minutes. Slides were then incubated in either 4G8 (1:500, Signet Labs Inc., Dedham, MA) or F4/80 (1:10, Serotec, Oxford, UK) overnight at 4°C, washed and incubated with a secondary biotinylated anti-mouse antibody for 4G8 or a biotinylated anti-rat antibody for F4/80 (DAKO LSAB+system, DakoCytomation) for 25 minutes. Sections were developed by DAB

(Vector Laboratories Inc., Burlington, ON), counterstained with Mayer's hematoxylin, dehydrated and mounted. Slides were examined under a Zeiss microscope and images were captured using OpenLab software. The number of plaques per cortical brain section per mouse was counted and analyzed. Data were collected from 4 equally spaced sections. The values for all sections from one mouse were averaged to obtain a single sample for statistical analysis.

2.12 Aβ and antibody injection

Fluorescent-labelled $A\beta_{1-40}$, PBS, bovine serum albumin (BSA) conjugated to Texas red (Sigma), anti-human Aβ antibody (4G8), Biotin labeled anti-human Aβ antibody (4G8) (Signet Labs Inc.) and biotin (Sigma) were injected intravenously (i.v.) into the tail veins of mice. For injections, a total volume of 200 µl was injected into each mouse containing 200 µg of protein. One hour after injection, the mice were anesthetized with ketamine (25 mg/kg i.p.) and xylazine (5 mg/kg i.p.) and perfused with 1 X PBS followed by 4% PFA. Following perfusion, the brains were dissected, embedded into paraffin and sectioned into 8 µM sections. Brain sections from mice injected with fluorescent Aβ, PBS and Texas-red conjugated BSA were examined directly by confocal microscopy without any processing. Brain sections for mice injected with anti-Aβ antibodies (both unlabelled and biotin labeled) were stained with secondary antibodies or processed with DAB respectively. Briefly, slides were deparaffinized and hydrated as described above. For mice injected with anti-Aβ antibodies, slides were blocked in 10% skin milk in PBS for 30 minutes, washed 2 times for 5 minutes in water and then incubated in Alexa 488 nm conjugated goat-anti mouse IgG secondary antibody (1:500)

(Molecular probes, Eugene, OR) diluted in 2% BSA/PBS for one hour. The slides were then washed 3 times for 5 minutes. The coverslip was mounted with 5 µl Antifade (Molecular probes) before sealing with nail polish. For mice injected with biotin labeled antibody or biotin alone, slides were developed with DAB (Vector laboratory) washed 3 times for 5 minutes in water, dehydrated in 3 washes of xylene and mounted with a coverslip using permount. The slides were then examined using a confocal microscope or a light microscope. All mice used for these studies were 6 weeks old and of similar weight.

2.13 Vaccination protocol

Prior to immunization each mouse was bled and serum collected. Two groups of mice were vaccinated beginning at 6 weeks and 11 months of age and sacrificed at 12 months and 15 months respectively. Aβ peptide was freshly prepared from lyophilized powder for each set of injections. For immunizations, 2 mg of Aβ (human $A\beta_{1-40}$; Bachem) was added to 0.9 ml of deionized water and mixed until a solution of uniform suspension was obtained. Then 100 µl of 10X PBS was added to obtain a final 1X PBS concentration. The solution was vortexed and placed at 37°C overnight until use the next day. $A\beta_{1-40}$ (100 µg antigen per injection) or PBS (control) was mixed 1:1 (v/v) with complete Freund's adjuvant (CFA) for the first immunization. This was followed by a boost with $A\beta_{1-40}$ (100 µg) or PBS mixed 1:1 (v/v) with incomplete Freund's adjuvant (ICFA) at two weeks and monthly thereafter. The 6 week old mice were vaccinated for a total of 11 months, and the 11 month old mice were vaccinated for a total of 4 months.

Aβ or PBS alone were injected from the fifth immunization onward. Antibody titres for anti-Aβ antibodies was assayed after the second immunization. Anti-Aβ antibody titres were determined by serial dilutions of sera against aggregated Aβ, which had been coated in microtitre wells. Detection was done by using goat anti-mouse immunoglobulin conjugated to horseradish peroxidase and ABTS (2'2-AZINO-bis (3-ethylbenzthiazoline-6-sulfonic acid; Sigma) as substrate. A fluorescence plate reader (Spectra Max 190; Molecular Devices) then measured fluorescence at 405 nm.

2.14 Evans blue assay

Quantitative Evans blue analysis was performed as previously described by Ujiie *et al.* [149] In brief, Tg2576 mice vaccinated with either Aβ or PBS alone and their age-matched controls were weighed and injected intra-peritoneal (i.p.) with 50 μg/g Evans blue dye (Sigma) in 1XPBS. Three hours after injection, the mice were anesthetized with ketamine (25 mg/kg i.p.) and xylazine (5 mg/kg i.p.) and perfused with 1XPBS for 5 minutes. Following perfusion, the brains were dissected, olfactory and cerebellum removed, weighed and dounce homogenized in 0.5 ml of 50% trichloroacetic acid. The sample was then centrifuged at 10000 rpm for 10 minutes. The supernatant was collected and diluted 1:4 in 100% ethanol. An ELISA plate reader (Spectra Max 190; Molecular Devices) then measured Evans blue fluorescence at 620 nm. Values are graphed as OD_{620}/brain weight, and the data were statistically analyzed with the student t-test. As a control for Evan blue distribution throughout the mouse, OD_{620} values for the liver, a

tissue known to be highly permeable, were also evaluated. All mice used in this study exhibited high levels of Evans blue dye in the liver.

2.15 Statistical analysis

All analyses were performed using the GraphPad Prism software. TNF-α ELISA data and Real-time PCR data were analyzed by performing ANOVA tests followed by Bonferroni analysis. All experiments were performed at least 3 times and in triplicate within each experiment. Statistical significance was established at a level of $P < 0.05$. Aβ vaccination studies were analyzed by comparing Aβ vaccinated transgenic mice and PBS vaccinated transgenic mice within each group by the student t-test. Transgenic and non-transgenic mice injected with Aβ and transgenic and non-transgenic mice injected with PBS were also compared to one another respectively. Statistical significance was established at a level of $P < 0.05$.

Chapter 3: P97 expression in activated microglia

3.1 Rationale

It is now becoming widely accepted that inflammatory processes are involved in the pathogenesis of AD. There have been extensive studies over the past 10 years which have characterized the increased expression of many pro-inflammatory cytokines, cell surface markers and various neurotoxins corresponding to the accumulation of Aβ and disease pathology. The findings that amyloid plaques are surrounded by activated microglia also provide evidence for the contribution of inflammation in AD. These observations provide the rationale for developing therapeutics for AD targeted against inflammation and thus activated microglia. Further support of such therapies came from epidemiological evidence from arthritic patients who were on long term NSAIDs in which NSAID use correlated with a significant decreased risk for AD by approximately 60-80% [102]. Furthermore, NSAID treatment appears to slow down disease progression, delay onset and diminish symptom severity [103]. While it has been established that the target of NSAIDs are microglia, it is unclear what intracellular process in microglia mediate the response elicited by NSAIDs. It has been suggested that either the COX-1/2 enzymes or the transcription factor, PPAR-γ, are involved [26].

Finding a specific marker for inflammation resulting from Aβ accumulation would aid in the diagnosis of AD as well as in evaluating the efficacy of new anti-inflammatory therapeutics. There have been many biomarkers suggested to aid in the diagnosis of AD. These are mostly limited to the ratio between $A\beta_{42}$ and $A\beta_{40}$ or total Tau or phosphorylated Tau levels in the CSF. There have also been some markers of

inflammation that have been investigated in AD, such as levels of IL-6 [191] and TNF [192] however; these markers are general for all forms of CNS inflammation and not specific for AD related inflammation. An alternative candidate that is believed to be specific for AD is a protein called melanotransferrin.

Melanotransferrin, also known as the human melanoma associated antigen p97, was originally identified as a cell surface marker associated with human skin cancer [193]. Woodbury *et al.* analyzed the expression of p97 in normal adult, fetal, and neoplastic tissues and found that the protein was highly expressed in fetal colon, lung and umbilical cord as compared to adult tissues [194]. Further studies revealed that p97 is also highly expressed in fetal liver, placenta and sweat glands [193]. Due to high p97 expression in fetal tissues, it has been suggested that p97 may play a role in fetal development. In addition to its expression in human tissues, p97 has been found to be expressed in many cultures of normal cells including liver, intestinal epithelial cells and fetal intestinal cells [195,196,197,198]. P97 exists in two forms: one is a glycosylphosphatidylinositol (GPI)-linked cell surface form and the other is a secreted soluble form generated by alternative splicing [199,200,201]. P97 is a member of a group of iron binding proteins that include serum transferrin, lactoferrin and ovotransferrin and maps to the same region of chromosome 3q in humans as the genes of other proteins involved in iron transport [202]. Human transferrin and p97 share 40% sequence identity and p97 is able to bind one iron molecule [203]. Thus, p97 may be one of the many uncharacterized iron transport molecules that operate in a transferrin independent fashion.

The relationship between p97 and AD remains to be elucidated in molecular detail. The distribution of p97 in the brains of AD and non-AD subjects was studied to identify

locations where p97 is expressed [204,110]. In previous studies comparing AD brains with brains of patients who died from neurodegenerative diseases other than AD, such as Huntington's disease or Parkinson's disease (PD), the distribution of p97 in the non-AD brains appeared to be limited to the endothelial cells, which make up the BBB, with occasional positive staining for astrocytes and oligodendrocytes. Interestingly, in the AD brain, p97 was also detected in reactive microglia associated with senile plaques. Reactive microglia that stained positive with HLA-DR antibody but were not closely positioned near senile plaques did not express p97 [110]. Further immunohistochemical and *in situ* hybridization studies [111] revealed a high expression of p97 mRNA in the reactive microglia associated with senile plaques and lower levels of p97 around endothelial cells. In the non-AD brain, endothelial cells stained weakly for p97 mRNA and there was no p97 mRNA or protein detected in microglia. It is possible that there is an increased requirement for the utilization and/or scavenging of iron by reactive microglia associated with senile plaques since, in addition to p97, increased concentrations of iron, transferrin [205] and ferritin [206,207] have been noted in the region.

With the finding that p97 is detected on the BBB and in the reactive microglia associated with the senile plaques of AD patients [110] it was postulated that p97 may be used as a biological marker for AD. Initial studies by Kennard *et al.* investigated this putative relationship and found evidence that the soluble form of p97 is elevated, up to 6 fold, in the serum taken from AD patients as compared to controls (n=17) [208]. Further regression analysis of these data revealed that there was no correlation between p97 levels and age. To eliminate the possibility that environmental factors may result in the increased levels observed, serum samples from AD patients and their cognitively normal

spouses (n=10) were obtained [208]. Again it was found that the levels of p97 in AD patients compared to their spouses were significantly elevated thereby suggesting that environmental factors have no influence on serum p97 levels.

A subsequent study by Feldman *et al.*, involving a larger cohort of subjects, showed that there is a 2 fold significant increase in serum p97 levels from patients with AD compared to non-AD controls (41 ng/ml versus 20 ng/ml, $p<0.001$) [209]. These results were corroborated by an independent group of investigators [210] who reported that there was a 3 to 5 fold significant increase in the serum p97 levels in AD cases compared to non-AD cases of dementia and controls. In addition, there was no correlation between p97 serum levels and age or severity of disease. Collectively these are compelling findings which independently support the potential of serum p97 levels as a biomarker of AD.

The role of p97 as an iron transporter in AD pathology is unclear. It has been established that in many neurodegenerative diseases, such as AD and PD, there is a dysfunction in iron metabolism and hence homeostasis (reviewed in Qian, 1998) [211]. How exactly iron gets into the brain remains unresolved. It is thought that most iron transport in the body is mediated by the classical transferrin-transferrin receptor (TfR) pathway. However, in regards to iron transport in the brain, it is possible that other proteins may be involved. This is supported by looking at TfR, transferrin and iron distribution in the brain. There appears to very little overlap between TfR and iron distribution and between TfR and transferrin distribution [212]. In addition, there is a difference in the rate of transfer of iron and transferrin across the BBB indicating that iron transport across the BBB is likely to be facilitated by other means. It has been

previously established that p97 is able to bind and internalize iron into cells independent of transferrin and TfR [199,200]. Furthermore, the rate of iron uptake by p97 was equivalent to the rate of iron uptake seen with transferrin/TfR. These data suggest that p97 may transport iron across the BBB in a manner similar to the TfR. Dysregulation of p97 may be one of the causes of iron deposition in AD. Studies have confirmed the presence of an iron-responsive element in the 5'UTR of the APP and that at the biochemical level, copper, zinc and iron are shown to accelerate the aggregation of the Aβ peptide and amyloid plaque formation [45]. Microglia may express p97 in response to Aβ as a means to help clear Aβ plaques by binding to iron deposited in the plaques and destabilizing it. Alternatively, p97 expression in microglia may be a harmful response. If there is an initial dysregulation of iron in the brain causing a decrease in the concentration of free iron, (for example sequestration in plaques) p97 may cross the BBB into the periphery, bind iron and cross back into the brain. Recently, it has been demonstrated that p97 may participate in the vascularization of solid tumors and promote endothelial cell migration [213]. This angiogenic activity may depend on activation of endogenous vascular endothelial growth factor (VEGF) expression [213]. We have established that the BBB is compromised in AD model mice [149] and it is known that there is an increase in VEGF expression in AD [214,215,216]. Thus p97 may contribute to the increased permeability of the BBB in AD. More studies are needed in order to determine if an increase in brain iron levels is associated with an increase in p97 expression. Also, the distribution of p97 in different brain regions and different cells types may help elucidate the role of p97 in brain iron homeostasis and possibly AD pathology.

The aims of this study were to determine if microglia upregulate the expression of p97 upon general activation or whether this occurs in response to AD specific stresses, and to investigate which signal transduction pathway is responsible for this up-regulation. Moreover, if p97 could be used as a marker for inflammation, it may be possible to use it as an indicator of anti-inflammatory drug efficacy. To further investigate this possibility, p97 expression was examined in cells treated with NSAIDs.

3.2 Results

3.2.1 Microglial activation

As a prerequisite for analysis of levels of p97 in activated microglia upregulate the expression of p97, it is important to confirm the state of microglia after treatment with known stimulants was confirmed. It has been well established that once microglia become activated they secrete many pro-inflammatory cytokines including IL-1β and TNF-α, as well as reactive oxygen and nitrogen radicals [26]. Therefore to determine if microglia were indeed in an activated state, TNF-α levels were measured by a sandwich ELISA with antibodies specific for murine TNF-α. Cultured BV-2 cells were incubated for 24 hours with known activators of microglia including 50 ng/ml LPS, 5 ng/ml IFN- γ or 10 μM fibrillar $A\beta_{1-40}$, which is a stress specifically associated with AD. As negative controls, cells were treated with 10 μM of the reverse Aβ peptide ($A\beta_{40-1}$) or PBS. Stimulation of BV-2 cells with $A\beta_{1-40}$, LPS and IFN-γ lead to an increase in the

production of TNF-α (Figure 3.1). Treatment with the $A\beta_{40-1}$ had some effect on TNF-α production likely due to non-specific effects of addition of peptides to the media..

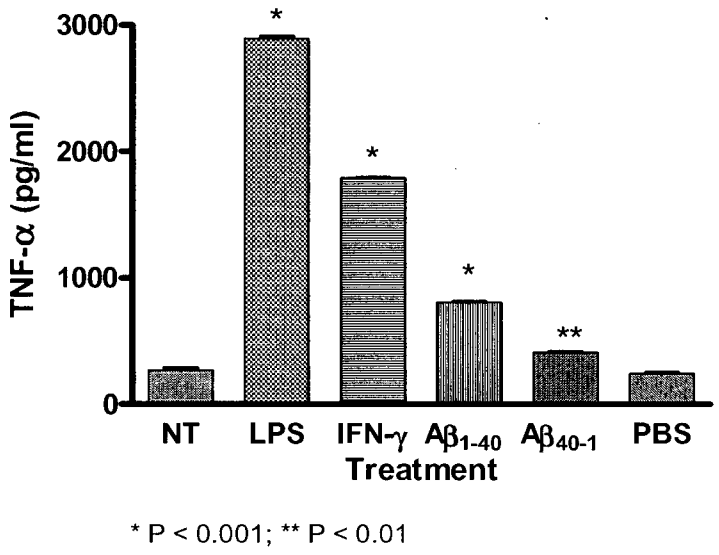

Figure 3.1. TNF-α production increased in BV-2 cells treated with various known activators. Cells were plated at a density of $5x10^5$ cells/ml and treated for 24 hours with 50 ng/ml LPS, 5 ng/ml IFN-γ, 10μM $A\beta_{1-40}$, 10 μM $A\beta_{40-1}$ and PBS. Cell culture supernatant was collected and TNF-α levels were measured using an ELISA specific for murine TNF-α. There was a significant increase in TNF-α production in cells treated with LPS, IFN-γ and $A\beta_{1-40}$ compared to no treatment (NT) (ANOVA, * $P < 0.001$, ** $P < 0.01$). Treatment with the reverse Aβ peptide had some effect, likely due to non-specific effects of added peptides while PBS had no significant effect on TNF-α production. All experiments were performed at least 3 times in triplicate. Error bars represent ± SD. The results above are representative of all replicates.

3.2.2 P97 expression in BV-2 cells

The expression of p97 was determined by RT-PCR in BV-2 cells under non-stimulating conditions and following treatment with fibrillar $A\beta_{1-40}$, LPS and IFN-γ. The results show that expression of p97 was largely increased in BV-2 cells in response to treatment with Aβ (Figure 3.2 a). Treatment with other known activators of microglia, such as IFN-γ had no significant effect on the expression of p97. There was an increase in treatment with LPS; however, not as large a magnitude as with treatment with Aβ. There was no effect on the expression of S15, a ribosomal subunit mRNA used as a loading control. In addition, there seemed to be no change in the expression of p97 in murine melanoma cells (JB/MS), murine brain endothelial cells (bEnd.3), nor in murine fibroblasts (3T3) in response to these stimuli (Figure 3.2 a). Real-time PCR analysis of p97 expression in BV-2 cells was performed in order to quantitate the change in mRNA expression. Treatment with Aβ resulted in an approximate 6 fold increase in p97 expression. The 6 fold increase corresponds to the increased protein serum levels previously reported in humans [208,209,210]. Treatment with LPS exhibited an approximate 4 fold increase in p97 expression (Figure 3.2 b). Since there is no monoclonal antibody to murine p97, BV-2 cells were transfected with the pEGFP-1 promoterless vector where the expression of GFP is under control of the p97 promoter (p1800-GFP). To investigate if protein levels of murine p97 corresponded to the increase in mRNA expression, Western blot analysis was performed on p1800-GFP transfected BV-2 cells and blotted for GFP expression. Treatment with Aβ and to a lesser extent LPS resulted in an increase in GFP expression compared no treatment (Figure 3.2 c).

Figure 3.2. P97 expression in treated cells.
p97 expression in BV-2 cells was upregulated ~6 fold in response to 10μM Aβ compared to no treatment and treatment with other known activators (IFN-γ) of microglia. Treatment with 50 ng/ml LPS resulted in an ~3.5 fold increase in p97 expression. (a-b). In addition, treatment of endothelial cells (bEnd.3), melanoma cells (JB/MS), and fibroblast cells (3T3) with 10 μM Aβ, 50 ng/ml LPS and 5 ng/ml IFN-γ had no effect on p97 expression. This increase in p97 expression was also observed at the protein level in response to 10 μM Aβ and 50 ng/ml LPS (c). S15 mRNA was used as a loading control for RT-PCR and GAPDH for western blot. (a) RT-PCR of p97 expression in BV-2, b.End3, JB/MS and 3T3 cells (b) P97 expression as determined by real-time PCR. Relative gene expression was determined by calculating the cycle threshold (C_T) for p97 as well as for S15. Treated sample thresholds were then compared to non-treated and fold induction of gene expression determined. Error bar represent ± SD for C_T values. (c) Western blot analysis of GFP expression in p1800-GFP transfected BV-2 cells after treatment with Aβ and LPS. All experiments were performed at least three times and data indicated here are representative of all trials.

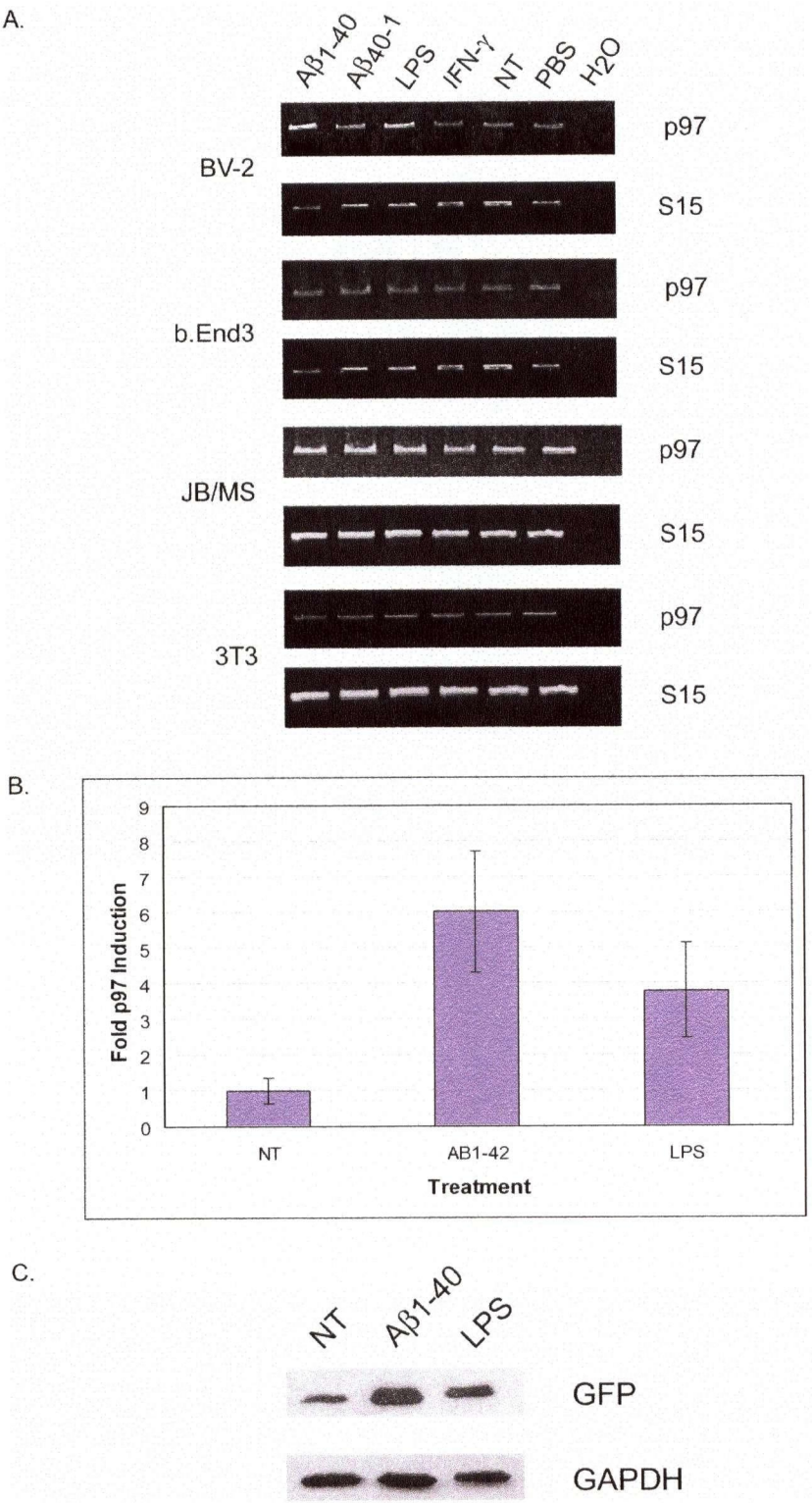
A.
Aβ1-40
Aβ40-1
LPS
IFN-γ
NT
PBS
H2O
BV-2
p97
S15
b.End3
p97
S15
JB/MS
p97
S15
3T3
p97
S15
B.
Fold p97 Induction
0
1
2
3
4
5
6
7
8
9
NT
AB1-42
LPS
Treatment
C.
NT
Aβ1-40
LPS
GFP
GAPDH

3.2.3 P97 expression in Tg2576 AD model mice

Finally, the mRNA expression levels of p97 in different brain regions of Tg2576 AD model mice was examined. Sixteen month old Tg2576 AD model mice, where there is a substantial presence of amyloid plaques and activated microglia, and their control littermates, were perfused with PBS and the brains were dissected into 6 different regions; frontal, hippocampal, occipital, olfactory, parietal, and temporal. The brains were then processed for total RNA extraction and subjected to RT-PCR to assess for p97 expression. Results illustrate that p97 expression is increased in the Tg2576 AD mouse in the brain regions associated with heavy plaque burden and activated microglia such as the temporal cortex and hippocampus (Figure 3.3).

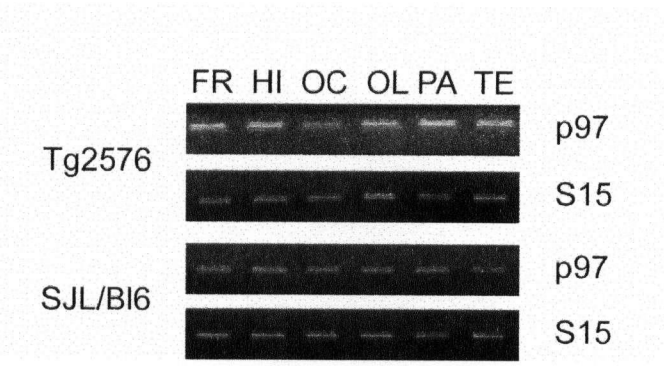

Figure 3.3. p97 expression is increased in affected brain regions in Tg2576 mice. Brains were dissected into 6 regions, RNA extracted and RT-PCR performed for p97 gene expression. Areas of the brain known to have significant amyloid deposition and activated microglia, FR, HI, PA and TE, also have an increase in p97 gene expression. Non-transgenic mice exhibit no change in the expression of p97. There was also no change in S15 mRNA levels in all brain regions in both transgenic and non-transgenic mice. FR-frontal; HI-hippocampal; OC-occipital; OL-olfactory; PA-parietal; TE-temporal. All experiments were performed at least three times and data indicated here are representative of all trials.

3.2.4 MAPK pathways control the expression of p97

To seek further insight in what signal transduction pathway is involved in p97 expression, the promoter region of p97 was studied to identify possible transcription factor binding sites. Within this region there are 3 AP-1 transcription factor binding sites, indicating a possible regulation by MAPK-dependent pathways. Moreover, Rozé-Heusse *et al.* found that increased mRNA levels of Jun/Fos, the transcription factors which constitute AP-1, correlated with mRNA levels of p97 in human melanoma cells [217]. To directly test which MAPK pathway is involved in the expression of p97, p1800-GFP transfected BV-2 cells were stimulated with 10 μM $A\beta_{1-40}$ or 50 ng/ml LPS with and without the addition of selective inhibitors of the p38 MAPK and ERK1/2 pathways. SB203580 (SB) is a selective inhibitor of p38 MAPK and has no effect on ERK1/2 or JNK while PD98059 (PD) is a selective inhibitor of upstream kinases, MEK 1/2, in the ERK pathway.

Cells were incubated with each of the MAPK inhibitors for 30 minutes and then stimulated with either 10 μM $A\beta_{1-40}$ or 50 ng/ml LPS for 6 hours. No treatment and treatment with inhibitor alone were used as controls. GFP protein levels were measured by Western blot. Treatment of p1800-GFP BV-2 cells with the inhibitor of p38MAPK (SB, 20 μM) resulted in a decrease in GFP expression in both Aβ and LPS treated samples (Figure 3.4 a). Treatment with inhibitors to ERK1/2 (PD; 50 μM) had no effect on GFP expression in stimulated cells (Figure 3.4 b). Cells transfected with vector alone, pEGFP-1, showed no change in GFP expression in all cases, but did show a difference in phospho-p38 and phospho-ERK expression upon treatment with Aβ or LPS with and

without respective inhibitors (Figure 3.4 b,d). This suggests that the p97 promoter region is regulated by the p38 MAPK pathway.

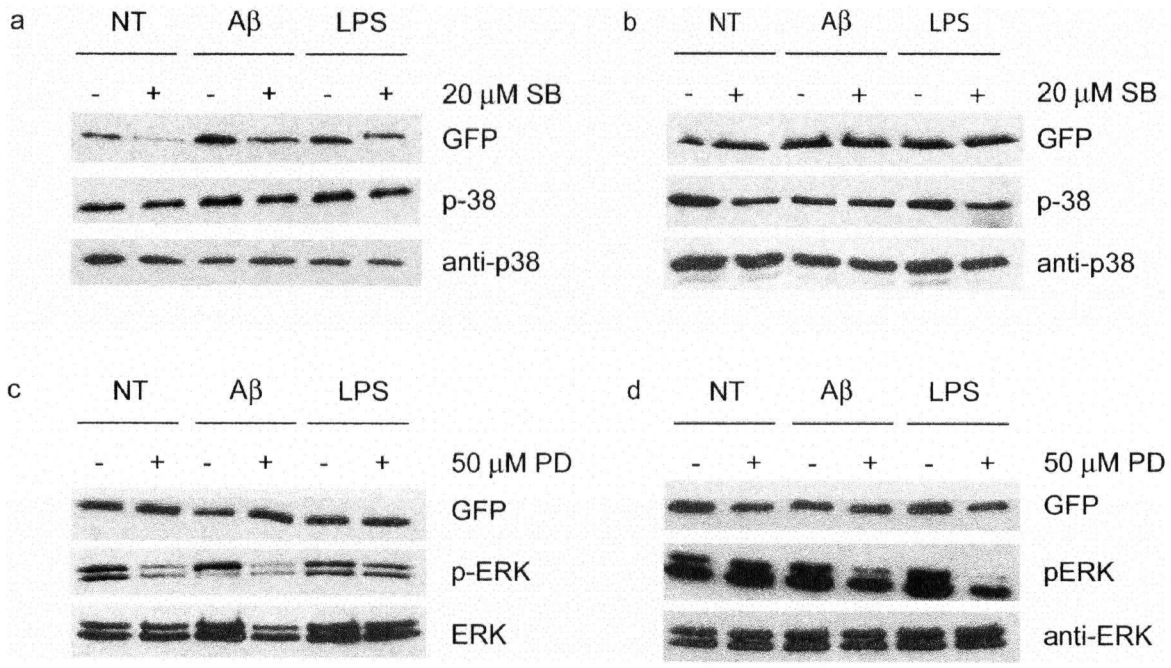

Figure 3.4. The p97 promoter appears to be regulated by the p38 MAPK pathway. BV-2 cells transfected with p1800-GFP were stimulated with 10 μM $A\beta_{1-40}$ and 50 ng/ml LPS as well as with inhibitors for p38 (20 μM) and p-ERK (50 μM) for 6 hours. GFP expression was measured by Western Blots of cell lysates with antibodies against GFP and the activated (phosphorylated) forms of p38 and p-ERK. Levels of extracellular regulated MAPKs were used as loading controls. GFP expression was decreased when treated with Aβ or LPS in conjunction with SB implying that the p38 MAPK pathway controls the regulation of the p97 promoter region. There was no change in GFP levels in cells treated with PD or in cells transfected with an empty vector. (a) GFP expression in p1800-GFP cells treated with p38 MAPK inhibitor, SB, (b) GFP expression in pEGFP-1 cells treated with p38 MAPK inhibitor, SB, (c) GFP expression in p1800-GFP cells treated with ERK1/2 inhibitor, PD and (d) GFP expression in pEGFP-1 cells treated with ERK1/2 inhibitor, PD. Each gel is a representative gel from three separate experiments.

3.2.5 P97 expression in BV-2 cells after treatment with NSAIDs

Next, the expression of p97 in microglia in the presence of NSAIDs, was tested. To assess if NSAID treatment reduced the activation of microglia, TNF-α production was again measured in cells either treated with stimulant alone or stimulant and NSAID. Treatment with two NSAIDs, 10 μM Ibu and 10 μM Nim, appeared to reduce the production of TNF-α from cells treated with both stimulant and drug (Figure 3.5 a-b). When examining the gene expression of p97, it appears that the expression was decreased in cells treated with both Ibu and Nim, where RT-PCR and real-time PCR show that the expression of p97 in NSAID treated cells was reduced close to the levels of non-treated cells (Figure 3.6 a-b and 3.7 a-b). Since previous studies have demonstrated that serum levels of p97 are elevated in AD, protein levels were also examined. Western blot analysis with p1800-GFP transfected BV-2 cells also shows a decrease, similar to the levels of mRNA. GFP levels were also decreased in cells treated with drug compared to treatment with Aβ and LPS alone (Figure 3.6 c and 3.7 c).

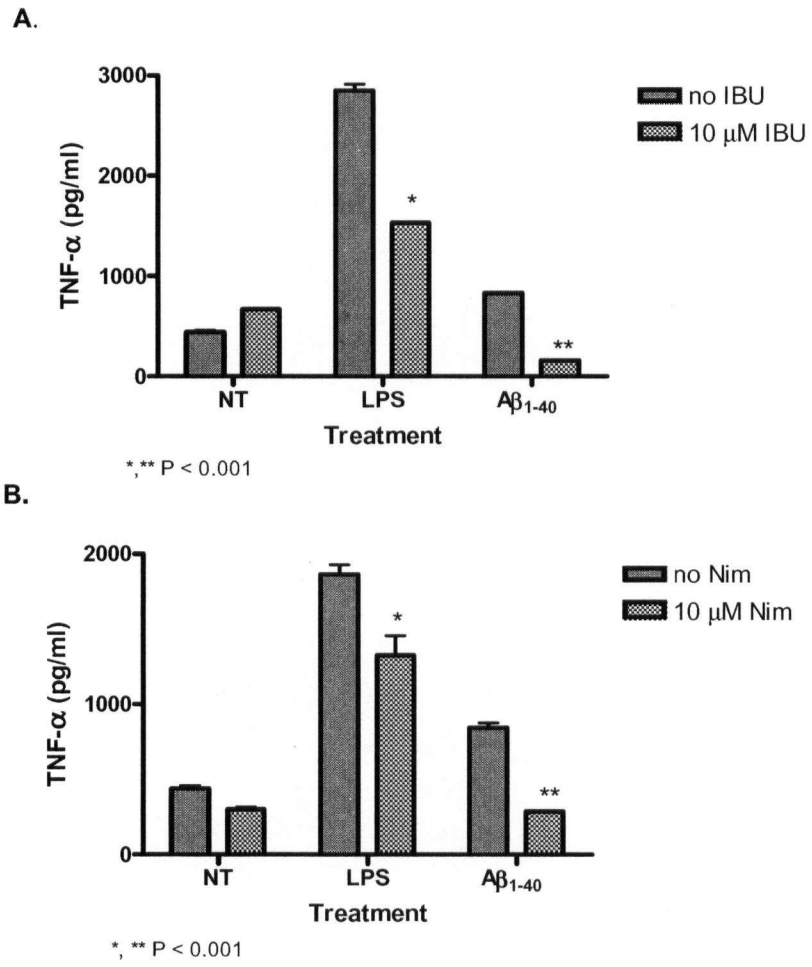

Figure 3.5. NSAID treatment decreased TNF-α production in activated BV-2 cells. Cells were plated at a density of 5 x 10^5 cells/ml and treated for 24 hrs with 10 μM $A\beta_{1-40}$ or 50 ng/ml LPS with or without the addition of 10 μM Ibu or 10 μM Nim. There was a significant decrease in TNF-α production in cells treated with drug compared to treatment with $A\beta_{1-40}$ or LPS alone (ANOVA, *, ** $P < 0.001$). (a) TNF-α production in BV-2 cells after treatment with 10 μM Ibu and (b) TNF-α production in BV-2 cells after treatment with 10 μM Nim. All experiments were performed at least 3 times in triplicate. Error bars represent ± SD. The results illustrated above are representative of all replicates.

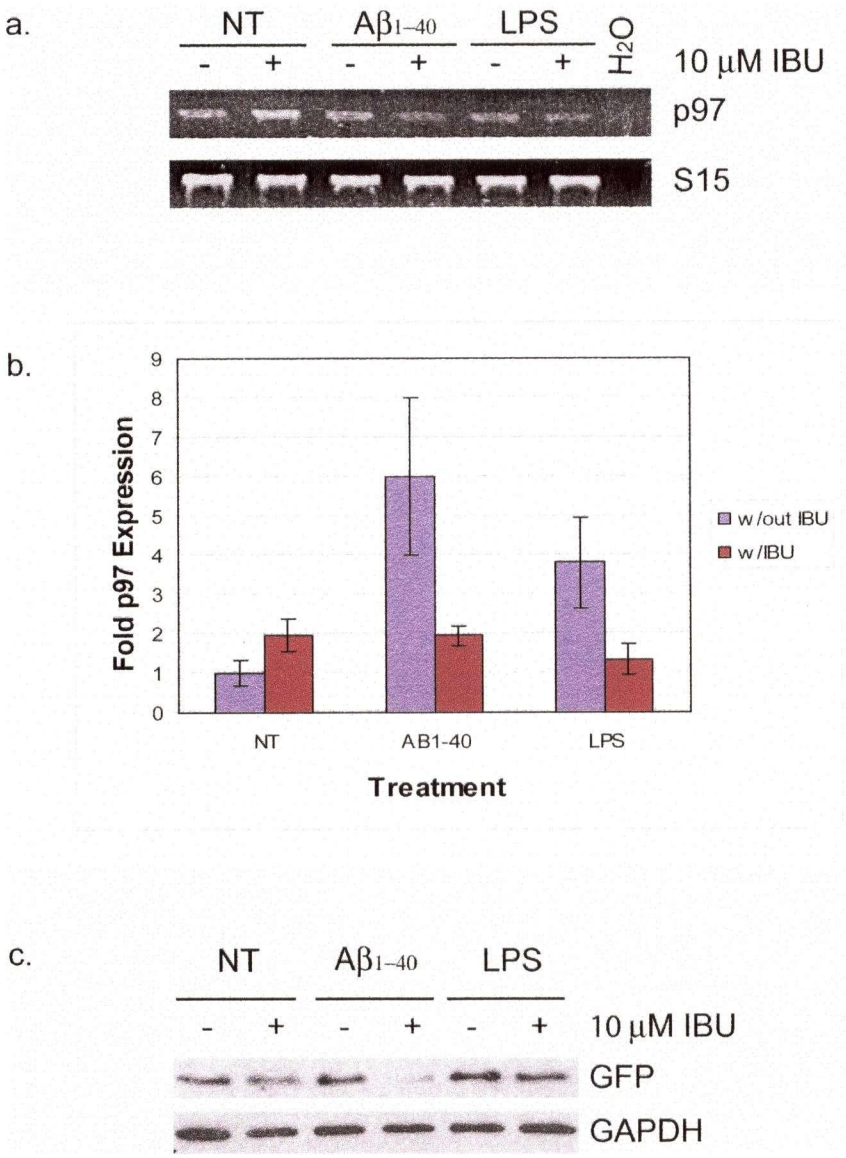

Figure 3.6. p97 expression is decreased in BV-2 cells treated with Ibuprofen.
Cells were plated at a density of 5 x 10^5 cells/ml and treated for 24 hrs with 10 μM $A\beta_{1-40}$ or 50 ng/ml LPS with and without the addition of 10 μm Ibu. There was a significant decrease in p97 expression in cells treated with Aβ or LPS in conjunction with Ibu compared to $A\beta_{1-40}$ and LPS treatment alone. (**a**) RT-PCR of BV-2 cells treated with $A\beta_{1-40}$, LPS and Ibu. (**b**) p97 expression as determined by real-time PCR. Relative gene expression was determined by calculating the cycle threshold (C_T) for p97 as well as for S15. Treated sample thresholds were then compared to non-treated and fold induction of gene expression determined. Error bar represent ± SD for C_T values. (**c**) Western blot of GFP protein levels in p1800-GFP transfected BV-2 cells after treatment with 10 μM $A\beta_{1-40}$ and 50 ng/ml LPS with and without the presence of 10 μM Ibu. The levels of the GAPDH loading control are also shown. All experiments were performed at least three times and data indicated here are representative of all trials.

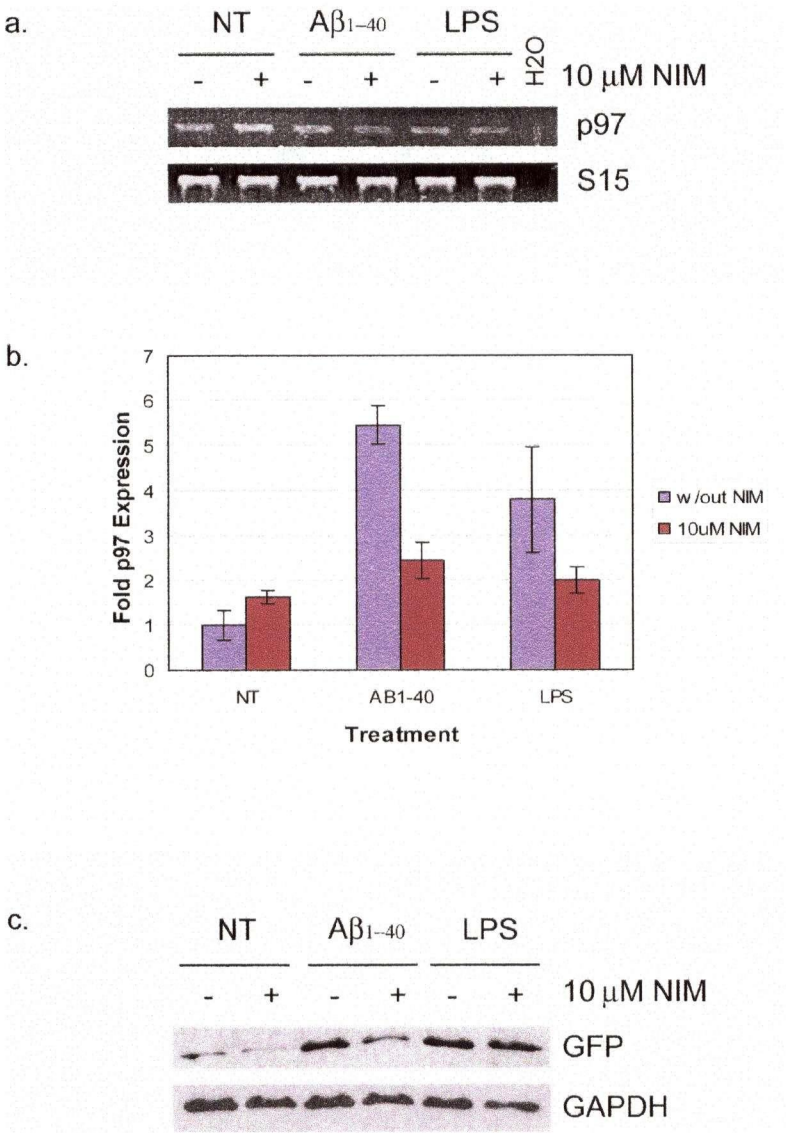

Figure 3.7. p97 expression is decreased in BV-2 cells treated with Nimesulide.
Cells were plated at a density of 5 x 10^5 cells/ml and treated for 24 hrs with 10 μM $A\beta_{1-40}$ or 50 ng/ml LPS with and without the addition of 10 μm Nim. There was a significant decrease in p97 expression in cells treated with Aβ or LPS in conjunction with Nim compared to $A\beta_{1-40}$ and LPS treatment alone. (**a**) RT-PCR of BV-2 cells treated with $A\beta_{1-40}$, LPS and Nim. (**b**) p97 expression as determined by real-time PCR. Relative gene expression was determined by calculating the cycle threshold (C_T) for p97 as well as for S15. Treated sample thresholds were then compared to non-treated and fold induction of gene expression determined. Error bar represent ± SD for C_T values. (**c**) Western blot of GFP protein levels in p1800-GFP transfected BV-2 cells after treatment with 10 μM $A\beta_{1-40}$ and 50 ng/ml LPS with and without the presence of 10 μM Nim. The levels of the GAPDH loading control are also shown. All experiments were performed at least three times and data indicated here are representative of all trials.

3.3 Discussion

In this study, it was demonstrated that fibrillar Aβ significantly promoted the up-regulation of p97 at both the mRNA and protein level in microglia. Furthermore, the signal transduction pathway involving p38 MAPK appears to be important in p97 production by stimulated microglia whereas the pathway involving ERK is not. It was also shown that the expression of p97 can be down-regulated with the use of NSAIDs. There have been a few studies that have proposed that p97 may be a putative biomarker for AD, with an ~4 fold increase in serum levels of p97 in AD patients [208,209,210]. In addition, p97 appears to be expressed in the active microglia closely associated with amyloid plaques in the AD brain [111]. However, there was no direct evidence that microglia upregulate p97 expression as a result of activation. In this regard, the results from this study are very intriguing. Not only is it demonstrated that p97 is upregulated in activated microglia, but the upregulation is largely specific to activation via Aβ, a stress specific to AD. It has been previously established by many groups, that in response to stimulation from molecules such as LPS and IFN-γ, microglia upregluate the expression and secretion of many cytokines and other proteins such as IL-1β, TNF-α and urokinase plasminogen-activator receptor [218,113]. Therefore, it is possible that p97 is one of few proteins whose expression may be regulated by Aβ in AD. It has been shown here by real-time PCR that the expression of p97 increased approximately 6 fold after treatment of microglia with 10 μM fibrillized Aβ. A previous gene expression study [219] using gene array chips supports these results and demonstrated that the expression of p97 increased 2 fold after 24 hrs of treatment with 2.5 μM Aβ.

A number of different parameters of microglial activation in AD have been defined both *in vivo* and *in vitro*. In particular, the phosphorylation of various proteins involved in the MAPK signal transduction pathway, such as p38 and ERK, are increased in activated microglia. The pathways downstream of these proteins share a common transcription factor, AP-1, which has 3 potential binding sites in the promoter region of p97, suggesting a regulatory role for this transcription factor [220]. Further evidence in human melanoma cells support this and show that the RNA levels of Jun and Fos, which make up AP-1, is correlated to the expression of p97 [217]. It is known that in microglia, LPS and Aβ stimulate the MAPK pathways and we have shown that Aβ and LPS treatment cause an increase in p97 expression. The present study also examined the expression of p97 in stimulated cells with and without the addition of p38 and ERK specific inhibitors. Inhibition of the p38 pathway resulted in a decrease of GFP expression in p1800-GFP transfected BV-2 cells. Inhibition of ERK had no effect on GFP expression. Thus, it would appear that the expression of p97 in Aβ and LPS stimulated microglia may be under control of the p38 MAPK signal transduction pathway. Since p97 expression was not completely abolished by SB, it is possible that p97 expression may also be controlled by other mediators or pathways.

The role of inflammation is becoming more evident in AD pathogenesis and it has been recently hypothesized that the neurodegeneration observed in AD is the consequence of an inflammatory response to Aβ and NFTs rather than as a result of these hallmarks [26]. Early epidemiological studies offer support for the role of inflammation in AD and have demonstrated that the use of NSAIDs confers protection against AD and appears to slow down disease progression [102,103]. *In vitro* experiments have shown that

NSAIDs, such as Ibu and indomethacin inhibit the gene expression of nitric oxide synthase in macrophage and decrease cytokine production in neuronal cells [221,222]. In addition, NSAIDs including Ibu, indomethacin and flurbiprophen, have been shown to reduce the amounts of $A\beta_{1-42}$ in human glioma cells by shifting the cleavage of Aβ to its shorter derivatives [223]. In animal models, it has been established that oral administration of Ibu approximately around the time of initial disease pathology, attenuated plaque pathology resulting in the decrease in both the size and number of plaques as well as a decrease in the number of dystrophic neuritis and activated microglia [224]. Moreover, $A\beta_{1-42}$ brain levels and the presence of activated microglia in NSAID treated mice were significantly lowered [225,223]. Conversely, recent clinical trials examining a variety of NSAIDs failed to report any beneficial effects of NSAID treatment. These trials are confounded by their small size and large withdrawal rates [226]. The findings from the many *in vitro*, *in vivo* and clinical studies suggest that the molecular targets of NSAIDs play a key role in the development of brain amyloidosis, however, what the exact targets are remain unclear. It is evident that more clinical trials are needed that focus on determining if anti-inflammatory drugs can delay and/or prevent disease onset. To date, there are no end-point criteria that can be used as a means to assess drug efficacy. Plasma levels of Aβ are not correlated with Aβ brain levels indicating that measuring Aβ plasma levels as an indicator of drug efficacy is inconclusive and erroneous [223]. Here it is shown that the expression of p97, at both the mRNA and protein level, is affected by the presence of Ibu and Nim, potent anti-inflammatory drugs, after 24 hours of treatment. Thus it is possible that p97 may be a potential marker to determine drug efficacy. It is still unclear as to what aspect of inflammation in AD NSAIDs target or if they target

inflammatory cells at all. Mechanistically, it has been shown that the beneficial effects of NSAIDs are a result of the drugs' ability to reduce or attenuate the activity of COX enzymes thereby precluding the synthesis of prostaglandins and thromboxanes from arachidonic acid [26]. There is still much debate as to the pathological role of each of the COX enzymes, COX-1 and COX-2. Alternatively, NSAIDs have been shown to work in a COX independent manner reducing the amounts of $A\beta_{1-42}$ by targeting the γ-secretase complex [227,223]. In this study, the effects of both a non-selective COX inhibitor, Ibu, and a COX-2 specific inhibitor, Nim, were examined. In both instances, p97 expression was decreased. This suggests that p97 expression may be dependent or related to the upregulation of the both the COX-1 and COX-2 enzymes. Both ERK and p38 MAPK pathways have been demonstrated to increase the transcription and to regulate the stabilization COX-2 [228]. In contrast, Ibu has also been shown to reduce $A\beta_{1-42}$ levels with little inhibition of COX enzymes [174,223]. In order to resolve this, treatment with NSAIDs that are COX-1 specific inhibitors and have no effect on the activity of COX enzymes, such as Thalidomide which inhibits TNF-α, needs to be examined. Nonetheless, these data indicate that expression of p97 is upregulated in response to microglia activation and that treatment with NSAIDs causes a down regulation of mRNA expression. Therefore, it is possible that serum levels of p97 may be used in future NSAID clinical trials as a criterion to resolve whether a certain drug is beneficial.

In summary, these data establish that p97 mRNA is upregulated in microglia in response to treatment with Aβ and that the expression of p97 is regulated by the AP-1 transcription factor downstream of the p38 MAPK pathway, which has also been shown to be highly active in microglia. Moreover, the expression of p97 can be modified by

anti-inflammatory drug treatment. It has been previously proposed that p97 may be a plausible biomarker for AD. These studies show that in addition to being a diagnostic biomarker for AD, p97 may be used as an indicator of Aβ specific mediated inflammation/microglial activation. P97 may also be used as an aid in determining the efficacy of new and already established anti-inflammatory therapies for AD.

Chapter 4: The role of microglia in amyloid deposition

4.1 Rationale

Activation of microglia is among the first cellular changes in the injured CNS. In an acute inflammatory response activated microglia produce many beneficial neuro-trophic and neuro-regenerative factors, in addition to pro-inflammatory mediators and potential neurotoxins. This response is short-lived and only the injured neurons are regenerated or removed. Alternatively, in a chronic inflammatory response, neurons are exposed to large amounts of neurotoxins for a prolonged period of time and this exposure ultimately leads to their demise. It has been proposed that microglia bring about the neurodegenerative changes in AD by eliciting an inflammatory response and by contributing to amyloid deposition. However, the decisive role of microglia in the accumulation of Aβ and the subsequent propagation of amyloid plaques remain to be clearly elucidated.

It has been demonstrated in AD, that activated microglia co-localize with and infiltrate amyloid plaques in both humans and APP transgenic mice [116,117,118,90]. Ultra-structural studies by Wisniewski *et al.* have found that plaque associated microglia displayed intracellular channels containing amyloid fibrils [229]. A subsequent study also found Aβ to be present in the secondary lysosomes of macrophage-like cells suggesting that microglia are involved in both the production and phagocytosis of Aβ [230]. Furthermore, microglia may be able to drive the fibrillization of Aβ monomers/oligomers into fibrils and plaques [119,231]. It is also been established that microglia are able to rapidly internalize and degrade microaggregates of Aβ by scavenger receptors or by activation of

complement pathways [60,232,233]. Regardless of the mechanism of internalization, the degradation of amyloid appears to be the main issue in Aβ accumulation. The ultimate fate of phagocytosed Aβ is still unclear. It has been shown that Aβ is degraded by microglia; however, this degradation is slow and can lead to the accumulation of Aβ inside the cell. Therefore, in the case of AD, the overproduction and thus the persistence of Aβ may become too overwhelming for the microglia thereby disrupting the dynamic balance between Aβ deposition and removal. Regardless of the mechanism it would appear that activated microglia contribute to the formation of amyloid plaques.

Many studies have focused on the role of complement in amyloid deposition and have shown that the activation of complement, both the classical and alternative pathways, results in the production of many complement opsonin proteins that bind to Aβ [116,234]. These opsonins promote microglial phagocytosis of Aβ, thereby implying that microglial activation promotes amyloid removal, precluding plaque formation [235]. In a study by Wyss-Coray *et al.* it was found that in mice which overexpress astroglial TGF-β1 and human $APP_{695,751,770}$, there was a 3 fold reduction in the number of Aβ parenchymal plaques and an overall 50% reduction in amyloid burden [236]. These mice also exhibited an increase in complement protein C3 as well as activated microglia suggesting the TGF-β1 promote the degradation of Aβ by microglia via complement activation [236]. Further studies involving the inhibition of C3 activation in AD model mice by expression of the soluble complement receptor-related protein, found that in C3 inhibited mice there were significant increases in amyloid plaque burden, the levels of $Aβ_{1-42}$, and the number of degenerating neurons [237]. Overall, these data suggest that certain inflammatory defense mechanisms are indeed neuroprotective. In contrast, other

studies involving complement C1q deficient hAPP mice showed that the absence of C1q resulted in a decrease in the degree of degenerating neurons compared to C1q sufficient mice, with no difference in amyloid burden [238]. This implies that complement plays a detrimental role in disease pathology.

A better understanding of the mechanisms that regulate amyloid accumulation and degradation may help facilitate the generation of therapeutics that will prevent the accumulation or enhance the degradation of Aβ and ameliorate AD treatments. It is hypothesized that microglia are activated in response to Aβ and phagocytose it removing it from the parenchyma. In time, the activated microglia may become overburdened and unable to remove the amyloid thereby facilitating its aggregation and subsequent plaque formation. This study addresses the role of microglia in plaque deposition using the Osteopetrotic (CSF-1 deficient; op/op) mouse. As a model for osteopetrosis, this mouse has a spontaneous frameshift mutation that results in a complete deficiency of the CSF-1 factor, an important mitogen for brain microglia promoting survival, proliferation and differentiation [182,183]. As a result, these animals possess a reduced number of mature, functioning microglia in their brains [187,186]. In culture, microglia isolated from op/op mice can be restored to full functionality with the addition of CSF-1 [186]. Moreover, daily CSF-1 administration, before BBB formation, can largely restore microglial function [239]. Animal models with a defective microglial response, such as osteopetrosis, provide an approach to explore the many relationships fostered by microglia in the CNS. To explore the course of Aβ plaque development, the op/op mouse was crossed with the Tg2576 AD model mouse to generate an AD mouse with reduced microglial capabilities. This new mouse model will hopefully help resolve the contribution of microglia to AD

pathogenesis. In this study, the role of microglia in amyloid deposition was investigated. In accordance with previous data on complement and amyloid pathology, it is hypothesized that in AD mice with reduced microglial function, there will be an increase in amyloid burden in the brain.

4.2 Results

4.2.1 Characterization of Tg/+;op/op mice

Tg2576;CSF-1 deficient (Tg/+;op/op) mice were generated by initially crossing Tg2576 (Tg/+;+/+) mice by CSF-1 deficient (+/+;op/op) mice. The F_1 generation of these mice (Tg/+;op/+) were crossed to get Tg/+;op/op mice. To distinguish between Tg/+ mice and wild-type (+/+;+/+), all mice were genotyped for the hAPP transgene (Figure 4.1). +/+;op/op mice were distinguished from +/+;+/+ mice by the absence of incisors and a domed skull 10 days after birth. Tg/+;op/op and +/+;op/op mice were separated from Tg/+;+/+ and +/+;+/+ mice and fed on wet chow. Tg/+;op/op mice were significantly smaller than their control littermates (Figure 4.2). Mouse growth and body weight was followed for a 3 month period. At 3 months, op/op mice were approximately 33% smaller from +/+ littermates. Body weight was also evaluated at 6 and 9 months of age at time of sacrifice. As depicted in Figure 4.2, Tg/+;op/op mice had a significantly lower body weight that control mice.

In accordance with the phenotype of the op/op mice, Tg/+;op/op mice appeared to be infertile. In addition, the viability of the Tg/+;op/op mice was reduced, as many mice died before the 9 month time point. The average life span of the op/op mouse is reported

to be 7 months of age (Jackson Laboratories); however, we have maintained this mouse for periods exceeding 12 months.

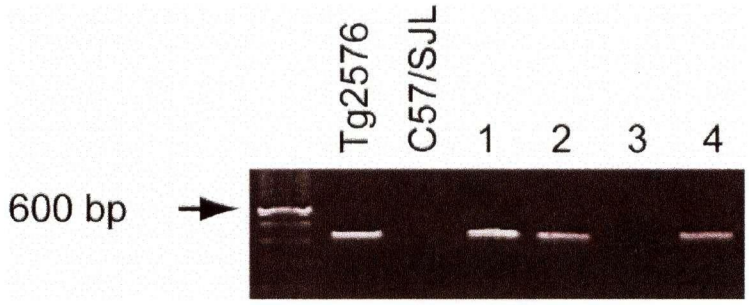

Figure 4.1. PCR genotyping of Tg2576 AD model mice.
Tg2576 hAPP transgenic mice and littermate controls were genotyped from ear punch DNA by PCR as previously described. The PCR products were analyzed on a 1% agarose gel and visualized. Tg2576 mice amplify a single 420 base pair (bp) product while control mice do not amplify any product. Each PCR was performed twice. Lane 1, Tg2576 founder control; Lane 2, C57/SJL non-transgenic control; Lane 3-6 genotyped mice. The gel shown is representative of all PCR reactions.

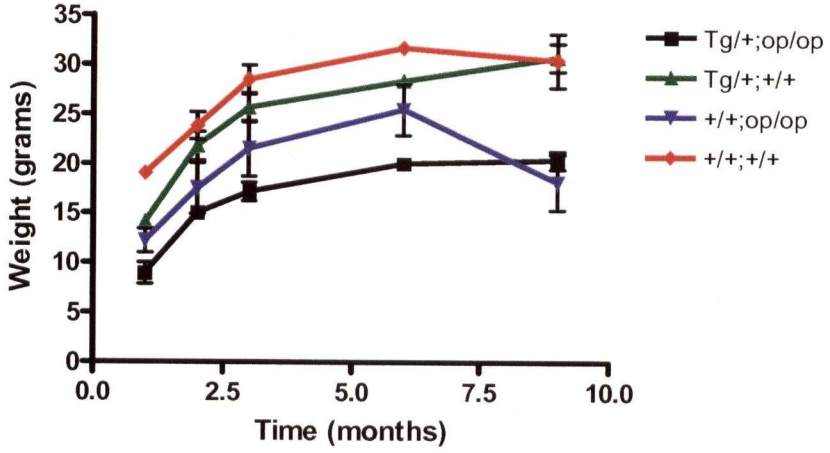

Figure 4.2. Tg/+;op/op mice are smaller than control littermates.
Mice were weighed beginning at one month of age until 9 months of age. Tg/+;op/op were significantly smaller than control littermates ;Tg/+;+/+ and +/+;+/+ at every age ($P < 0.01$, two-way ANOVA followed by Bonferroni analysis). Tg/+;op/op mice were smaller than +/+;op/op mice at all time points, however the difference was not significant ($P > 0.05$; two-way ANOVA followed by Bonferroni analysis).

4.2.2 Amyloid burden in Tg/+;op/op mice

Amyloid plaques are first seen in Tg2576 mice at approximately 9 months of age, therefore this time point was used to evaluate plaque burden. In addition, Tg/+;op/op mice have a high mortality and generally die at 10 months of age. At 9 months of age, Tg/+;op/op mice exhibited similar amounts of Aβ immunostaining as Tg/+;+/+ mice (Figure 4.3 a-c. $P = 0.1$; t-test). There was no presence of Aβ in +/+;op/op and +/+;+/+ mice (Figure 4.3 d and e). At 6 months and 3 months there was no Aβ immunostaining present in all animal brains. Interestingly, there appeared to be Aβ deposition in cerebral blood vessels of Tg/+;op/op mice compared to Tg/+;+/+ mice (Figure 4.4). Therefore, it is possible that the absence of microglia increases vascular angiopathy.

Figure 4.3. Amyloid plaque burden in 9 month Tg/+;op/op mice compared to controls. Amyloid plaques in cortical sections from mice were visualized with an anti-human Aβ antibody. There was no significant difference in the total number of Aβ plaques in Tg/+;op/op mice compared to Tg/+;+/+ controls. There was no detection of Aβ plaques in +/+;op/op and +/+;+/+ mice (a) Quantitative assessment of plaque burden in Tg/+;op/op mice and Tg/+;+/+ mice, T-test; $P \doteq 0.1$. Qualitative assessment of Aβ in (b) Tg/+;op/op mice, (c) Tg/+;+/+ mice, (d) +/+;op/op mice, and (e) +/+;+/+ mice. Brain sections shown are representative of their respective groups (n=3 for Tg/+;op/op, n=4 for Tg/+;+/+, +/+;op/op and +/+;+/+).

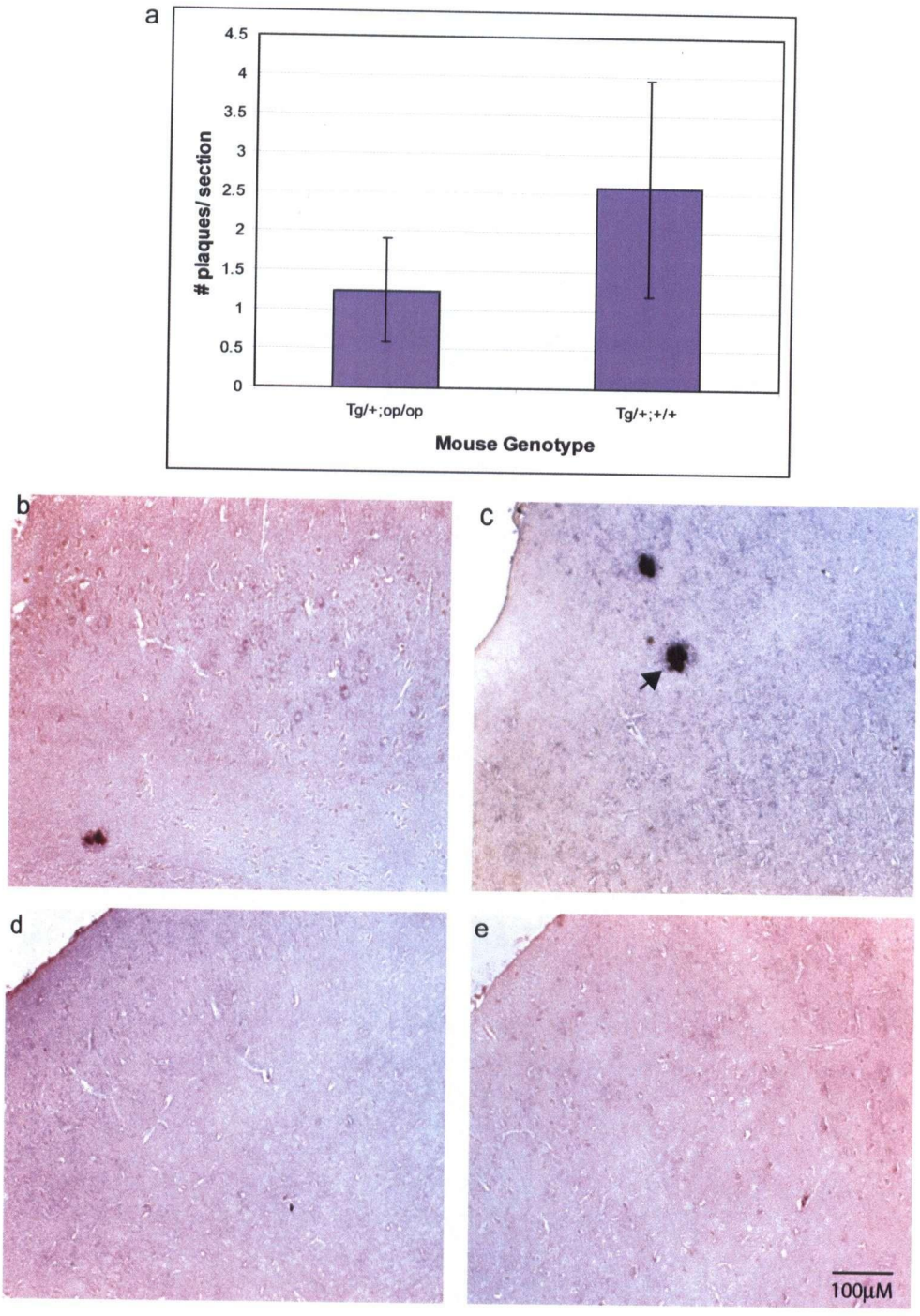
a
4.5
4
3.5
3
2.5
2
1.5
1
0.5
0
plaques/ section
Tg/+;op/op
Tg/+;+/+
Mouse Genotype
b
c
d
e
100µM

Figure 4.4. Amyloid accumulation in cerebral blood vessels of Tg/+;op/op mice. Amyloid accumulation in cerebral blood vessels (thin arrow) in the brains of Tg/+;op/op mice compared to Tg/+;+/+ controls as visualized with an anti-human Aβ antibody. (**a**) Tg/+;op/op mice (**b**) Tg/+;+/+ mice. Brain sections shown are representative of their respective groups (n=3 for Tg/+;op/op, n=4 for Tg/+;+/+).

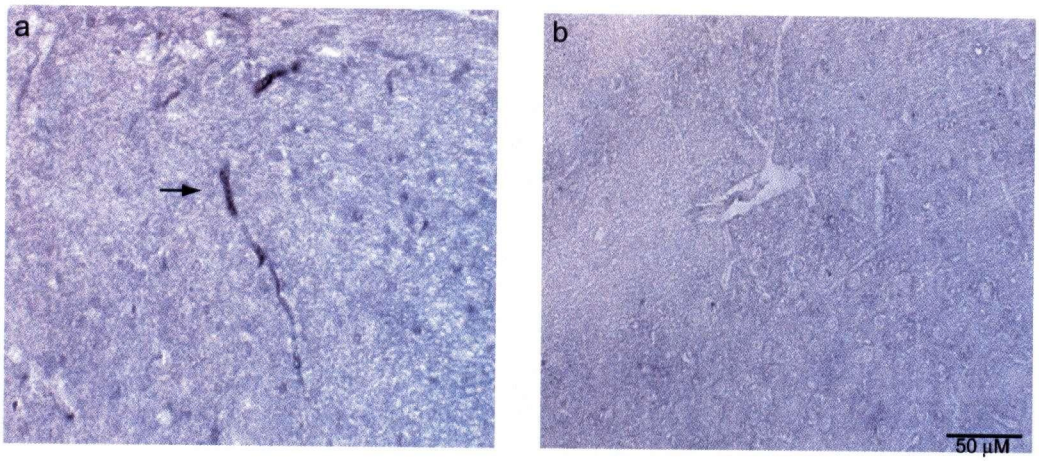
a
b
50 µM

4.2.3 Microgliosis in Tg/+;op/op mice

Many studies examining the number and morphology of microglia in op/op mice are controversial [183,186,187,240]. This study demonstrates that there is a decrease in the number of activated microglia in the Tg/+;op/op mice compared to the Tg/+;+/+ mice. In addition, the majority of the microglia in the Tg/+;op/op mice exhibited a resting morphology with small cell bodies and thin ramified processes whereas the microglia in the Tg/+ mice had a more activated morphology with more condensed cell bodies and thicker processes (Figure 4.5). These results are supported by previous studies indicating a reduced number and altered morphology of microglia in the op/op mouse [187].

Figure 4.5. Reduced number and altered morphology of microglia in Tg/+;op/op mice. Brain sections were stained with F4/80 to reveal the presence of microglia. Tg/+;op/op mice exhibited an overall decrease in the number of microglia than Tg/+;+/+ mice and fewer activated microglia than Tg/+;+/+ mice. +/+;op/op mice and +/+;+/+ mice exhibited resting microglia, with +/+;op/op mice having a reduced number if cells. Activated microglia can be distinguished from resting microglia by the presence of ramified processes and condensed cell bodies (black arrow) compared to small cell bodies and thin ramified processes (white arrow). Control littermates exhibited no microgliosis (a) Tg/+;op/op mice, (b) Tg/+;+/+ mice; (c) +/+;op/op mice, and (d) +/+;+/+ mice. Brain sections shown are representative of their respective groups (n=3 for Tg/+;op/op, n=4 for Tg/+;+/+, +/+;op/op and +/+;+/+).

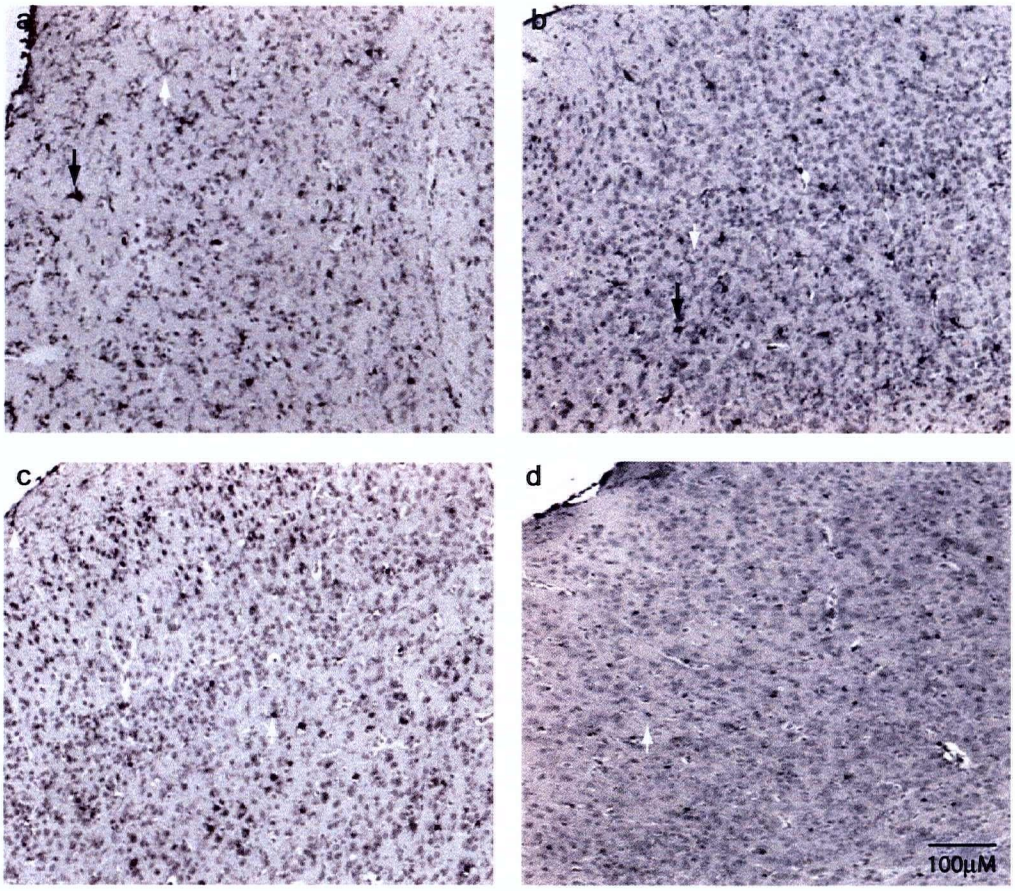
a
b
c
d
100µM

4.3 Discussion

It has been hypothesized that microglia play an integral role in the formation of amyloid plaques and results from many *in vitro* and *in vivo* studies support this premise. These previous studies established that activated microglia are attracted to and surround amyloid plaques [116,117,118,90]. However, whether microglia promote plaque formation by converting monomeric/oligomeric Aβ to fibrillized Aβ or whether microglia prevent Aβ deposition by complement mediated phagocytosis *in vivo* remains unresolved. The present study uses a CSF-1 deficient hAPP transgenic model to assess the implication of activated microglia in AD pathogenesis. Tg2576 were bred with mice deficient for CSF-1 and hence lacked mature, differentiated microglia. The results obtained here indicated that the Tg/+;op/op mouse was smaller in weight than control littermates and had a higher mortality rate. This was in accordance with previous studies on op/op mice, which found that op/op mice were smaller than +/op and +/+ littermates, had a decreased life-span and poor reproductive performance [188,182]. In this study, the oldest age group was 9 months of age, the age of initial plaque formation in the Tg2576 AD mouse. Older age groups were not examined due to the fact that no Tg/+;op/op mice survived past 10 months of age.

The amount of plaque pathology has been investigated in many mouse models of AD. In the mouse model created in this study, levels of fibrillar Aβ in Tg/+;op/op mice appeared to accumulate at rates comparable to Tg/+;+/+ mice since there was no significant difference in plaque burden in the cortices of 9 month old mice. No plaques were observed in the brains of 6 month old animals. It was also observed that there was more Aβ accumulated in the cerebral blood vessels of the Tg/+;op/op mice than in the

Tg/+;+/+ mice. With the high incidence of CAA in AD such deposits are likely to be found. Since there were few Tg/+;op/op mice in the study, it was difficult to clearly determine a difference in plaque deposition as well as establish an explanation in the shift of Aβ deposition patterns. It is possible that with a decrease in the amount of activated microglia in the brains of these animals, other cells, such as astrocytes and pericytes, compensated and upregulated the production of certain cytokines and other important factors. For instance, TGF-β, a known immunosuppressive cytokine, is upregulated in AD and has been implicated in AD in astrocytosis, microglial activation, and accumulation and regional distribution of Aβ [26]. Recently, TGF-β1 was implicated as an inducer of vascular amyloid deposition [236,241]. In addition, Lesne *et al.* demonstrated that TGF-β1 potentiated Aβ production in human astrocytes and, as a result, may enhance the formation of amyloid deposits [242]. However, the role of TGF-β, beneficial or detrimental, in the CNS is still unresolved. It is also feasible that with the functional deficiency of microglia in the op/op mouse the number or proportions of factors produced by activated microglia is skewed. This, in turn, may be amplifying certain pathological changes such as amyloidogenesis and amyloid accumulation in the blood vessels. A more detailed analysis on brain Aβ levels and vascular Aβ levels is required in order to determine if there is indeed a shift towards vascular amyloid deposition and what cellular and molecular processes are involved.

There is still great controversy as to the state of microglia in the op/op mouse. Initial studies by Blevins and Fedoroff found that microglia were not affected by the mutation in CSF-1, in that they have normal morphology and are present at normal frequency [186]. They did find that the microglia isolated from op/op mice needed CSF-1 in

order to differentiate and proliferate in culture, implying a possible deficiency in function [186]. Other studies established that there was indeed a reduction in the number of microglia in the brains of op/op mice; 47% in the corpus callosum, 37% in the parietal cortex and 34% in the parietal cortex compared to +/+ and +/op controls [243,244,187]. Morphological differences, such as, smaller size and shorter cytoplasmic processes were also found and limited to the frontal cortex. [187]. There have also been some studies focused on the response of microglia to acute CNS injury in the op/op mouse. In the facial motor nucleus paradigm, there was a lack of cell proliferation, mobilization and change in morphology in op/op mice compared to controls [245]. Microglia in the op/op mouse responded to neuronal signals but there was a decrease in neuronal regeneration due to the lack of proliferation and mobilization. Further studies examining the role of microglial mediated neurodegeneration found similar results. Here, endotoxins were injected directly into the brains of animals and microglial activation and neuronal degeneration were assessed. It was found that microglia in the op/op mouse have normal activated morphological phenotype, however, only 30-40% of activated microglia were observed in the brains of op/op mice compared to controls [240]. Moreover, levels of TNF-α were increased in response to injury [246] and were at par with the amount of activated cells with op/op mice having 48% of levels to that of controls [240]. In regards to neurodegeneration, it appears that microglia in the op/op mice were able to promote neurotoxicity potentially by TNF-α mediated expression of IL-1β, IL-6 and other pro-inflammatory cytokines [246,240]. Therefore, it is now evident that the microglia in op/op mice are deficient in their proliferative ability but are able to elicit neurodegeneration and removal of debris. It should be noted that all the aforementioned experiments focused on

acute CNS injury. The response of microglia in op/op mice in chronic inflammatory reactions is not well documented. This is where the experiment outlined in this study is unique.

From the data presented in the literature one can speculate that, with respect to the CSF-1 deficient hAPP, there may be more Aβ deposition at a later age due to the inability of microglia to proliferate. The microglia present in the brain may be able to accommodate and degrade accumulated Aβ at the initial stages of the disease, but as the amount of Aβ increases there is not enough activated microglia to remove it. This also is in agreement with the complement experiments by Wyss-Coray *et al.* where inhibition of complement (which results from microglial activation) results in an increase in plaque development [237]. With fewer cells able to express complement proteins and activate complement pathways there may be a reduction in the effective removal of Aβ. According to the "microglial dysfunction" hypothesis [109], one can also anticipate an accelerated accumulation of Aβ since with age it is thought that microglia become senescent and/or dysfunctional therefore their ability to support neurons and to act as phagocytic macrophage would be diminished. With fewer microglia present in the brain, the degree of senescence would be greater in Tg/+;op/op mice than Tg/+;+/+ mice perhaps hastening AD pathology. Moreover, the extent of neurodegeneration, like Aβ deposition, may start at the same rate in Tg/+;op/op and Tg/+;+/+ mice. The Aβ deposition may then accelerate in Tg/+;op/op mice due to the increase in amyloid and its toxic effects on neurons, as well as, the presence of microglial neurotoxins. Also, it is possible that microglia in op/op mice have a diminished ability to undergo phagocytosis and support neuronal survival due to the lack of CSF-1 which may result in an alteration

in the expression and response of many cytokines and other neurotrophic factors that microglia provide to the CNS.

The number and ages of mice used in this study were limited due to the high mortality of the Tg/+;op/op mouse. It is possible that with a larger subject cohort and/or at later age, there could be differences in plaque burden between the different mice. Moreover, differences in other pathological hallmarks of AD, such as neurodegeneration, may be evident at later ages. In a study by Fonseca *et al.*, C1q deficient hAPP transgenic mice had similar plaque burden to hAPP mice at 9 and 16 months of age where older C1q deficient hAPP mice exhibited less neuropathology than controls. [238]. Studies by Wyss-Coray *et al.* on TGF-β1 overexpression hAPP mice and on C3 inhibited hAPP mice, demonstrated brain pathology at 10-12 months of age after significant plaque deposition occurs [236,237]. In addition, the hAPP mice used in these studies express mutated $hAPP_{695,751,770}$ under control of the platelet derived growth factor β chain promoter and develop plaques at approximately 6 months of age [247]. Therefore, since the op/op mouse has a shortened life span it would be beneficial to use an AD mouse that develops significant Aβ deposition prior to 9 months of age to evaluate the relationship between microglial activation and plaque formation.

Many studies have demonstrated that genetic background regulates the extent of APP processing, Aβ deposition and mouse mortality. Initial attempts by Hsiao *et al.* to create transgenic mice failed in part due to host strain effect on transgene expression [84]. These mice were generated in the FVB/N inbred strain. The second attempt utilized a C57BL/6 x C57B6/SJL hybrid proved more successful and is the basis for the Tg2576 AD transgenics used in this study. These mice also had some initial complicating factors.

The life span of the Tg2576 mouse on the inbred C57BL/6 background is approximately 6 months whereas on a mixed background of C57BL/6;SJL mice can survive for over 2 years (Younkin, personal communication). Gene dosage also has an effect on mouse mortality. For example, the Tg2576 AD mouse exists only as a hemizygote and is lethal in a homozygous state. It is possible that the Tg/+;op/op generated in this study contained more of the C57BL/6 background which impacted its life span, since very few of these mice survived past 9 months of age. Recently studies on APP proteolysis, Aβ metabolism and Aβ deposition in transgenic mice have demonstrated that these processes are regulated by genetic background [248]. The C57BL/6 background exhibits greater plaque burden, earlier age of Aβ deposition, and increased levels of brain and plasma levels of $A\beta_{1-40}$ and $A\beta_{1-42}$, compared to DBA/2J and 129S1/SvImJ strains [248]. These results suggest that certain gene alleles in some mouse strains, such as C57BL/6, are dominant over alleles present in other strains, such as DBA/2J, and alter Aβ-related pathologies in AD. As a consequence of host effects, most transgenic mice used in AD research have hybrid backgrounds.

The diversity of the response seen from this study and many others examining microglia and their induction of inflammatory and complement pathways, indicates the complexity of microglial responses and the multiplicity of microglial activation states in AD. A considerable amount of investigation is required and necessary to elucidate these interactions.

Chapter 5: Aβ immunization and the blood-brain barrier

5.1 Rationale

Conflicting with the concept that $A\beta_{1-40}$ and $A\beta_{1-42}$ are cytotoxic are noteworthy advances in recent AD research which advocated the use of peripherally administered Aβ peptides as a vaccine in an effort to reduce senile plaque loads of AD model mice [179,178]. While the exact relationship between Aβ production and deposition and its role in AD neurodegeneration remains unclear, one cannot dispute that treatments aimed at reducing the amyloid burden have resulted in reduction in senile plaques and behavioral benefits. Recent vaccination studies aimed at reducing the burden of all Aβ types in the brain have proven successful in transgenic mice. The first of such studies by Schenk *et al.* injected fibrillar $A\beta_{1-42}$ into six week old PDAPP mice, prior to AD symptom onset, and in 11 month old PDAPP mice, after noticeable Aβ deposition has occurred in the brain [175,249]. After eleven months, mice which had been vaccinated since they were six weeks old showed an almost total absence of amyloid plaques, and a reduced amount of dystrophic neuritis, astrogliosis and microgliosis in the brain compared to PBS injected controls. After five months, mice which had been vaccinated since they were 11 months old showed a significant decrease in plaque burden and in the amount of diffuse Aβ, as well as a reduction in dystrophic neuritis and astro- and microgliosis [175]. Many other immunization studies, utilizing both active and passive immunization protocols, have been performed in the same and different AD model mice and have found similar results in regard to the pathological features of AD [177,250,251]. On the other hand, some studies in different AD mouse models have found that immunization had little effect on plaque

burden if dense plaques were pre-existing [252]. Studies focused on memory impairment have found that immunization with Aβ or passive transfer of antibodies against Aβ protected mice from learning and age-related memory deficits behavioral impairment [178,179] as well as in a significantly delay the onset of memory deficits [253,254]. Recently, it was determined that Aβ immunotherapy can clear early Tau pathology but not late hyperphosphorylated Tau aggregates [181]. With the success of amyloid immunization in mice, clinical trails in humans were undertaken. These trials were halted when approximately 5% of the test subjects showed signs of inflammation of the CNS, clinically described as aseptic meningoencephalitis [255,256]. Subsequent studies in APP23 mice found the same results as in the human trials. In these mice Aβ immunization did reduce plaque burden, as in other studies; however, there was also an increase in cerebral microhemorrhages associated with amyloid-laden vessels [257].

Regardless of the early success in animals, it remains unclear how peripheral immunization can affect plaque burden in 'immunoprivileged' tissues such as the brain that possess vasculature that limit immune surveillance. This vasculature, also known as the BBB, is formed by a continuous layer of capillary endothelium joined by tight junctions that are generally impermeable, except by active transport, to most large molecules including antibodies and other proteins. With this in mind, three possible mechanisms have been proposed to explain the effects of vaccination in AD. The first suggests that the antibodies against Aβ, normally excluded from the CNS, enter the brain by an obscure mechanism involving receptor mediated transport and then proceed to bind to Aβ. Entry into the brain may be facilitated by binding of the antibody to Aβ in the periphery creating an Aβ-antibody complex which is then transported in the brain via

receptor mediated transcytosis by receptors that recognize Aβ [258]. The Aβ-antibody complex is then degraded by the microglia via Fc receptor (FcR) mediated phagocytosis [259,176,260,261]. However, when fragments of antibodies were administered there was reduction in Aβ load in the brain [262,263]. This indicates that non-FcR mediated clearance of Aβ is also occurring. A second possible mechanism suggests that antibodies against Aβ are actively transported into the brain, again by an unknown mechanism, and bind directly to Aβ fibrils resulting in plaque disaggregation. In this instance, the antibodies sequester the Aβ and prevent further fibril/plaque formation [261]. Finally, it is also postulated that there is an equilibrium formed by active transport of Aβ into and out of the brain by receptor mediated transcytosis and by antibodies against Aβ, binding Aβ in the periphery removing it from circulation. This then causes a shift in the equilibrium between Aβ in the plasma and CNS, resulting in a suppression of Aβ deposition in the brain [177,264,265,266]. Studies involving intravenous administration of Aβ specific antibodies demonstrated an efflux of Aβ from the brain to the plasma [264]. In addition, administration of a ^{125}I-Aβ-antibody complex into the periphery inhibited the movement of ^{125}I-Aβ into the brain [266].

The permeability of the BBB to Aβ peptides and antibodies to Aβ is addressed in this study. In addition, the effect of Aβ immunization on the integrity of the BBB is also examined. It is hypothesized that, as with previous immunization studies where there was a reversal of pathology, amyloid immunization will restore BBB integrity in Tg2576 mice. These results will aid in further substantiating this form of therapy in AD research and will also serve as a means to explain the mechanism by which immunization reverses plaque pathology.

5.2 Results

5.2.1 Aβ peptide and anti-Aβ antibodies and their ability to cross the BBB

To investigate the possible mechanisms involved in Aβ vaccination, the ability of both the $A\beta_{1-40}$ peptide and antibodies against Aβ to cross from the periphery into the brain was examined. First, fluorescent labeled $A\beta_{1-40}$ or PBS were injected i.v. into 6 week Tg2576 mice and control littermates. The fluorescent Aβ was detected in the brain parenchyma of both groups of animals (Figure 5.1 a-d). Since it has been previously shown that Aβ can gain entry into the brain via receptor mediated transcytosis, this data also supports this hypothesis. Other studies focused on the movement of Aβ into the brain support these results. Yan *et al.* found that the endothelial cells which make up the BBB express the RAGE receptor [68]. This receptor has been shown to bind to Aβ with high affinity and transport Aβ into the brain. As a control for BBB permeability, BSA, a protein known not to be able to cross the BBB, was conjugated to Texas Red and injected into mice. As seen in Figure 5.1 (e and f), the BSA was primarily localized in the vessels indicating an intact BBB; however, there is some BSA found in the brain parenchyma of transgenic mice. The presence of BSA in the brain may be an indicator of the beginning of stages of increased BBB permeability in the Tg2576 mouse. Next an anti-human Aβ antibody, clone 4G8, was injected into 6 week old transgenic and non-transgenic mice. In contrast to the Aβ peptide, there was no presence of anti-Aβ antibodies in the brain parenchyma (Figure 5.2 a-d). This experiment was repeated using a biotin-labeled anti-Aβ antibody. In this instance either the labeled antibody or biotin alone was injected. As with the above experiment, biotin conjugated anti-Aβ antibodies were only present in the

vessels and not in brain parenchyma (Figure 5.2 e-h). This would indicate that anti-Aβ antibodies cannot gain access to the brain from the periphery. However, recent studies using iodinated antibodies against Aβ indicated that antibodies can cross the BBB but with very low efficiency [258]. In the study by Poduslo *et al.* the mice used were significantly older than the ones used here [258] and it has been established that the BBB in Tg2576 AD model mice is compromised by 4 months of age [149]. Thus at 6 weeks of age, there is little damage to the BBB and it is possible that antibodies cannot gain access to the brain.

Figure 5.1. Aβ peptides can cross the BBB in both transgenic and wild-type mice. Fluorescent labeled $A\beta_{1-40}$ was injected i.v. into 6 week old transgenic and control littermates. Aβ was able to cross the BBB and enter the brain parenchyma in both transgenic and non-transgenic mice thereby suggesting a receptor mediated transport across the BBB. (a) cortical section of a Tg2576 mouse injected with Aβ, (b) cortical section of a control littermate injected with Aβ, (c) cortical section of a Tg2576 mouse injected with PBS control and (d) cortical section of a control littermate injected with PBS. As a control for BBB integrity, Texas red conjugated BSA was injected into both mice. As seen in (e) Tg2576 mouse and (f) non transgenic littermate, the BBB is relatively intact. There appears to be a small amount of BSA in the brain parenchyma of the transgenic mouse indicating the beginning of the BBB breakdown. *, brain parenchyma with Aβ peptide, arrow, brain vasculature.

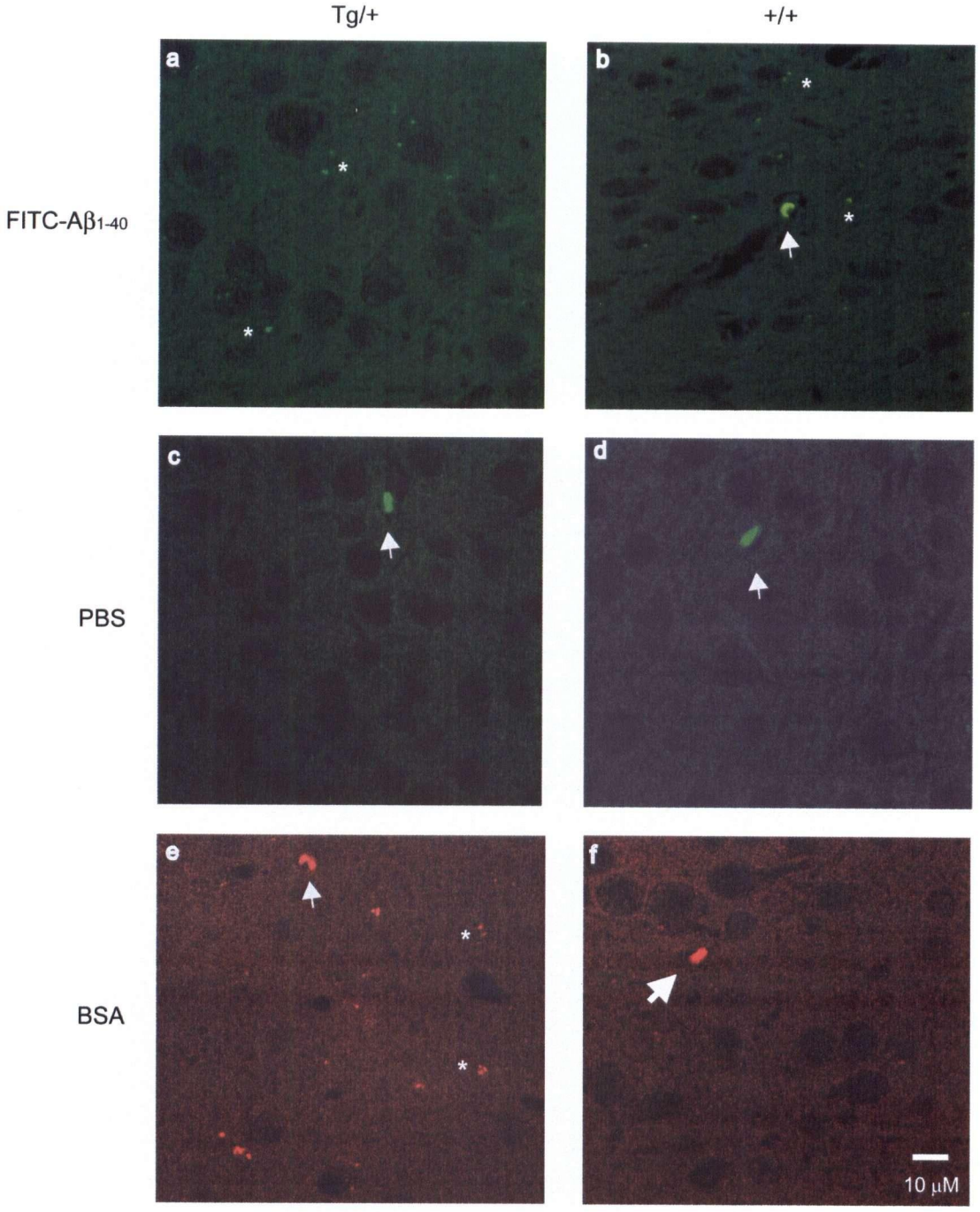
Tg/+
+/+
FITC-Aβ1-40
PBS
BSA
a
b
c
d
e
f
10 μM

Figure 5.2. anti-Aβ antibodies cannot cross the BBB in both transgenic and wild-type mice. Anti-Aβ antibodies, clone 4G8 against human $A\beta_{1-42}$, were injected i.v. into 6 week old transgenic and control littermates. Both unlabeled antibodies (visualized by immunofluorescence) and biotin labeled antibodies (visualized by light microscopy) were used. In both cases anti-Aβ antibodies were localized to the vasculature (white and black arrows) and were unable to cross the BBB and access the brain in both Tg2576 and control littermates. (a) cortical section of a Tg2576 mouse injected with anti-Aβ antibodies, (b) cortical section of a control littermate injected with anti-Aβ antibodies, (c) cortical section of a Tg2576 mouse injected with PBS control and (d) cortical section of a control littermate injected with PBS. (e) cortical section of a Tg2576 mouse injected with biotin labeled anti-Aβ antibodies, (f) cortical section of a control littermate injected with biotin labeled anti-Aβ antibodies , (g) cortical section of a Tg2576 mouse injected with biotin (control) and (h) cortical section of a control littermate injected with biotin (control).

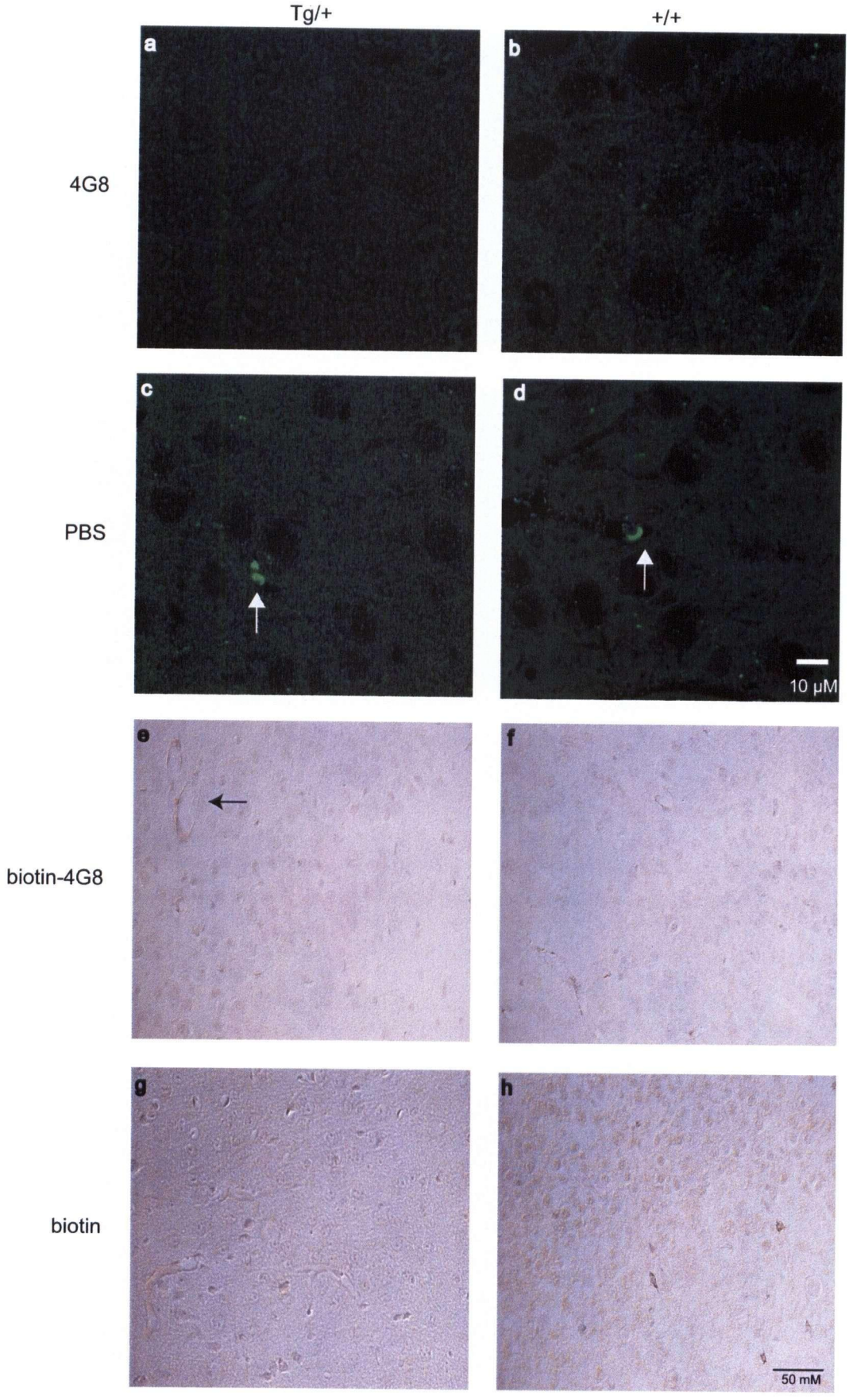
Tg/+
+/+
4G8
PBS
biotin-4G8
biotin
a
b
c
d
e
f
g
h
10 μM
50 mM

5.2.2 Anti-Aβ antibody titres in immunized animals

To assess the immune response of the mice to immunization with Aβ, antibody titres for antibodies against Aβ were measured. Serological analysis of serum samples collected from transgenic and non-transgenic mice vaccinated with Aβ and PBS were analyzed for the titres of anti-Aβ antibodies by ELISA using synthetic $A\beta_{1-40}$ peptide. Serum samples from mice in all groups were collected after the second injection and results indicated that transgenic and non-transgenic mice vaccinated with Aβ produced a high IgG response to $A\beta_{1-40}$. No detectable antibodies were detected in transgenic and non-transgenic mice vaccinated with PBS (Figure 5.3). Mice vaccinated with Aβ, which did not exhibit high anti-Aβ antibody titres, were not used in the study.

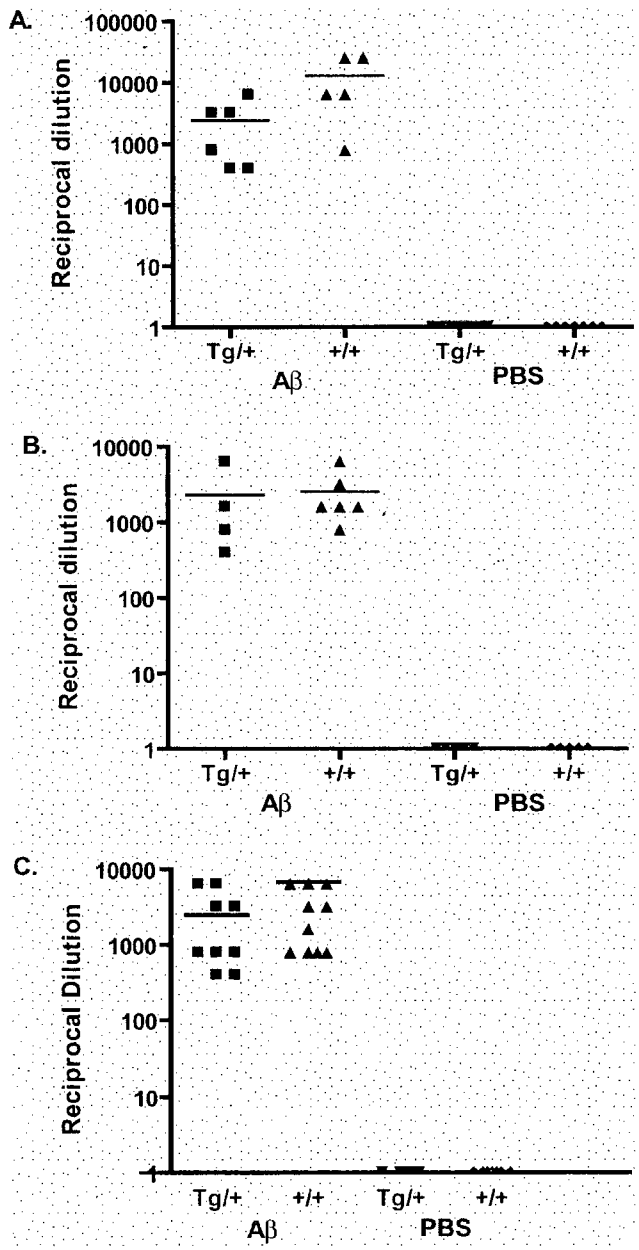

Figure 5.3. Antibody titre in serum of transgenic and non-transgenic mice immunized with either Aβ or PBS. Serum antibody titres were measured after the second vaccination by ELISA. In all cases, mice (transgenic and non-transgenic) immunized with fibrillar $A\beta_{1-40}$ exhibited a high anti-Aβ antibody titre against Aβ peptide. No anti-Aβ antibodies were detected in mice immunized with PBS. A. 15 month age group, B. 12 month age group, C. 6 month age group.

5.2.3 Amyloid plaque burden in immunized animals

Next, amyloid plaque burden was assessed in both Aβ and PBS immunized transgenic and non-transgenic animals. As noted in other immunization studies[175,176,267,178,177,180,181] there was a significant reduction in the plaque burden in the cortex and hippocampus of transgenic mice immunized with Aβ compared to those immunized with PBS. In 15 month old mice, which were immunized with Aβ after disease onset, there was a decrease in plaque burden with a reduction in both the size and number of plaques, whereas brain sections from PBS-treated transgenic mice contained numerous amyloid deposits (Figure 5.4 a-b; Figure 5.5 a). These data agree with previous studies where there was not a total elimination or prevention of plaques in these animals. In mice immunized with Aβ prior to disease onset (12 month) there was an almost complete prevention of Aβ deposition. In Aβ immunized transgenic mice, 4 out of 6 had no detectable amyloid deposits. Two mice from this treatment group had a single isolated plaque in the 4 brain sections examined. As with the 15 month group of mice, 12 month old, PBS-treated transgenic mice exhibited numerous amyloid deposits in their cortical and hippocampal regions (Figure 5.4 e-f; Figure 5.5 b). There were no detectable plaques in non-transgenic controls vaccinated with either Aβ or PBS (Figure 5.4 c-d, g-h). No amyloid plaques were found in 6 month old mice since amyloid plaques do not manifest in Tg2576 mice until 9 months of age. Non-transgenic mice injected with either Aβ and PBS exhibited no plaque burden (Figure 5.5 c-d, g-h). This confirms that immunization with Aβ may prevent plaque formation and thereby protect against disease.

Figure 5.4. Amyloid Pathology in Tg2576 Mice Immunized with Aβ or PBS.
Amyloid plaques in cortical sections from mice were visualized with 4G8, an antibody against human Aβ. There was a significant reduction in the total number of Aβ plaques in Tg2576 mice vaccinated with Aβ compared to those vaccinated with PBS at 11 months of age and at 6 weeks of age. Very few 4G8 positive plaques were found in brains of mice vaccinated at 6 weeks of age with Aβ. (**a**) 15 month Tg2576 mice vaccinated with PBS, (**b**) 15 month Tg2576 mice vaccinated with Aβ, (**c**) 15 month wild-type controls vaccinated with PBS and (**d**) 15 month wild-type controls vaccinated with Aβ, (**e**) 12 month Tg2576 mice vaccinated with PBS, (**f**) 12 month Tg2576 mice vaccinated with Aβ, (**g**) 12 month wild-type controls vaccinated with PBS and (**h**) 12 month wildtype controls vaccinated with Aβ. No plaques were present in all 6 month old mice. Brain sections shown are representative of their respective treatment groups.

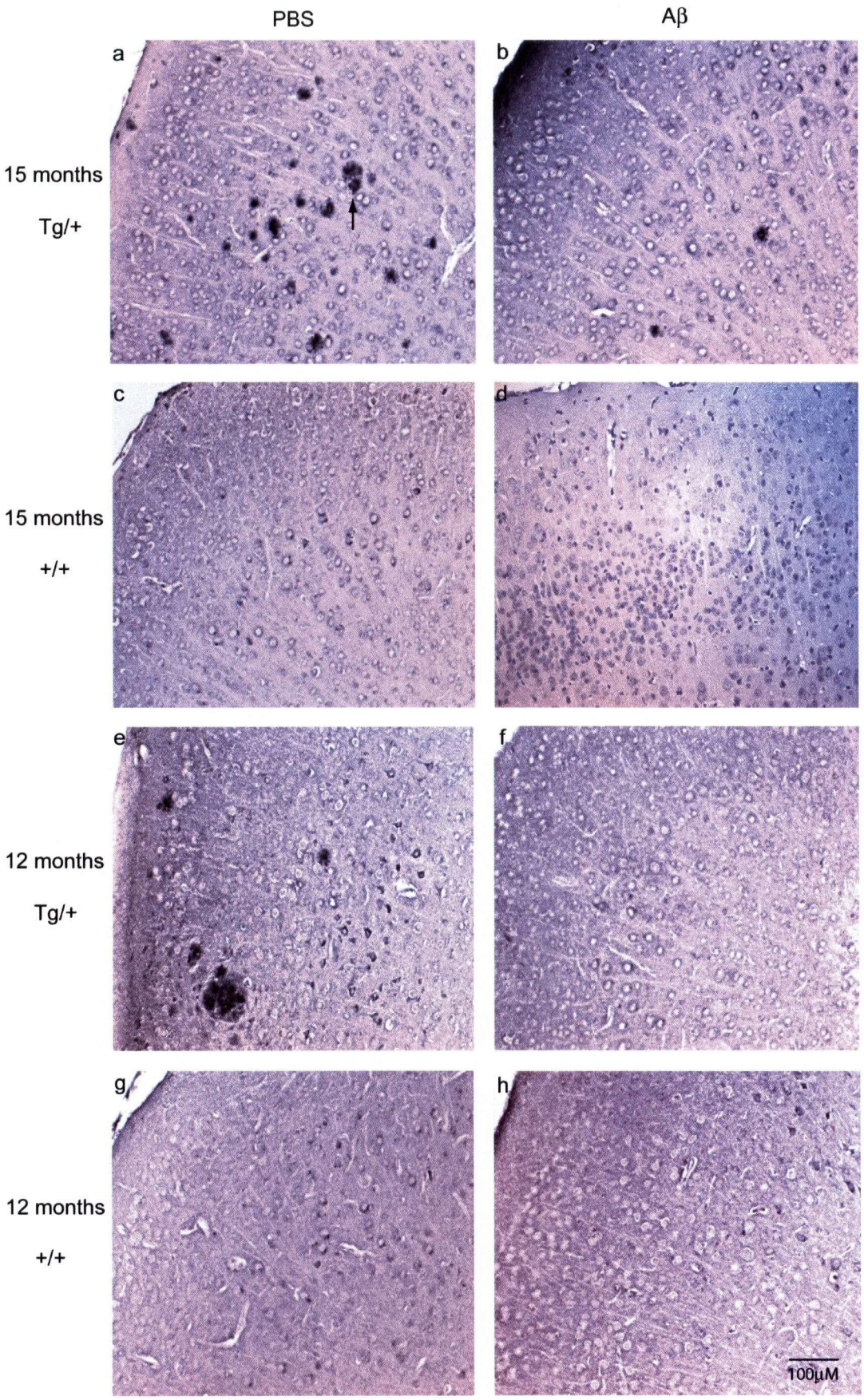
PBS
Aβ
a
b
15 months
Tg/+
c
d
15 months
+/+
e
f
12 months
Tg/+
g
h
12 months
+/+
100μM

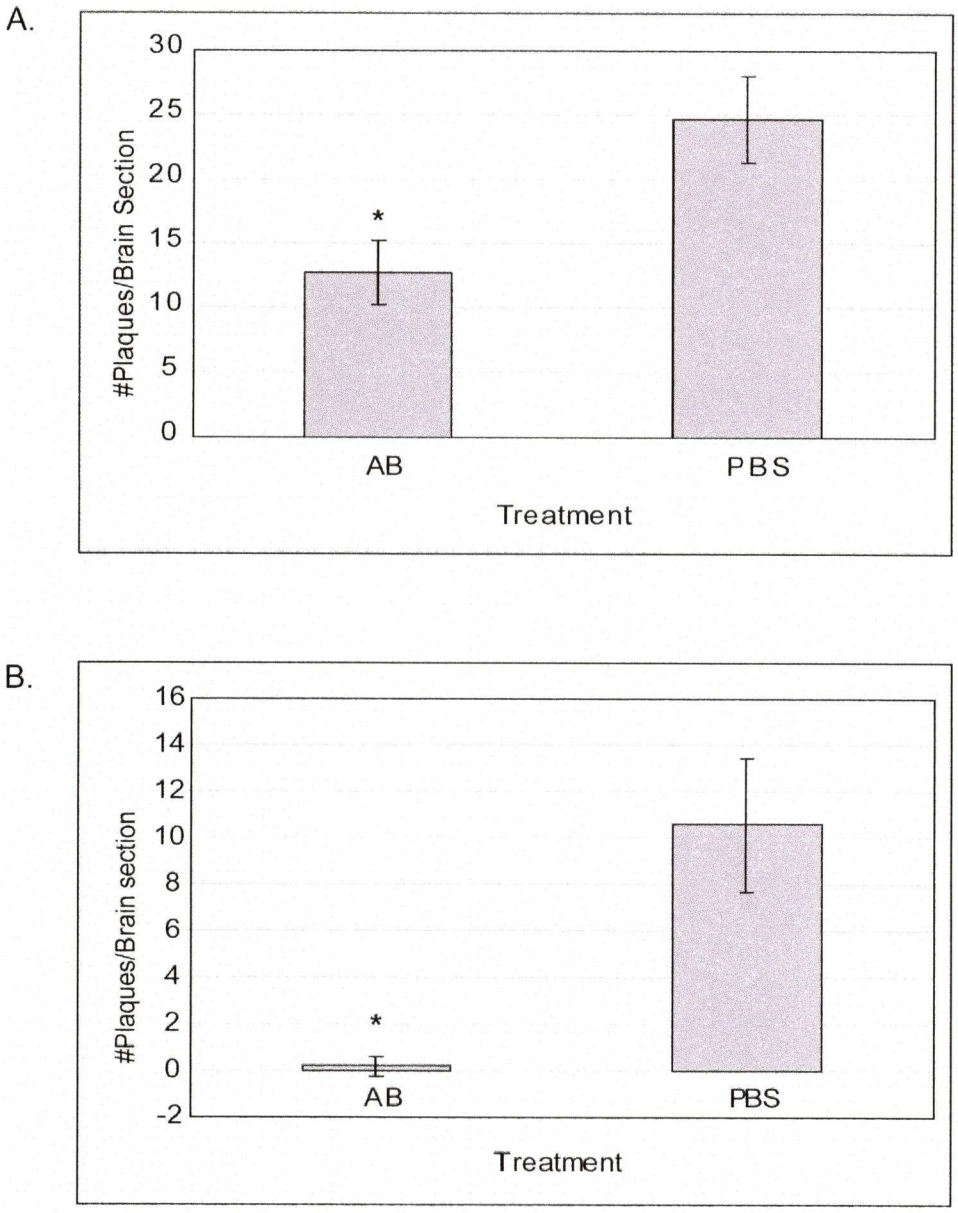

Figure 5.5. Cerebral amyloid levels are reduced in Tg2576 mice following Aβ immunization. Plaques were detected using an anti-human Aβ antibody, 4G8, on sequential brain sections. The presence of discrete plaques made it feasible to count the number of plaques in the entire section. Plaques were counted by visual inspection under the microscope for each of 4 sections at equal plane for each mouse. Total averaged number of plaques is presented. There was a significant reduction in the total number of Aβ plaques in Tg2576 mice vaccinated with Aβ compared to those vaccinated with PBS for both the 15 moth and 12 moth age groups. No plaques were seen in all 6 month old mice. (t-test * $P < 0.05$).

5.2.4 Microgliosis in immunized animals

The presence of activated microglia in immunized and non-immunized animals was also analyzed. Activated microglia are usually found associated with the amyloid plaques and can be distinguished from resting microglia by the expression of specific proteins, such as IL-1β, CD11b and major histocompatibility class II, and by distinct morphology [26]. Activated microglia exhibit an altered morphology from resting microglia first by the presence of thickened ramified processes and larger cell bodies which progresses to a final amoeboid/phagocytic state [104,105]. Sections of mouse brains were reacted with an antibody specific for the F4/80 antigen. The F4/80 antigen is expressed by a majority of mature macrophages, including microglia [268]. In agreement with previous studies [175], there appeared to be a reduction in the presence of activated, microglia in the brains of Aβ immunized mice compared to PBS controls suggesting a dampening of the inflammatory response. In 15 month transgenic mice immunized with PBS there are more plaque infiltrating microglia present compared to those immunized with Aβ (Figure 5.6 a,b). There were more densely stained F4/80 positive microglia with swelled cell bodies and thickened processes in PBS-treated transgenic mice compared to Aβ-treated mice. Similarly, in 12 month old transgenic mice immunized with PBS there were more amoeboid shaped and thick ramified microglia, whereas there microglia in the Aβ immunized mice have smaller cell bodies and more extensively ramified processes (Figure 5.6 e,h). The microglia present in non-transgenic mice displayed largely a non-activated morphology with small cell bodies and thin, highly branched processes (Figure 5.6 c-d, g-h).

Figure 5.6. Microgliosis in Immunized Mice.
Brain sections were stained with F4/80 to reveal the presence of microglia. Activated microglia can be distinguished from resting microglia by the presence of ramified processes and condensed cell bodies. Cortical sections from Tg2576 mice immunized with PBS or with Aβ, both at 11 months and at 6 weeks, show that Aβ immunized mice have reduction of activated, plaque associated microglia (black arrow). Control littermates exhibited no microgliosis (**a**) 15 month Tg2576 mice vaccinated with PBS, (**b**) 15 month Tg2576 mice vaccinated with Aβ, (**c**) 15 month non-transgenic controls vaccinated with PBS and (**d**) 15 month non-transgenic controls vaccinated with Aβ, (**e**) 12 month Tg2576 mice vaccinated with PBS, (**f**) 12 month Tg2576 mice vaccinated with Aβ, (**g**) 12 month non-transgenic controls vaccinated with PBS and (**h**) 12 month non-transgenic controls vaccinated with Aβ. Brain sections shown are representative of their respective treatment groups.

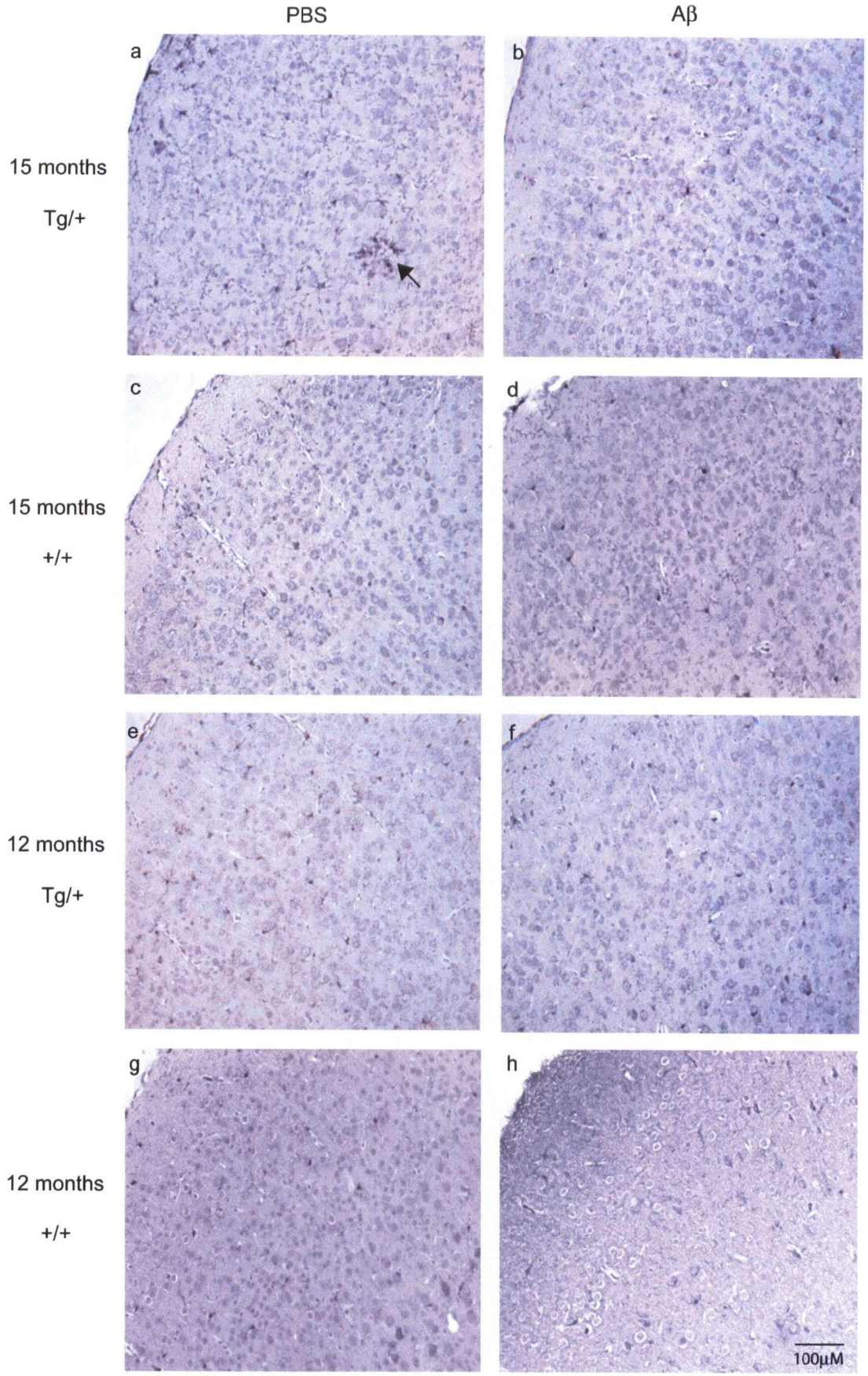
PBS
Aβ
a
b
15 months
Tg/+
c
d
15 months
+/+
e
f
12 months
Tg/+
g
h
12 months
+/+
100μM

5.2.5 BBB permeability in immunized animals

To test the effect of vaccination on the BBB, BBB permeability was assessed in mice at various time points. The first group was immunized with either Aβ peptide or PBS at 11 months of age, after disease onset, and immunized for a 4 month period (15 month old mice). The second group was immunized beginning at 6 weeks of age, well before any pathological disease symptoms, for an 11 month period (12 month old mice), similar to previous studies by Schenk *et al.* [175]. The final group was immunized beginning at 6 weeks of age for a 4 month period (6 month old mice). This last group was only immunized for a short duration since it has been demonstrated that BBB permeability can be compromised as early as 4 months of age. BBB permeability was assessed using the quantitative Evans blue assay [269,270]. Organs with a selective barrier, such as the brain, only take up a small amount of the dye. If there is a breach in the BBB then Evans blue will enter the parenchyma, whereas it is excluded from the brain with an intact BBB.

In all groups of mice (15 month, 12 month and 6 month mice), the integrity of the BBB of transgenic mice was compromised compared with that of non-transgenic controls (** $P < 0.05$). These data concur with the study by Ujiie *et al.* where BBB integrity was compromised in 4 month and 10 month old Tg2576 mice [149]. Upon immunization with Aβ, the AD transgenic mice displayed a significant decrease in BBB permeability, indicating a possible restoration of the BBB. Transgenic mice injected with Aβ had a significantly lower amount of Evans blue dye in their brain parenchyma compared to AD transgenic mice injected with PBS alone (Figure 5.7 a,b; * $P < 0.05$). This was true for both 15 month old mice and 12 month old mice immunized with Aβ. In the 12 month old mice, it is possible that vaccination with Aβ maintained an intact BBB, with little to no

compromise in BBB function. There was no change in BBB permeability in non-transgenic mice injected with Aβ or PBS. This latter observation is interesting as Aβ has been shown to be cytotoxic to endothelial cells and neuron *in-vitro* by eliciting apoptosis [271,151,54] and angiogenesis [272], yet the low amounts used in this study do not appear to affect BBB integrity in normal mice.

Finally, results from the 6 month old group are intriguing. In this instance, transgenic mice vaccinated with Aβ appeared to exhibit a breach in BBB integrity, similar to that of transgenic mice immunized with PBS (Figure 5.7 c). There was no effect elicited by Aβ immunization on the BBB as seen with the other groups. As demonstrated above, transgenic mice vaccinated with PBS had a compromised BBB in comparison to non-transgenic mice and no changes in BBB integrity were evident in non-transgenic mice injected with either Aβ or PBS. There was in an increase in the permeability of the BBB between transgenic and non-transgenic mice (Figure 5.7 c; ** $P < 0.05$). These data agree with previous data demonstrating that BBB integrity can become compromised as early as 4 month of age [149].

Figure 5.7. BBB permeability as determined by Evans Blue in cortical regions of Aβ and PBS immunized mice. In all groups the permeability of the BBB in Tg2576 is greater than non-transgenic controls (t-test, $^{**}P < 0.05$) (A) 15 months Tg2576 mice immunized with Aβ (n=5) show a decrease in the permeability of the BBB compared to PBS controls (n=4) (t-test, $^{*}P < 0.05$). The level of BBB permeability in Aβ immunized mice is similar to the permeability of non-transgenic littermates. (B) 12 months Tg2576 mice immunized with Aβ (n=6) show a decrease in the permeability of the BBB compared to PBS controls (n=6) (t-test, $^{*}P < 0.05$). The level of BBB permeability in Aβ immunized mice is similar to the permeability of non-transgenic littermates. (C) 6 month Tg2576 mice immunized with Aβ (n=9) show no difference in BBB permeability compared to PBS controls (N=9). Tg2676 mice (both Aβ and PBS vaccinated) do exhibit an increase in BBB permeability compared to control littermates.

A.

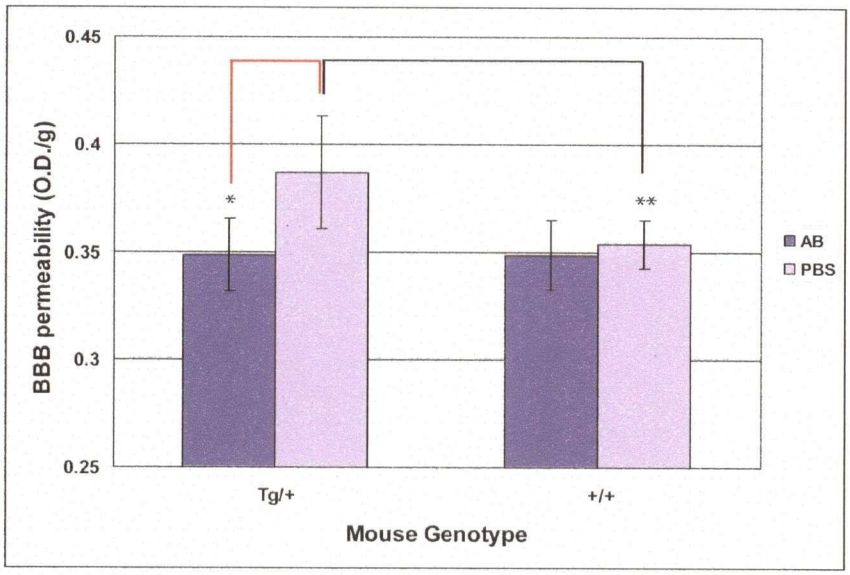
0.45
0.4
0.35
0.3
0.25
BBB permeability (O.D./g)
*
**
AB
PBS
Tg/+
+/+
Mouse Genotype

B.

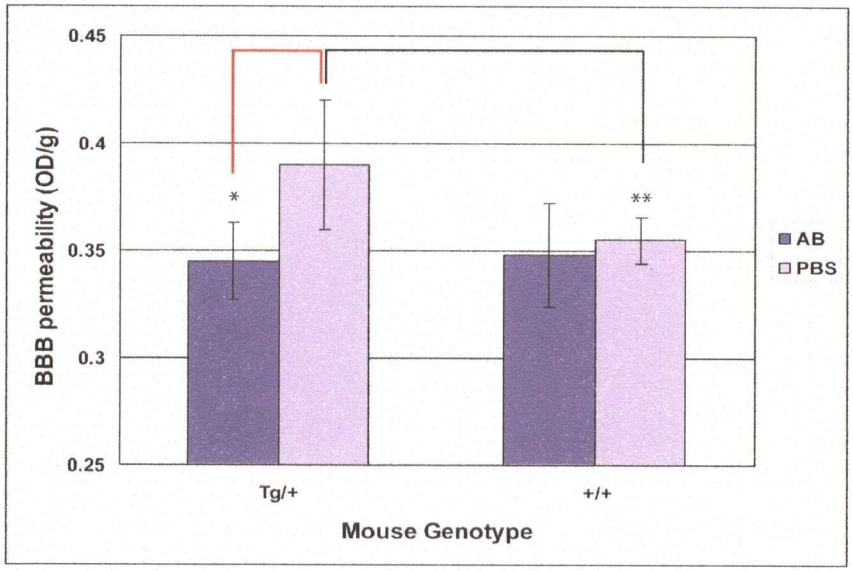
0.45
0.4
0.35
0.3
0.25
BBB permeability (OD/g)
*
**
AB
PBS
Tg/+
+/+
Mouse Genotype

C.

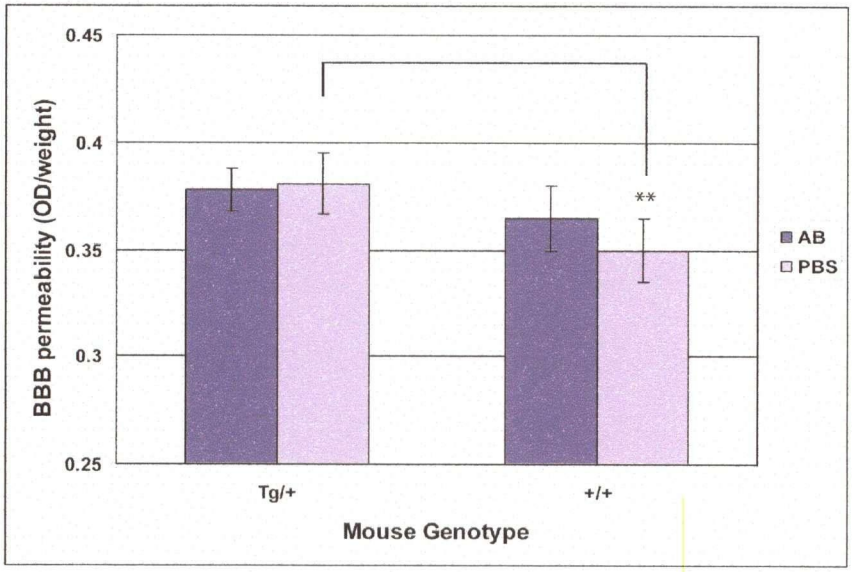
0.45
0.4
0.35
0.3
0.25
BBB permeability (OD/weight)
**
AB
PBS
Tg/+
+/+
Mouse Genotype

5.3 Discussion

Research focused on systemic Aβ-lowering strategies is becoming more important in the development of therapeutics for AD. Recent advances have focused on immunotherapy using amyloid. These studies have proven successful in mice and have reached clinical trials in humans. What remains unclear is the mechanism by which Aβ immunotherapy alleviates the pathology seen in AD. This issue was first addressed by examining the ability of Aβ peptides to pass through the BBB and demonstrated that Aβ was able to access the brain in both transgenic and non-transgenic mice. This suggests that Aβ can gain entry into the brain via receptor mediated transcytosis [273], [274], [70]. Aβ transport across the BBB has been investigated by many groups and all results indicate an active transport of Aβ across the BBB. In a recent study it was shown that soluble Aβ can be transported from the CNS to the plasma since direct injection of radiolabelled Aβ into the brain was recovered in the plasma. Moreover, when radiolabelled Aβ was injected into the periphery, radioactive counts were found in the brain [70]. Banks *et al.* examined the influx of both $A\beta_{1-42}$ and $A\beta_{1-40}$ (mouse and human) in the different mouse models, CD-1 and SAMP8 [275]. They found that all forms of Aβ were transported into the brain, with mouse 1-42 and human 1-40 being the fastest. In addition, all forms of Aβ were also transported out of the CNS. When examining the permeability coefficient x surface area product (PS) of proteins known to cross the BBB via receptor-mediated transcytosis (i.e. insulin) and of proteins known to have limited entry into the brain (i.e. albumin) it was shown that the PS value of Aβ was similar to that of insulin [274,258]. Further studies have suggested that the RAGE receptor is a receptor on the BBB that is responsible for the influx of Aβ from the blood to the brain [68,273]. RAGE, is a multiligand

receptor in the immunoglobulin superfamily, binding ligands such as Aβ, the S100/calgranulin family of pro-inflammatory cytokine-like mediators, the high mobility group 1DNA binding protein amphoterin and products of nonenzymatic glycoxidation [67]. The expression of RAGE is ligand dependant. In transgenic mice, RAGE expression correlates with Aβ deposition and is localized to affected cerebral vessels, neurons and activated microglia. The increase in expression may facilitate an increase in Aβ transport into the brain thereby exacerbating cellular dysfunction and disease progression [67]. Other studies in animal models have shown that RAGE mediates the transport of Aβ from the blood to the brain and deletion of RAGE results in the inhibition of Aβ transport thus protecting the CNS from the accumulation of peripheral Aβ pools [69].

When an antibody against human Aβ, was injected into mice there was no apparent presence of antibody in the brain parenchyma. Whether antibodies can cross into the brain from the periphery is under debate. It is possible that in this study, the amount of antibody used was insufficient to cross the BBB. Antibody injected into the periphery could have bound to circulating peripheral amyloid thereby preventing its movement into the brain. In this study the mice used were 6 weeks old. In other studies, where there was a presence of antibody in the brain, the mice were significantly older. It has been previously shown that the BBB is compromised in AD mice as early as 4 months of age. Thus, it is possible that at 6 weeks of age antibodies cannot gain access into the brain whereas in older animals the BBB is damaged thereby facilitating the entrance of antibodies to the brain. When evaluating the PS values of antibodies across the BBB, Podsulo *et al.* found that the PS value of non-specific IgG and Aβ specific antibodies were similar, 0.5 to 1.1 X 10^{-6} ml/g/s and 0.6 to 1.4 X10^{-6} ml/g/s respectively, and less

than that for albumin [147]. This indicates that the passage of antibodies across the BBB occurs at a very low efficiency [258]. Furthermore, Demattos *et al.* were unable to identify any plaque associated anti-Aβ antibodies after immunization [177]. Conversely, there is abundant evidence which illustrates that anti-Aβ antibodies can cross the BBB. In a study using active immunization with Aβ peptides there was the appearance of anti-Aβ antibodies associated with microglia localized with plaques [175]. In addition, antibodies to Aβ may be able to enter the brain once in complex with Aβ [258]. It has also been demonstrated that anti-Aβ antibodies can enter the brain at a rate similar to that of albumin; however, due to the long half-life of the antibody in the blood there was a longer clearance time from the brain [276]. Taken together, the disruption of the BBB likely facilitates an increase of antibodies across the BBB efficiently enough to explain the action of the vaccine.

The most significant finding in this study demonstrates that immunization with Aβ tends to repair the damage found in BBB in Tg2576 AD mice. In 15 month old transgenic mice, which have been inoculated for 4 months, there is a decrease in Evans blue uptake compared to PBS-treated transgenic mice. The significant decrease in Evans blue uptake observed in Aβ immunized transgenic mice compared to the PBS mice suggest that Aβ immunization results in the restoration of the BBB. In 12 month old mice inoculated for 11 months starting at 6 weeks of age, Aβ immunization may be able to actually prevent further disease progression. In these mice, Evans blue uptake is comparable to non-transgenic mice, where there is no measurable decreased integrity of the BBB. One possible explanation of the restoration of the BBB in older mice is that the vaccination leads to the decrease in the amount of circulating Aβ that could directly or

indirectly affect the function of endothelium in the BBB. As demonstrated in this study and in many other studies [175,178,250,180,251,181], there is a significant decrease in Aβ deposits and microgliosis following immunization. With the removal of Aβ from the brain and the subsequent deactivation of microglia, there will be a decrease in the brain in the amount of reactive oxygen and nitrogen compounds and inflammatory cytokines produced by these cells which have been shown to activate vascular endothelial cells [155,277,153]. Studies focused on vasculature activation found that in response to systemic inflammation from either the periphery or brain parenchyma, endothelial cells up-regulate the expression of molecules that are generally associated with inflammatory processes such as prostaglandin E2, nitric oxide, CD40 and COX-2 [153,154,155]. These then can act agonistically on microglia and neuronal cells to further intensify inflammation and disease pathology.

Aβ has also been demonstrated to elicit many pro-apoptotic and pro-angiogenic responses in the endothelial cells that make up the BBB [152,151,150]. These effects are dependent on the amount of Aβ present. It has been exhibited *in vitro* that exposure of endothelial cells to μM concentrations (5-25 μM) elicits pro-apoptotic signals [272,271,151] whereas treatment with nM concentrations (50-250 nM) of Aβ elicits pro-inflammatory signals and increased monocyte migration with minimal disruptions to the endothelial monolayer [278,279]. Treatment of primary cerebral mouse endothelial cells with $A\beta_{25-35}$ resulted in the activation of AP-1 and the subsequent expression of Bim, a member of the BH3 only family of proapoptotic proteins [151]. Moreover, Aβ treatment also resulted in the translocation of second-mitochondria derived activator of caspase (Smac), a regulator of apoptosis, from the mitochondria to the cytosol where it can bind to the X

chromosome linked inhibitor of apoptosis protein (XIAP), resulting in cell death [151]. Cytochrome C release from the mitochondria and the subsequent activation of several caspases, such as caspase 8 and caspase 3, all important events on the apoptotic cascade, have also been reported [150]. Several studies have also shown that exposure of endothelial cells to Aβ results in cytotoxic damage elicited from the generation of reactive oxygen species and increased calcium levels causing alterations in endothelial cell structure and function [280,272]. Angiogenesis is also observed in endothelial cells in AD. Inflammatory mediators such as TNF-α, IL-1β, and IL-6 stimulate angiogenesis [281]. These inflammatory mediators, as well as COX-2 and amyloid, have been found to cause an increase in the expression of may angiogenic factors including VEGF, TGF-β and TNF-α [215,282]. Moreover, in AD patients there is an increase in VEGF expression in the brain as well as an increase in the serum and CSF [214,215]. Recently, it was discovered that VEGF binds to Aβ with high affinity and specificity and is thus co-localized to the plaques. Therefore, it is possible that in response to pro-angiogenic and pro-apoptotic signals from Aβ and activated microglia, tight junctions disappear, cells round up creating a leaky barrier [216]. The endothelial cells in turn release neurotoxins, free oxygen radicals, APP and more pro-angiogenic factors such as VEGF and TGF-β. With the removal of signal provided by Aβ and inflammation, it is possible that the endothelial cells quiesce, terminate the release of toxic substances, reform tight junctions reforming an intact, tight barrier.

In regards to the mechanism by with Aβ immunization effectively reduces AD pathology; it is possible that the debate as to whether antibodies can cross the BBB is resolved. With a leaky BBB, antibodies are able to gain access into the brain, bind to Aβ

and are either degraded by microglia via FcR mediated phagocytosis or the Aβ-antibody complex can leave the brain. Alternatively, with a leaky BBB the efflux of Aβ from the brain can occur at a faster rate than by active transport by specific receptors, such as LRP [70], thereby re-establishing equilibrium between plasma and CNS Aβ pools [258]. Once the excess amyloid is removed, by microglia or by efflux into the periphery, amyloid levels return to tolerable a threshold, microglia become deactivated, the BBB reforms and the brain becomes an 'immunoprivileged' site once again. In summary, these new observations provide an intellectual framework for understanding the efficiency of vaccination to modify disease progression. In addition, resealing of the BBB provides a previously undescribed intervention point for modifying disease outcome in amyliodopathies such as AD.

Chapter 6: Concluding remarks and future directions

Since the eponym "Alzheimer's disease" was coined, there has been much debate as to the exact etiology and pathology of the disease. Many view that AD is not a single, uniform disease. Rather, AD is more likely a heterogeneous and multifactorial disease influenced by the interactions of various susceptibility genes and environmental factors. Intriguingly, as with other medical conditions, AD represents a disease with heterogeneity in its origins (EOFAD compared to LOAD) and homogeneity in its clinical appearance and pathology. Therefore, it is hypothesized that AD results from a complex sequence of steps involving multiple factors that extend well beyond the accumulation of Aβ. This thesis concentrates on many facets of one of the main foundation of AD, the contribution of microglia in disease progression. In particular the relationship of Aβ to the activation of microglia, subsequent signal transduction pathways and gene expression and the impact of microglia on Aβ deposition and clearance and its effect on another pathological hallmark, the BBB, were addressed.

According to the "amyloid cascade hypothesis" it is thought that Aβ accumulation is the principle event in AD. A possible discrepancy with this theory is that there is no direct evidence linking Aβ accumulation to neuronal death. Neuroinflammatory processes may be this missing link and have been suggested to exacerbate neuronal damage/death seen in AD. With the current understanding of the role of activated microglia in disease progression many therapeutic strategies directed against inflammatory processes have been pursued. Epidemiological studies on NSAID use demonstrated a reduced risk and decrease in the rate of cognitive decline [102,103] and treatment of hAPP transgenic mice with anti-inflammatories decreased plaque size and

slowed down cognitive deficits [224]. However, the use of NSAIDs appears to be effective only when administered prior to disease onset and not once symptoms are manifest, as indicated from current clinical trials where no beneficial effect of NSAID use is reported [226]. The development of new anti-inflammatory therapies that interfere with one or more specific steps in the inflammatory cascade is underway. Nevertheless, it is essential to establish a specific, reliable and non-invasive biomarker to assess the efficacy of new drug treatments. Results from the studies performed in this thesis support the use of p97 as a marker of inflammation. The levels of p97, mRNA and protein, were upregulated in activated microglia. Interestingly, the increase in p97 expression occurred largely in response to Aβ stimulation and not in response to other known AD stresses such as IFN-γ. Further investigation into the expression of p97 found that p97 production appears to be controlled by the p38 MAPK signal transduction pathway. This is intriguing since many studies have demonstrated that Aβ is able to induce the activation of p38 MAPK in vitro and that p38 MAPK phosphorylation is increased in affected brain regions in the AD brain [57,128,129]. In addition, this thesis has demonstrated that p97 levels can be altered with treatment of activated microglia with NSAIDs, Ibu and Nim, promoting its potential role as an AD inflammatory biomarker.

Understanding the mechanism of amyloid aggregation and clearance will ultimately lead to new advances in therapeutic development. Clearance of Aβ through microglial activation, chemotaxis, proliferation and phagocytosis has received a lot of interest over the years, in particular from the recent immunization studies. Activated microglia displaying a variety of cell surface markers that distinguish them from resting microglia are often found within and immediately surrounding maturing amyloid plaques

[118,26,283]. Whether activated microglia contribute to or aid in the clearance of plaques is controversial. Using a hAPP AD mouse model which lacked functional microglia it was found that, at the early stages of the disease, there was no significant difference in plaque burden in Tg/+;op/op and Tg/+;+/+ mice. Interestingly there were deposits of cerebral amyloid in the Tg/+;op/op mice implying a possible shift in amyloid deposition patterns. These results are intriguing but more mice need to be examined in order to resolve the complex relationship between activated microglia and Aβ aggregation and clearance.

One of the latest therapies to combat AD employs active or passive immunization with Aβ peptide or antibodies against Aβ. This method was successful in transgenic mice, but failed during clinical trials due to the incidence of meningio-encephalitis [256,255]. It has previously been established that there is increased permeability in the BBB of Tg2576 AD mice compared to age match controls at 10 months of age, as the signs of the disease become manifest, and as early as 4 months of age, prior to disease onset and plaque deposition [149]. Therefore, it was hypothesized that disruption of the BBB is another pathological hallmark of AD that may explain the mechanism by which immunization therapies have proven successful. Specifically, peripheral antibodies are able to pass into the brain via a breached barrier and bind to and sequester brain amyloid. The antibody-amyloid complex is then degraded by FcR mediated phagocytosis by activated microglia. The present study addressed the effect of Aβ immunization on the integrity of the BBB and revealed that immunization with Aβ, prior to and after disease onset, resulted in a decrease in permeability and a restoration of BBB integrity. These observations provide an intellectual framework for understanding the efficiency of

vaccination to modify disease progression as well as providing new possible therapeutic interventions.

It is clear that there are several directions this project could take in the future. For instance: studies focused on further establishing p97 as a biomarker for AD and as an indicator for drug efficacy in an *in vitro* and *in vivo* system could be addressed. Measuring p97 levels in primary mouse and/or human microglia with or without exposure to Aβ and in AD model mice treated with various putative drug treatments would clarify if indeed p97 can be used as a monitoring system. If successful, this assay could serve as a means to test new drug development initially in an *in vitro* system and, if efficacious, move into an *in vivo* system before clinical trials. In order to do these experiments monoclonal antibodies to mouse p97 need to be generated. In addition, it is possible that, since p97 is an iron transport molecule, it may play a role in disease progression. Therefore, determining if p97 contributes to disease pathology could be investigated. One way to address this hypothesis would be by creating transgenic mice overexpressing p97 and breeding these mice to hAPP mice and examining the brains for signs of AD pathology.

In regards to the role of activated microglia in Aβ accumulation and plaque formation, it was found that the amount of Aβ plaques in hAPP mice with dysfunctional microglia was similar to the amount in hAPP mice. However, the number of animals used in this study was small and since there is variability between mice, a larger cohort is needed in order to draw a more definite conclusion. Moreover, since CSF-1 deficient mice have a short life span it would be beneficial to use an AD mouse model that develops pathological symptoms at an earlier age than the Tg2576 mouse model. As

well, it would be interesting to assess the other hallmarks of AD in these mice, namely neurodegeneration, vascular amyloid burden and BBB permeability. Furthermore, measuring the levels of certain complement proteins and other indicators of microglial activation would be of interest to see if Aβ had a direct or indirect effect on microglial maturation and function.

It was demonstrated in this thesis that Aβ immunization restores BBB integrity in mice immunized after disease onset and possibly prevents BBB deterioration when immunized prior to disease onset. In this thesis, the permeability of the BBB was investigated on a global level. It would be interesting to see if there is a difference in permeability in specific brain regions, in particular, regions of the brain more severely affected in AD and if the decrease in BBB permeability coincides with the decrease in Aβ burden. Some studies have shown the occurrence of micro-hemorrhages in the brain after immunization. However, these micro-hemorrhages may have been due to the type of anti-Aβ antibody used as an immunogen. It is possible that immunization could result in small hemorrhages in specific areas of the brain but an overall restoration of BBB integrity. This needs to be investigated more thoroughly. Dissecting the brains of immunized mice into various regions and performing the Evans blue assay is a quantitative way of assessing regional permeability. Alternatively, qualitative analysis using sections from Evans blue perfused animals can be done since Evans blue fluoresces under specific light wavelengths. Recently, Ujiie, *et al.* developed a new technique for assessing BBB permeability using succinimidyl ester of carboxyfluorescein diacetate [149]. Perfusing immunized mice with succinimidyl ester of carboxyfluorescein diacetate is another way to assess regional permeability. Moreover, it will allow one to determine if

the BBB is more permeable in plaque laden regions. Finally, it would be interesting to examine which cells in the brain are responsible for the damage and re-establishment on the BBB.

Overall, there is an important link between microglial activation, plaque formation and degradation and the progression of other pathological hallmarks, which needs to be clearly elucidated. Determining the mechanism of Aβ clearance in the normal brain and upon Aβ immunization is required in order to facilitate the design of specific treatment regimens, allowing exclusive targeting of plaques without inducing detrimental side effects. Such experiments are difficult since transgenic mice have less genetic variability than humans, and their plaques have a different chemical composition, making them far more soluble and easier to remove. Furthermore, there is no transgenic mouse to date that can clearly mimic all the hallmarks of AD. In regards to immunization regimes, the consequences are different between human and mouse. Vaccination of transgenic mice removes human Aβ while leaving endogenous mouse Aβ intact, whereas in humans the immune response is directed against an endogenous target that occurs naturally and plays an essential role in maintaining healthy brain tissue. In conclusion the results from this thesis shed significant new light on activated microglial gene expression in AD and also on the role of microglia in plaque development and clearance possibly due to alterations in BBB integrity.

Appendix I: Domain Structure of APP

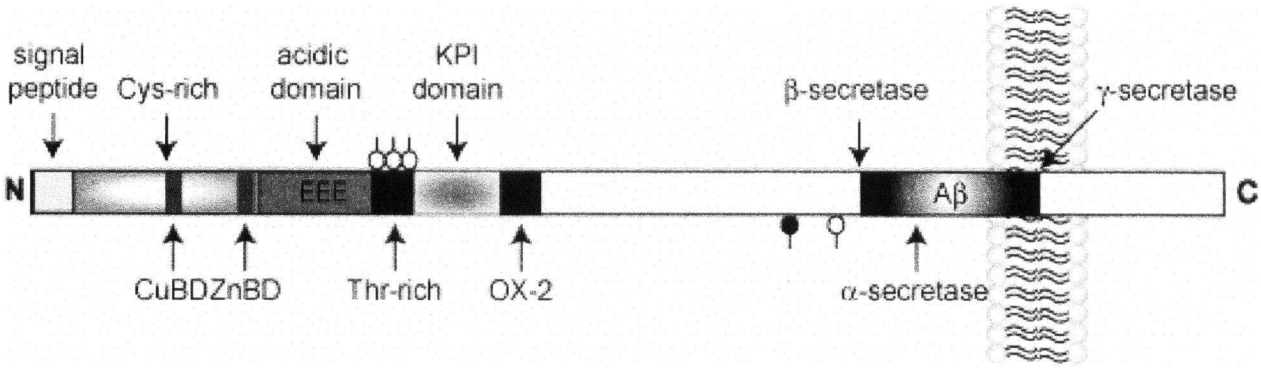

Schematic representation of the domain structure of APP.
Full length APP contains a signal peptide at the N-terminal end; a cysteine residue-rich region (Cys-rich) with copper binding (CuBD) and zinc binding sites (ZnBD); an acidic domain; a threonine residue-rich domain; Kinitz protease inhibitor domain (KPI); and an OX-2 homology domain (OX2). The Aβ fragment is flanked by the β- and γ-secretase cleavage sites and contains the α-sectretase cleavage site.

Appendix II: Regional diagram of the brain

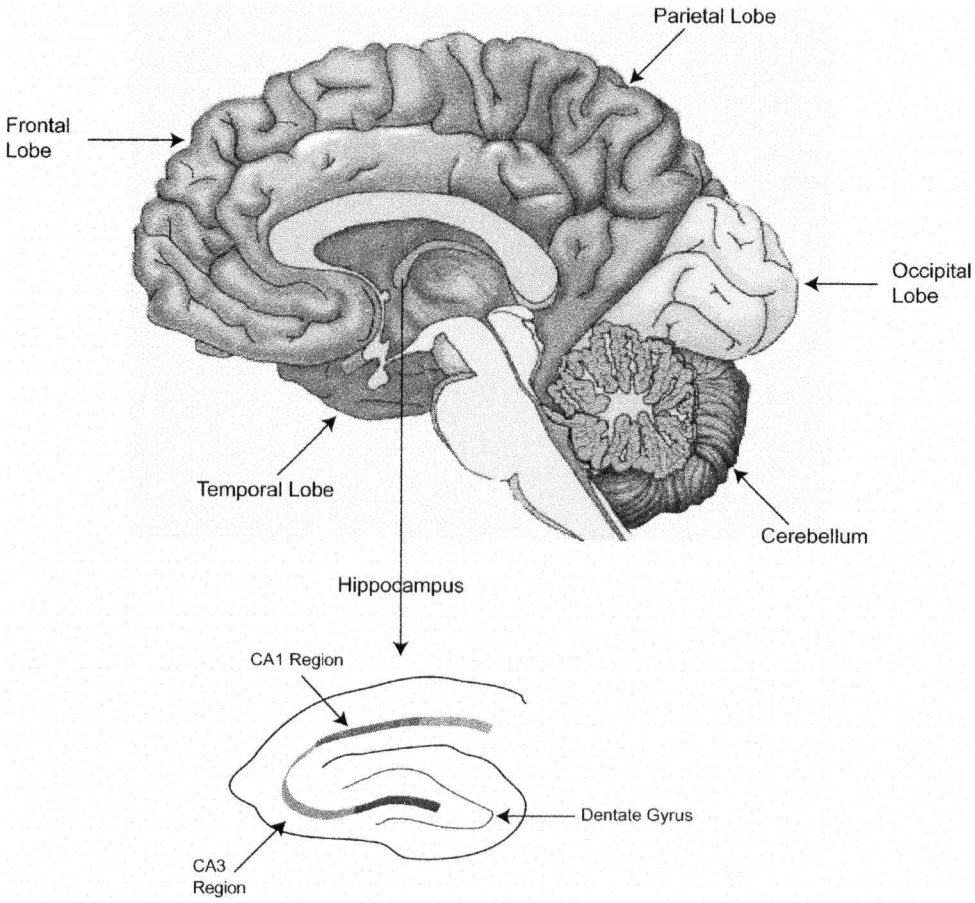

References

1. Turner, P. R., O'Connor, K., Tate, W. P. & Abraham, W. C. Roles of amyloid precursor protein and its fragments in regulating neural activity, plasticity and memory. *Prog Neurobiol* **70**, 1-32 (2003).
2. Verbeek, M. M., Ruiter, D. J. & de Waal, R. M. The role of amyloid in the pathogenesis of Alzheimer's disease. *Biol Chem* **378**, 937-50 (1997).
3. Selkoe, D. J. & Schenk, D. Alzheimer's disease: molecular understanding predicts amyloid-based therapeutics. *Annu Rev Pharmacol Toxicol* **43**, 545-84 (2003).
4. Small, D. H. The role of the amyloid protein precursor (APP) in Alzheimer's disease: does the normal function of APP explain the topography of neurodegeneration? *Neurochem Res* **23**, 795-806 (1998).
5. Price, D. L., Tanzi, R. E., Borchelt, D. R. & Sisodia, S. S. Alzheimer's disease: genetic studies and transgenic models. *Annu Rev Genet* **32**, 461-93 (1998).
6. Nunan, J. & Small, D. H. Regulation of APP cleavage by alpha-, beta- and gamma-secretases. *FEBS Lett* **483**, 6-10 (2000).
7. Allsop, D., Landon, M. & Kidd, M. The isolation and amino acid composition of senile plaque core protein. *Brain Res* **259**, 348-52 (1983).
8. Hardy, J. A. & Higgins, G. A. Alzheimer's disease: the amyloid cascade hypothesis. *Science* **256**, 184-5 (1992).
9. Tanzi, R. E. A genetic dichotomy model for the inheritance of Alzheimer's disease and common age-related disorders. *J Clin Invest* **104**, 1175-9 (1999).
10. Tanzi, R. E. & Bertram, L. New frontiers in Alzheimer's disease genetics. *Neuron* **32**, 181-4 (2001).
11. Wisniewski, K. E., Wisniewski, H. M. & Wen, G. Y. Occurrence of neuropathological changes and dementia of Alzheimer's disease in Down's syndrome. *Ann Neurol* **17**, 278-82 (1985).
12. Rumble, B. et al. Amyloid A4 protein and its precursor in Down's syndrome and Alzheimer's disease. *N Engl J Med* **320**, 1446-52 (1989).
13. Tanzi, R. E. Neuropathology in the Down's syndrome brain. *Nat Med* **2**, 31-2 (1996).
14. Suzuki, N. et al. An increased percentage of long amyloid beta protein secreted by familial amyloid beta protein precursor (beta APP717) mutants. *Science* **264**, 1336-40 (1994).
15. Cai, X. D., Golde, T. E. & Younkin, S. G. Release of excess amyloid beta protein from a mutant amyloid beta protein precursor. *Science* **259**, 514-6 (1993).
16. Selkoe, D. J. Alzheimer's disease: genes, proteins, and therapy. *Physiol Rev* **81**, 741-66 (2001).
17. Wolfe, M. S. et al. Two transmembrane aspartates in presenilin-1 required for presenilin endoproteolysis and gamma-secretase activity. *Nature* **398**, 513-7 (1999).
18. Luo, W. J. et al. PEN-2 and APH-1 coordinately regulate proteolytic processing of presenilin 1. *J Biol Chem* **278**, 7850-4 (2003).

19. Gu, Y. et al. APH-1 interacts with mature and immature forms of presenilins and nicastrin and may play a role in maturation of presenilin.nicastrin complexes. *J Biol Chem* **278**, 7374-80 (2003).
20. Kimberly, W. T. et al. Gamma-secretase is a membrane protein complex comprised of presenilin, nicastrin, Aph-1, and Pen-2. *Proc Natl Acad Sci U S A* **100**, 6382-7 (2003).
21. Selkoe, D. J. The cell biology of beta-amyloid precursor protein and presenilin in Alzheimer's disease. *Trends Cell Biol* **8**, 447-53 (1998).
22. Russo, C. et al. Presenilin-1 mutations in Alzheimer's disease. *Nature* **405**, 531-2 (2000).
23. Strittmatter, W. J. et al. Apolipoprotein E: high-avidity binding to beta-amyloid and increased frequency of type 4 allele in late-onset familial Alzheimer disease. *Proc Natl Acad Sci U S A* **90**, 1977-81 (1993).
24. Mahley, R. W. Apolipoprotein E: cholesterol transport protein with expanding role in cell biology. *Science* **240**, 622-30 (1988).
25. LaDu, M. J. et al. Isoform-specific binding of apolipoprotein E to beta-amyloid. *J Biol Chem* **269**, 23403-6 (1994).
26. Akiyama, H. et al. Inflammation and Alzheimer's disease. *Neurobiol Aging* **21**, 383-421 (2000).
27. Selkoe, D. J. Clearing the brain's amyloid cobwebs. *Neuron* **32**, 177-80 (2001).
28. McGeer, P. L. & McGeer, E. G. Inflammation, autotoxicity and Alzheimer disease. *Neurobiol Aging* **22**, 799-809 (2001).
29. Yoshikai, S., Sasaki, H., Doh-ura, K., Furuya, H. & Sakaki, Y. Genomic organization of the human amyloid beta-protein precursor gene. *Gene* **87**, 257-63 (1990).
30. Tanaka, S. et al. Tissue-specific expression of three types of beta-protein precursor mRNA: enhancement of protease inhibitor-harboring types in Alzheimer's disease brain. *Biochem Biophys Res Commun* **165**, 1406-14 (1989).
31. Storey, E., Beyreuther, K. & Masters, C. L. Alzheimer's disease amyloid precursor protein on the surface of cortical neurons in primary culture co-localizes with adhesion patch components. *Brain Res* **735**, 217-31 (1996).
32. Annaert, W. G. et al. Interaction with telencephalin and the amyloid precursor protein predicts a ring structure for presenilins. *Neuron* **32**, 579-89 (2001).
33. Allinson, T. M., Parkin, E. T., Turner, A. J. & Hooper, N. M. ADAMs family members as amyloid precursor protein alpha-secretases. *J Neurosci Res* **74**, 342-52 (2003).
34. Ling, Y., Morgan, K. & Kalsheker, N. Amyloid precursor protein (APP) and the biology of proteolytic processing: relevance to Alzheimer's disease. *Int J Biochem Cell Biol* **35**, 1505-35 (2003).
35. Vassar, R. et al. Beta-secretase cleavage of Alzheimer's amyloid precursor protein by the transmembrane aspartic protease BACE. *Science* **286**, 735-41 (1999).
36. Cai, H. et al. BACE1 is the major beta-secretase for generation of Abeta peptides by neurons. *Nat Neurosci* **4**, 233-4 (2001).
37. Acquati, F. et al. The gene encoding DRAP (BACE2), a glycosylated transmembrane protein of the aspartic protease family, maps to the down critical region. *FEBS Lett* **468**, 59-64 (2000).

38. Duff, K. et al. Increased amyloid-beta42(43) in brains of mice expressing mutant presenilin 1. *Nature* **383**, 710-3 (1996).
39. LaVoie, M. J. et al. Assembly of the gamma-secretase complex involves early formation of an intermediate subcomplex of Aph-1 and nicastrin. *J Biol Chem* **278**, 37213-22 (2003).
40. Roher, A. E. et al. Oligomerizaiton and fibril assembly of the amyloid-beta protein. *Biochim Biophys Acta* **1502**, 31-43 (2000).
41. Small, D. H. & McLean, C. A. Alzheimer's disease and the amyloid beta protein: What is the role of amyloid? *J Neurochem* **73**, 443-9 (1999).
42. Braak, H. & Braak, E. Development of Alzheimer-related neurofibrillary changes in the neocortex inversely recapitulates cortical myelogenesis. *Acta Neuropathol (Berl)* **92**, 197-201 (1996).
43. Gabuzda, D., Busciglio, J., Chen, L. B., Matsudaira, P. & Yankner, B. A. Inhibition of energy metabolism alters the processing of amyloid precursor protein and induces a potentially amyloidogenic derivative. *J Biol Chem* **269**, 13623-8 (1994).
44. Mattson, M. P. & Pedersen, W. A. Effects of amyloid precursor protein derivatives and oxidative stress on basal forebrain cholinergic systems in Alzheimer's disease. *Int J Dev Neurosci* **16**, 737-53 (1998).
45. Atwood, C. S. et al. Amyloid-beta: a chameleon walking in two worlds: a review of the trophic and toxic properties of amyloid-beta. *Brain Res Brain Res Rev* **43**, 1-16 (2003).
46. Cherny, R. A. et al. Aqueous dissolution of Alzheimer's disease Abeta amyloid deposits by biometal depletion. *J Biol Chem* **274**, 23223-8 (1999).
47. Querfurth, H. W. & Selkoe, D. J. Calcium ionophore increases amyloid beta peptide production by cultured cells. *Biochemistry* **33**, 4550-61 (1994).
48. Ueda, K., Shinohara, S., Yagami, T., Asakura, K. & Kawasaki, K. Amyloid beta protein potentiates Ca2+ influx through L-type voltage-sensitive Ca2+ channels: a possible involvement of free radicals. *J Neurochem* **68**, 265-71 (1997).
49. Pierrot, N., Ghisdal, P., Caumont, A. S. & Octave, J. N. Intraneuronal amyloid-beta1-42 production triggered by sustained increase of cytosolic calcium concentration induces neuronal death. *J Neurochem* **88**, 1140-50 (2004).
50. Wertkin, A. M. et al. Human neurons derived from a teratocarcinoma cell line express solely the 695-amino acid amyloid precursor protein and produce intracellular beta-amyloid or A4 peptides. *Proc Natl Acad Sci U S A* **90**, 9513-7 (1993).
51. Takahashi, R. H. et al. Intraneuronal Alzheimer abeta42 accumulates in multivesicular bodies and is associated with synaptic pathology. *Am J Pathol* **161**, 1869-79 (2002).
52. Echeverria, V. et al. Rat transgenic models with a phenotype of intracellular Abeta accumulation in hippocampus and cortex. *J Alzheimers Dis* **6**, 209-19 (2004).
53. Takahashi, R. H. et al. Oligomerization of Alzheimer's beta-amyloid within processes and synapses of cultured neurons and brain. *J Neurosci* **24**, 3592-9 (2004).

54. Dickson, D. W. Apoptotic mechanisms in Alzheimer neurofibrillary degeneration: cause or effect? *J Clin Invest* **114**, 23-7 (2004).
55. Schultz, D. R. & Harrington, W. J., Jr. Apoptosis: programmed cell death at a molecular level. *Semin Arthritis Rheum* **32**, 345-69 (2003).
56. Lustbader, J. W. et al. ABAD directly links Abeta to mitochondrial toxicity in Alzheimer's disease. *Science* **304**, 448-52 (2004).
57. McDonald, D. R., Bamberger, M. E., Combs, C. K. & Landreth, G. E. beta-Amyloid fibrils activate parallel mitogen-activated protein kinase pathways in microglia and THP1 monocytes. *J Neurosci* **18**, 4451-60 (1998).
58. McDonald, D. R., Brunden, K. R. & Landreth, G. E. Amyloid fibrils activate tyrosine kinase-dependent signaling and superoxide production in microglia. *J Neurosci* **17**, 2284-94 (1997).
59. Verdier, Y., Zarandi, M. & Penke, B. Amyloid beta-peptide interactions with neuronal and glial cell plasma membrane: binding sites and implications for Alzheimer's disease. *J Pept Sci* **10**, 229-48 (2004).
60. Paresce, D. M., Ghosh, R. N. & Maxfield, F. R. Microglial cells internalize aggregates of the Alzheimer's disease amyloid beta-protein via a scavenger receptor. *Neuron* **17**, 553-65 (1996).
61. Husemann, J., Loike, J. D., Anankov, R., Febbraio, M. & Silverstein, S. C. Scavenger receptors in neurobiology and neuropathology: their role on microglia and other cells of the nervous system. *Glia* **40**, 195-205 (2002).
62. Grewal, R. P., Yoshida, T., Finch, C. E. & Morgan, T. E. Scavenger receptor mRNAs in rat brain microglia are induced by kainic acid lesioning and by cytokines. *Neuroreport* **8**, 1077-81 (1997).
63. Bamberger, M. E., Harris, M. E., McDonald, D. R., Husemann, J. & Landreth, G. E. A cell surface receptor complex for fibrillar beta-amyloid mediates microglial activation. *J Neurosci* **23**, 2665-74 (2003).
64. Christie, R. H., Freeman, M. & Hyman, B. T. Expression of the macrophage scavenger receptor, a multifunctional lipoprotein receptor, in microglia associated with senile plaques in Alzheimer's disease. *Am J Pathol* **148**, 399-403 (1996).
65. Cui, Y., Le, Y., Yazawa, H., Gong, W. & Wang, J. M. Potential role of the formyl peptide receptor-like 1 (FPRL1) in inflammatory aspects of Alzheimer's disease. *J Leukoc Biol* **72**, 628-35 (2002).
66. Yazawa, H. et al. Beta amyloid peptide (Abeta42) is internalized via the G-protein-coupled receptor FPRL1 and forms fibrillar aggregates in macrophages. *Faseb J* **15**, 2454-62 (2001).
67. Yan, S. D. et al. Receptor-dependent cell stress and amyloid accumulation in systemic amyloidosis. *Nat Med* **6**, 643-51 (2000).
68. Yan, S. D. et al. RAGE and amyloid-beta peptide neurotoxicity in Alzheimer's disease. *Nature* **382**, 685-91 (1996).
69. Deane, R. et al. RAGE mediates amyloid-beta peptide transport across the blood-brain barrier and accumulation in brain. *Nat Med* **9**, 907-13 (2003).
70. Shibata, M. et al. Clearance of Alzheimer's amyloid-ss(1-40) peptide from brain by LDL receptor-related protein-1 at the blood-brain barrier. *J Clin Invest* **106**, 1489-99 (2000).

71. Zlokovic, B. V. Clearing amyloid through the blood-brain barrier. *J Neurochem* **89**, 807-11 (2004).
72. Kang, D. E. et al. Modulation of amyloid beta-protein clearance and Alzheimer's disease susceptibility by the LDL receptor-related protein pathway. *J Clin Invest* **106**, 1159-66 (2000).
73. Van Uden, E. et al. Increased extracellular amyloid deposition and neurodegeneration in human amyloid precursor protein transgenic mice deficient in receptor-associated protein. *J Neurosci* **22**, 9298-304 (2002).
74. Marx, J. Major setback for Alzheimer's models. *Science* **255**, 1200-2 (1992).
75. Quon, D. et al. Formation of beta-amyloid protein deposits in brains of transgenic mice. *Nature* **352**, 239-41 (1991).
76. Andra, K. et al. Expression of APP in transgenic mice: a comparison of neuron-specific promoters. *Neurobiol Aging* **17**, 183-90 (1996).
77. Borchelt, D. R. et al. A vector for expressing foreign genes in the brains and hearts of transgenic mice. *Genet Anal* **13**, 159-63 (1996).
78. Kulnane, L. S. & Lamb, B. T. Neuropathological characterization of mutant amyloid precursor protein yeast artificial chromosome transgenic mice. *Neurobiol Dis* **8**, 982-92 (2001).
79. Games, D. et al. Alzheimer-type neuropathology in transgenic mice overexpressing V717F beta-amyloid precursor protein. *Nature* **373**, 523-7 (1995).
80. Irizarry, M. C. et al. Abeta deposition is associated with neuropil changes, but not with overt neuronal loss in the human amyloid precursor protein V717F (PDAPP) transgenic mouse. *J Neurosci* **17**, 7053-9 (1997).
81. Dodart, J. C. et al. Behavioral disturbances in transgenic mice overexpressing the V717F beta-amyloid precursor protein. *Behav Neurosci* **113**, 982-90 (1999).
82. Chen, G. et al. A learning deficit related to age and beta-amyloid plaques in a mouse model of Alzheimer's disease. *Nature* **408**, 975-9 (2000).
83. Irizarry, M. C., McNamara, M., Fedorchak, K., Hsiao, K. & Hyman, B. T. APPSw transgenic mice develop age-related A beta deposits and neuropil abnormalities, but no neuronal loss in CA1. *J Neuropathol Exp Neurol* **56**, 965-73 (1997).
84. Hsiao, K. K. et al. Age-related CNS disorder and early death in transgenic FVB/N mice overexpressing Alzheimer amyloid precursor proteins. *Neuron* **15**, 1203-18 (1995).
85. Hsiao, K. et al. Correlative memory deficits, Abeta elevation, and amyloid plaques in transgenic mice. *Science* **274**, 99-102 (1996).
86. McGowan, E. et al. Amyloid phenotype characterization of transgenic mice overexpressing both mutant amyloid precursor protein and mutant presenilin 1 transgenes. *Neurobiol Dis* **6**, 231-44 (1999).
87. Chapman, P. F. et al. Impaired synaptic plasticity and learning in aged amyloid precursor protein transgenic mice. *Nat Neurosci* **2**, 271-6 (1999).
88. Schauwecker, P. E. & Steward, O. Genetic determinants of susceptibility to excitotoxic cell death: implications for gene targeting approaches. *Proc Natl Acad Sci U S A* **94**, 4103-8 (1997).

89. Sturchler-Pierrat, C. et al. Two amyloid precursor protein transgenic mouse models with Alzheimer disease-like pathology. *Proc Natl Acad Sci U S A* **94**, 13287-92 (1997).
90. Stalder, M. et al. Association of microglia with amyloid plaques in brains of APP23 transgenic mice. *Am J Pathol* **154**, 1673-84 (1999).
91. Kelly, P. H. et al. Progressive age-related impairment of cognitive behavior in APP23 transgenic mice. *Neurobiol Aging* **24**, 365-78 (2003).
92. Calhoun, M. E. et al. Neuron loss in APP transgenic mice. *Nature* **395**, 755-6 (1998).
93. Calhoun, M. E. et al. Neuronal overexpression of mutant amyloid precursor protein results in prominent deposition of cerebrovascular amyloid. *Proc Natl Acad Sci U S A* **96**, 14088-93 (1999).
94. Holcomb, L. et al. Accelerated Alzheimer-type phenotype in transgenic mice carrying both mutant amyloid precursor protein and presenilin 1 transgenes. *Nat Med* **4**, 97-100 (1998).
95. Carlson, G. A. et al. Genetic modification of the phenotypes produced by amyloid precursor protein overexpression in transgenic mice. *Hum Mol Genet* **6**, 1951-9 (1997).
96. Moechars, D., Lorent, K., De Strooper, B., Dewachter, I. & Van Leuven, F. Expression in brain of amyloid precursor protein mutated in the alpha-secretase site causes disturbed behavior, neuronal degeneration and premature death in transgenic mice. *Embo J* **15**, 1265-74 (1996).
97. Moechars, D., Gilis, M., Kuiperi, C., Laenen, I. & Van Leuven, F. Aggressive behaviour in transgenic mice expressing APP is alleviated by serotonergic drugs. *Neuroreport* **9**, 3561-4 (1998).
98. Moechars, D. et al. Early phenotypic changes in transgenic mice that overexpress different mutants of amyloid precursor protein in brain. *J Biol Chem* **274**, 6483-92 (1999).
99. Janus, C., Chishti, M. A. & Westaway, D. Transgenic mouse models of Alzheimer's disease. *Biochim Biophys Acta* **1502**, 63-75 (2000).
100. Janus, C. & Westaway, D. Transgenic mouse models of Alzheimer's disease. *Physiol Behav* **73**, 873-86 (2001).
101. Gotz, J. et al. Transgenic animal models of Alzheimer's disease and related disorders: histopathology, behavior and therapy. *Mol Psychiatry* (2004).
102. McGeer, P. L., Schulzer, M. & McGeer, E. G. Arthritis and anti-inflammatory agents as possible protective factors for Alzheimer's disease: a review of 17 epidemiologic studies. *Neurology* **47**, 425-32 (1996).
103. Stewart, W. F., Kawas, C., Corrada, M. & Metter, E. J. Risk of Alzheimer's disease and duration of NSAID use. *Neurology* **48**, 626-32 (1997).
104. Streit, W. J., Walter, S. A. & Pennell, N. A. Reactive microgliosis. *Prog Neurobiol* **57**, 563-81 (1999).
105. Nelson, P. T., Soma, L. A. & Lavi, E. Microglia in diseases of the central nervous system. *Ann Med* **34**, 491-500 (2002).
106. Perry, V. H. & Gordon, S. Macrophages and the nervous system. *Int Rev Cytol* **125**, 203-44 (1991).

107. Kaur, C., Hao, A. J., Wu, C. H. & Ling, E. A. Origin of microglia. *Microsc Res Tech* **54**, 2-9 (2001).
108. Streit, W. J. & Graeber, M. B. Heterogeneity of microglial and perivascular cell populations: insights gained from the facial nucleus paradigm. *Glia* **7**, 68-74 (1993).
109. Streit, W. J. Microglia as neuroprotective, immunocompetent cells of the CNS. *Glia* **40**, 133-9 (2002).
110. Jefferies, W. A. et al. Reactive microglia specifically associated with amyloid plaques in Alzheimer's disease brain tissue express melanotransferrin. *Brain Res* **712**, 122-6 (1996).
111. Yamada, T. et al. Melanotransferrin is produced by senile plaque-associated reactive microglia in Alzheimer's disease. *Brain Res* **845**, 1-5 (1999).
112. Schipper, H. M. et al. Evaluation of heme oxygenase-1 as a systemic biological marker of sporadic AD. *Neurology* **54**, 1297-304 (2000).
113. Walker, D. G., Lue, L. F. & Beach, T. G. Increased expression of the urokinase plasminogen-activator receptor in amyloid beta peptide-treated human brain microglia and in AD brains. *Brain Res* **926**, 69-79 (2002).
114. Espey, M. G., Chernyshev, O. N., Reinhard, J. F., Jr., Namboodiri, M. A. & Colton, C. A. Activated human microglia produce the excitotoxin quinolinic acid. *Neuroreport* **8**, 431-4 (1997).
115. Piani, D., Spranger, M., Frei, K., Schaffner, A. & Fontana, A. Macrophage-induced cytotoxicity of N-methyl-D-aspartate receptor positive neurons involves excitatory amino acids rather than reactive oxygen intermediates and cytokines. *Eur J Immunol* **22**, 2429-36 (1992).
116. McGeer, P. L., Akiyama, H., Itagaki, S. & McGeer, E. G. Immune system response in Alzheimer's disease. *Can J Neurol Sci* **16**, 516-27 (1989).
117. Styren, S. D., Civin, W. H. & Rogers, J. Molecular, cellular, and pathologic characterization of HLA-DR immunoreactivity in normal elderly and Alzheimer's disease brain. *Exp Neurol* **110**, 93-104 (1990).
118. Frautschy, S. A. et al. Microglial response to amyloid plaques in APPsw transgenic mice. *Am J Pathol* **152**, 307-17 (1998).
119. Itagaki, S., McGeer, P. L., Akiyama, H., Zhu, S. & Selkoe, D. Relationship of microglia and astrocytes to amyloid deposits of Alzheimer disease. *J Neuroimmunol* **24**, 173-82 (1989).
120. Mackenzie, I. R., Hao, C. & Munoz, D. G. Role of microglia in senile plaque formation. *Neurobiol Aging* **16**, 797-804 (1995).
121. Sasaki, A., Yamaguchi, H., Ogawa, A., Sugihara, S. & Nakazato, Y. Microglial activation in early stages of amyloid beta protein deposition. *Acta Neuropathol (Berl)* **94**, 316-22 (1997).
122. Ard, M. D., Cole, G. M., Wei, J., Mehrle, A. P. & Fratkin, J. D. Scavenging of Alzheimer's amyloid beta-protein by microglia in culture. *J Neurosci Res* **43**, 190-202 (1996).
123. Paresce, D. M., Chung, H. & Maxfield, F. R. Slow degradation of aggregates of the Alzheimer's disease amyloid beta-protein by microglial cells. *J Biol Chem* **272**, 29390-7 (1997).

124. Frackowiak, J. et al. Ultrastructure of the microglia that phagocytose amyloid and the microglia that produce beta-amyloid fibrils. *Acta Neuropathol (Berl)* **84**, 225-33 (1992).
125. Akiyama, H. et al. Granules in glial cells of patients with Alzheimer's disease are immunopositive for C-terminal sequences of beta-amyloid protein. *Neurosci Lett* **206**, 169-72 (1996).
126. Rogers, J. et al. Elucidating molecular mechanisms of Alzheimer's disease in microglial cultures. *Ernst Schering Res Found Workshop*, 25-44 (2002).
127. Chung, H., Brazil, M. I., Soe, T. T. & Maxfield, F. R. Uptake, degradation, and release of fibrillar and soluble forms of Alzheimer's amyloid beta-peptide by microglial cells. *J Biol Chem* **274**, 32301-8 (1999).
128. Combs, C. K., Johnson, D. E., Cannady, S. B., Lehman, T. M. & Landreth, G. E. Identification of microglial signal transduction pathways mediating a neurotoxic response to amyloidogenic fragments of beta-amyloid and prion proteins. *J Neurosci* **19**, 928-39 (1999).
129. Savage, M. J., Lin, Y. G., Ciallella, J. R., Flood, D. G. & Scott, R. W. Activation of c-Jun N-terminal kinase and p38 in an Alzheimer's disease model is associated with amyloid deposition. *J Neurosci* **22**, 3376-85 (2002).
130. Koistinaho, M. & Koistinaho, J. Role of p38 and p44/42 mitogen-activated protein kinases in microglia. *Glia* **40**, 175-83 (2002).
131. Hensley, K. et al. p38 kinase is activated in the Alzheimer's disease brain. *J Neurochem* **72**, 2053-8 (1999).
132. Xie, Z., Smith, C. J. & Van Eldik, L. J. Activated glia induce neuron death via MAP kinase signaling pathways involving JNK and p38. *Glia* **45**, 170-9 (2004).
133. Pyo, H., Jou, I., Jung, S., Hong, S. & Joe, E. H. Mitogen-activated protein kinases activated by lipopolysaccharide and beta-amyloid in cultured rat microglia. *Neuroreport* **9**, 871-4 (1998).
134. Ballabh, P., Braun, A. & Nedergaard, M. The blood-brain barrier: an overview: structure, regulation, and clinical implications. *Neurobiol Dis* **16**, 1-13 (2004).
135. Hirase, T. et al. Occludin as a possible determinant of tight junction permeability in endothelial cells. *J Cell Sci* **110 (Pt 14)**, 1603-13 (1997).
136. Prat, A., Biernacki, K., Wosik, K. & Antel, J. P. Glial cell influence on the human blood-brain barrier. *Glia* **36**, 145-55 (2001).
137. Janzer, R. C. & Raff, M. C. Astrocytes induce blood-brain barrier properties in endothelial cells. *Nature* **325**, 253-7 (1987).
138. Ramsauer, M., Krause, D. & Dermietzel, R. Angiogenesis of the blood-brain barrier in vitro and the function of cerebral pericytes. *Faseb J* **16**, 1274-6 (2002).
139. Kern, T. S. & Engerman, R. L. Capillary lesions develop in retina rather than cerebral cortex in diabetes and experimental galactosemia. *Arch Ophthalmol* **114**, 306-10 (1996).
140. Lindahl, P., Johansson, B. R., Leveen, P. & Betsholtz, C. Pericyte loss and microaneurysm formation in PDGF-B-deficient mice. *Science* **277**, 242-5 (1997).
141. Saunders, N. R., Habgood, M. D. & Dziegielewska, K. M. Barrier mechanisms in the brain, I. Adult brain. *Clin Exp Pharmacol Physiol* **26**, 11-9 (1999).
142. Kastin, A. J., Pan, W., Maness, L. M. & Banks, W. A. Peptides crossing the blood-brain barrier: some unusual observations. *Brain Res* **848**, 96-100 (1999).

143. Jolliet-Riant, P. & Tillement, J. P. Drug transfer across the blood-brain barrier and improvement of brain delivery. *Fundam Clin Pharmacol* **13**, 16-26 (1999).
144. Rothenberger, S. et al. Coincident expression and distribution of melanotransferrin and transferrin receptor in human brain capillary endothelium. *Brain Res* **712**, 117-21 (1996).
145. Claudio, L. Ultrastructural features of the blood-brain barrier in biopsy tissue from Alzheimer's disease patients. *Acta Neuropathol (Berl)* **91**, 6-14 (1996).
146. Caserta, M. T., Caccioppo, D., Lapin, G. D., Ragin, A. & Groothuis, D. R. Blood-brain barrier integrity in Alzheimer's disease patients and elderly control subjects. *J Neuropsychiatry Clin Neurosci* **10**, 78-84 (1998).
147. Poduslo, J. F., Curran, G. L., Wengenack, T. M., Malester, B. & Duff, K. Permeability of proteins at the blood-brain barrier in the normal adult mouse and double transgenic mouse model of Alzheimer's disease. *Neurobiol Dis* **8**, 555-67 (2001).
148. Perry, V. H., Anthony, D. C., Bolton, S. J. & Brown, H. C. The blood-brain barrier and the inflammatory response. *Mol Med Today* **3**, 335-41 (1997).
149. Ujiie, M., Dickstein, D. L., Carlow, D. A. & Jefferies, W. A. Blood-brain barrier permeability precedes senile plaque formation in an Alzheimer disease model. *Microcirculation* **10**, 463-70 (2003).
150. Xu, J. et al. Amyloid beta peptide-induced cerebral endothelial cell death involves mitochondrial dysfunction and caspase activation. *J Cereb Blood Flow Metab* **21**, 702-10 (2001).
151. Yin, K. J., Lee, J. M., Chen, S. D., Xu, J. & Hsu, C. Y. Amyloid-beta induces Smac release via AP-1/Bim activation in cerebral endothelial cells. *J Neurosci* **22**, 9764-70 (2002).
152. Vagnucci, A. H., Jr. & Li, W. W. Alzheimer's disease and angiogenesis. *Lancet* **361**, 605-8 (2003).
153. Wong, M. L. et al. Inducible nitric oxide synthase gene expression in the brain during systemic inflammation. *Nat Med* **2**, 581-4 (1996).
154. Ek, M. et al. Inflammatory response: pathway across the blood-brain barrier. *Nature* **410**, 430-1 (2001).
155. Uchikado, H. et al. Activation of vascular endothelial cells and perivascular cells by systemic inflammation-an immunohistochemical study of postmortem human brain tissues. *Acta Neuropathol (Berl)* **107**, 341-51 (2004).
156. Attems, J., Lintner, F. & Jellinger, K. A. Amyloid beta peptide 1-42 highly correlates with capillary cerebral amyloid angiopathy and Alzheimer disease pathology. *Acta Neuropathol (Berl)* **107**, 283-91 (2004).
157. Weller, R. O., Massey, A., Kuo, Y. M. & Roher, A. E. Cerebral amyloid angiopathy: accumulation of A beta in interstitial fluid drainage pathways in Alzheimer's disease. *Ann N Y Acad Sci* **903**, 110-7 (2000).
158. Vinters, H. V. Cerebral amyloid angiopathy. A critical review. *Stroke* **18**, 311-24 (1987).
159. Bergeron, C., Ranalli, P. J. & Miceli, P. N. Amyloid angiopathy in Alzheimer's disease. *Can J Neurol Sci* **14**, 564-9 (1987).

160. Prelli, F., Castano, E., Glenner, G. G. & Frangione, B. Differences between vascular and plaque core amyloid in Alzheimer's disease. *J Neurochem* **51**, 648-51 (1988).
161. Plassman, B. L. & Breitner, J. C. Recent advances in the genetics of Alzheimer's disease and vascular dementia with an emphasis on gene-environment interactions. *J Am Geriatr Soc* **44**, 1242-50 (1996).
162. Munch, G. & Robinson, S. R. Potential neurotoxic inflammatory responses to Abeta vaccination in humans. *J Neural Transm* **109**, 1081-7 (2002).
163. Nicoll, J. A. et al. Neuropathology of human Alzheimer disease after immunization with amyloid-beta peptide: a case report. *Nat Med* **9**, 448-52 (2003).
164. Golde, T. E. Alzheimer disease therapy: can the amyloid cascade be halted? *J Clin Invest* **111**, 11-8 (2003).
165. Luo, Y. et al. Mice deficient in BACE1, the Alzheimer's beta-secretase, have normal phenotype and abolished beta-amyloid generation. *Nat Neurosci* **4**, 231-2 (2001).
166. Wolozin, B., Kellman, W., Ruosseau, P., Celesia, G. G. & Siegel, G. Decreased prevalence of Alzheimer disease associated with 3-hydroxy-3-methyglutaryl coenzyme A reductase inhibitors. *Arch Neurol* **57**, 1439-43 (2000).
167. Notkola, I. L. et al. Serum total cholesterol, apolipoprotein E epsilon 4 allele, and Alzheimer's disease. *Neuroepidemiology* **17**, 14-20 (1998).
168. Simons, M. et al. Cholesterol depletion inhibits the generation of beta-amyloid in hippocampal neurons. *Proc Natl Acad Sci U S A* **95**, 6460-4 (1998).
169. Fassbender, K. et al. Simvastatin strongly reduces levels of Alzheimer's disease beta -amyloid peptides Abeta 42 and Abeta 40 in vitro and in vivo. *Proc Natl Acad Sci U S A* **98**, 5856-61 (2001).
170. Shie, F. S., Jin, L. W., Cook, D. G., Leverenz, J. B. & LeBoeuf, R. C. Diet-induced hypercholesterolemia enhances brain A beta accumulation in transgenic mice. *Neuroreport* **13**, 455-9 (2002).
171. George, A. J. et al. APP intracellular domain is increased and soluble Abeta is reduced with diet-induced hypercholesterolemia in a transgenic mouse model of Alzheimer disease. *Neurobiol Dis* **16**, 124-32 (2004).
172. Refolo, L. M. et al. A cholesterol-lowering drug reduces beta-amyloid pathology in a transgenic mouse model of Alzheimer's disease. *Neurobiol Dis* **8**, 890-9 (2001).
173. Friedhoff, L. T., Cullen, E. I., Geoghagen, N. S. & Buxbaum, J. D. Treatment with controlled-release lovastatin decreases serum concentrations of human beta-amyloid (A beta) peptide. *Int J Neuropsychopharmacol* **4**, 127-30 (2001).
174. Weggen, S. et al. A subset of NSAIDs lower amyloidogenic Abeta42 independently of cyclooxygenase activity. *Nature* **414**, 212-6 (2001).
175. Schenk, D. et al. Immunization with amyloid-beta attenuates Alzheimer-disease-like pathology in the PDAPP mouse. *Nature* **400**, 173-7 (1999).
176. Bard, F. et al. Peripherally administered antibodies against amyloid beta-peptide enter the central nervous system and reduce pathology in a mouse model of Alzheimer disease. *Nat Med* **6**, 916-9 (2000).

177. DeMattos, R. B. et al. Peripheral anti-A beta antibody alters CNS and plasma A beta clearance and decreases brain A beta burden in a mouse model of Alzheimer's disease. *Proc Natl Acad Sci U S A* **98**, 8850-5 (2001).
178. Morgan, D. et al. A beta peptide vaccination prevents memory loss in an animal model of Alzheimer's disease. *Nature* **408**, 982-5 (2000).
179. Janus, C. et al. A beta peptide immunization reduces behavioural impairment and plaques in a model of Alzheimer's disease. *Nature* **408**, 979-82 (2000).
180. Lemere, C. A. et al. Evidence for peripheral clearance of cerebral Abeta protein following chronic, active Abeta immunization in PSAPP mice. *Neurobiol Dis* **14**, 10-8 (2003).
181. Oddo, S., Billings, L., Kesslak, J. P., Cribbs, D. H. & LaFerla, F. M. Abeta Immunotherapy Leads to Clearance of Early, but Not Late, Hyperphosphorylated Tau Aggregates via the Proteasome. *Neuron* **43**, 321-32 (2004).
182. Yoshida, H. et al. The murine mutation osteopetrosis is in the coding region of the macrophage colony stimulating factor gene. *Nature* **345**, 442-4 (1990).
183. Wiktor-Jedrzejczak, W. et al. Total absence of colony-stimulating factor 1 in the macrophage-deficient osteopetrotic (op/op) mouse. *Proc Natl Acad Sci U S A* **87**, 4828-32 (1990).
184. Pollard, J. W., Morgan, C. J., Dello Sbarba, P., Cheers, C. & Stanley, E. R. Independently arising macrophage mutants dissociate growth factor-regulated survival and proliferation. *Proc Natl Acad Sci U S A* **88**, 1474-8 (1991).
185. Stanley, E. R. et al. Biology and action of colony--stimulating factor-1. *Mol Reprod Dev* **46**, 4-10 (1997).
186. Blevins, G. & Fedoroff, S. Microglia in colony-stimulating factor 1-deficient op/op mice. *J Neurosci Res* **40**, 535-44 (1995).
187. Wegiel, J. et al. Reduced number and altered morphology of microglial cells in colony stimulating factor-1-deficient osteopetrotic op/op mice. *Brain Res* **804**, 135-9 (1998).
188. Marks, S. C., Jr. & Lane, P. W. Osteopetrosis, a new recessive skeletal mutation on chromosome 12 of the mouse. *J Hered* **67**, 11-18 (1976).
189. Blasi, E., Barluzzi, R., Bocchini, V., Mazzolla, R. & Bistoni, F. Immortalization of murine microglial cells by a v-raf/v-myc carrying retrovirus. *J Neuroimmunol* **27**, 229-37 (1990).
190. Li, M., Pisalyaput, K., Galvan, M. & Tenner, A. J. Macrophage colony stimulatory factor and interferon-gamma trigger distinct mechanisms for augmentation of beta-amyloid-induced microglia-mediated neurotoxicity. *J Neurochem* **91**, 623-33 (2004).
191. Hampel, H. et al. Decreased soluble interleukin-6 receptor in cerebrospinal fluid of patients with Alzheimer's disease. *Brain Res* **780**, 356-9 (1998).
192. Fillit, H. et al. Elevated circulating tumor necrosis factor levels in Alzheimer's disease. *Neurosci Lett* **129**, 318-20 (1991).
193. Brown, J. P., Woodbury, R. G., Hart, C. E., Hellstrom, I. & Hellstrom, K. E. Quantitative analysis of melanoma-associated antigen p97 in normal and neoplastic tissues. *Proc Natl Acad Sci U S A* **78**, 539-43 (1981).

194. Woodbury, R. G., Brown, J. P., Loop, S. M., Hellstrom, K. E. & Hellstrom, I. Analysis of normal neoplastic human tissues for the tumor-associated protein p97. *Int J Cancer* **27**, 145-9 (1981).
195. Brown, J. P. et al. Human melanoma-associated antigen p97 is structurally and functionally related to transferrin. *Nature* **296**, 171-3 (1982).
196. Real, F. X. et al. Class 1 (unique) tumor antigens of human melanoma: identification of unique and common epitopes on a 90-kDa glycoprotein. *Proc Natl Acad Sci U S A* **85**, 3965-9 (1988).
197. Sciot, R. et al. In situ localization of melanotransferrin (melanoma-associated antigen P97) in human liver. A light- and electronmicroscopic immunohistochemical study. *Liver* **9**, 110-9 (1989).
198. Alemany, R. et al. Glycosyl phosphatidylinositol membrane anchoring of melanotransferrin (p97): apical compartmentalization in intestinal epithelial cells. *J Cell Sci* **104 (Pt 4)**, 1155-62 (1993).
199. Food, M. R. et al. Transport and expression in human melanomas of a transferrin-like glycosylphosphatidylinositol-anchored protein. *J Biol Chem* **269**, 3034-40 (1994).
200. Kennard, M. L., Richardson, D. R., Gabathuler, R., Ponka, P. & Jefferies, W. A. A novel iron uptake mechanism mediated by GPI-anchored human p97. *Embo J* **14**, 4178-86 (1995).
201. McNagny, K. M., Rossi, F., Smith, G. & Graf, T. The eosinophil-specific cell surface antigen, EOS47, is a chicken homologue of the oncofetal antigen melanotransferrin. *Blood* **87**, 1343-52 (1996).
202. Plowman, G. D. et al. Assignment of the gene for human melanoma-associated antigen p97 to chromosome 3. *Nature* **303**, 70-2 (1983).
203. Baker, E. N. et al. Human melanotransferrin (p97) has only one functional iron-binding site. *FEBS Lett* **298**, 215-8 (1992).
204. Jefferies, W. A. et al. Transferrin receptor on endothelium of brain capillaries. *Nature* **312**, 162-3 (1984).
205. Loeffler, D. A. et al. Transferrin and iron in normal, Alzheimer's disease, and Parkinson's disease brain regions. *J Neurochem* **65**, 710-24 (1995).
206. Grundke-Iqbal, I. et al. Ferritin is a component of the neuritic (senile) plaque in Alzheimer dementia. *Acta Neuropathol (Berl)* **81**, 105-10 (1990).
207. Kaneko, Y., Kitamoto, T., Tateishi, J. & Yamaguchi, K. Ferritin immunohistochemistry as a marker for microglia. *Acta Neuropathol (Berl)* **79**, 129-36 (1989).
208. Kennard, M. L., Feldman, H., Yamada, T. & Jefferies, W. A. Serum levels of the iron binding protein p97 are elevated in Alzheimer's disease. *Nat Med* **2**, 1230-5 (1996).
209. Feldman, H. et al. Serum p97 levels as an aid to identifying Alzheimer's disease. *J Alzheimers Dis* **3**, 507-516 (2001).
210. Kim, D. K. et al. Serum melanotransferrin, p97 as a biochemical marker of Alzheimer's disease. *Neuropsychopharmacology* **25**, 84-90 (2001).
211. Qian, Z. M. & Wang, Q. Expression of iron transport proteins and excessive iron accumulation in the brain in neurodegenerative disorders. *Brain Res Brain Res Rev* **27**, 257-67 (1998).

212. Dwork, A. J., Schon, E. A. & Herbert, J. Nonidentical distribution of transferrin and ferric iron in human brain. *Neuroscience* **27**, 333-45 (1988).
213. Sala, R. et al. The human melanoma associated protein melanotransferrin promotes endothelial cell migration and angiogenesis in vivo. *Eur J Cell Biol* **81**, 599-607 (2002).
214. Kalaria, R. N. et al. Vascular endothelial growth factor in Alzheimer's disease and experimental cerebral ischemia. *Brain Res Mol Brain Res* **62**, 101-5 (1998).
215. Tarkowski, E. et al. Increased intrathecal levels of the angiogenic factors VEGF and TGF-beta in Alzheimer's disease and vascular dementia. *Neurobiol Aging* **23**, 237-43 (2002).
216. Yang, S. P. et al. Co-accumulation of vascular endothelial growth factor with beta-amyloid in the brain of patients with Alzheimer's disease. *Neurobiol Aging* **25**, 283-90 (2004).
217. Roze-Heusse, A., Houbiguian, M. L., Debacker, C., Zakin, M. M. & Duchange, N. Melanotransferrin gene expression in melanoma cells is correlated with high levels of Jun/Fos family transcripts and with the presence of a specific AP1-dependent ternary complex. *Biochem J* **318 (Pt 3)**, 883-8 (1996).
218. McGeer, E. G. & McGeer, P. L. Inflammatory processes in Alzheimer's disease. *Prog Neuropsychopharmacol Biol Psychiatry* **27**, 741-9 (2003).
219. Walker, D. G., Lue, L. F. & Beach, T. G. Gene expression profiling of amyloid beta peptide-stimulated human post-mortem brain microglia. *Neurobiol Aging* **22**, 957-66 (2001).
220. Nakamasu, K. et al. Structure and promoter analysis of the mouse membrane-bound transferrin-like protein (MTf) gene. *Eur J Biochem* **268**, 1468-76 (2001).
221. Ogawa, O. et al. Inhibition of inducible nitric oxide synthase gene expression by indomethacin or ibuprofen in beta-amyloid protein-stimulated J774 cells. *Eur J Pharmacol* **408**, 137-41 (2000).
222. Blasko, I. et al. Ibuprofen decreases cytokine-induced amyloid beta production in neuronal cells. *Neurobiol Dis* **8**, 1094-101 (2001).
223. Eriksen, J. L. et al. NSAIDs and enantiomers of flurbiprofen target gamma-secretase and lower Abeta 42 in vivo. *J Clin Invest* **112**, 440-9 (2003).
224. Lim, G. P. et al. Ibuprofen suppresses plaque pathology and inflammation in a mouse model for Alzheimer's disease. *J Neurosci* **20**, 5709-14 (2000).
225. Netland, E. E., Newton, J. L., Majocha, R. E. & Tate, B. A. Indomethacin reverses the microglial response to amyloid beta-protein. *Neurobiol Aging* **19**, 201-4 (1998).
226. Etminan, M., Gill, S. & Samii, A. Effect of non-steroidal anti-inflammatory drugs on risk of Alzheimer's disease: systematic review and meta-analysis of observational studies. *Bmj* **327**, 128 (2003).
227. Weggen, S. et al. Evidence that nonsteroidal anti-inflammatory drugs decrease amyloid beta 42 production by direct modulation of gamma-secretase activity. *J Biol Chem* **278**, 31831-7 (2003).
228. Matsuura, H. et al. Regulation of cyclooxygenase-2 by interferon gamma and transforming growth factor alpha in normal human epidermal keratinocytes and squamous carcinoma cells. Role of mitogen-activated protein kinases. *J Biol Chem* **274**, 29138-48 (1999).

229. Wisniewski, H. M., Wegiel, J., Wang, K. C., Kujawa, M. & Lach, B. Ultrastructural studies of the cells forming amyloid fibers in classical plaques. *Can J Neurol Sci* **16**, 535-42 (1989).
230. Wisniewski, H. M., Barcikowska, M. & Kida, E. Phagocytosis of beta/A4 amyloid fibrils of the neuritic neocortical plaques. *Acta Neuropathol (Berl)* **81**, 588-90 (1991).
231. Wegiel, J., Wang, K. C., Tarnawski, M. & Lach, B. Microglia cells are the driving force in fibrillar plaque formation, whereas astrocytes are a leading factor in plague degradation. *Acta Neuropathol (Berl)* **100**, 356-64 (2000).
232. Brazil, M. I., Chung, H. & Maxfield, F. R. Effects of incorporation of immunoglobulin G and complement component C1q on uptake and degradation of Alzheimer's disease amyloid fibrils by microglia. *J Biol Chem* **275**, 16941-7 (2000).
233. Webster, S. D. et al. Antibody-mediated phagocytosis of the amyloid beta-peptide in microglia is differentially modulated by C1q. *J Immunol* **166**, 7496-503 (2001).
234. Rogers, J. et al. Complement activation by beta-amyloid in Alzheimer disease. *Proc Natl Acad Sci U S A* **89**, 10016-20 (1992).
235. Bradt, B. M., Kolb, W. P. & Cooper, N. R. Complement-dependent proinflammatory properties of the Alzheimer's disease beta-peptide. *J Exp Med* **188**, 431-8 (1998).
236. Wyss-Coray, T. et al. Alzheimer's disease-like cerebrovascular pathology in transforming growth factor-beta 1 transgenic mice and functional metabolic correlates. *Ann N Y Acad Sci* **903**, 317-23 (2000).
237. Wyss-Coray, T. et al. Prominent neurodegeneration and increased plaque formation in complement-inhibited Alzheimer's mice. *Proc Natl Acad Sci U S A* **99**, 10837-42 (2002).
238. Fonseca, M. I., Zhou, J., Botto, M. & Tenner, A. J. Absence of C1q leads to less neuropathology in transgenic mouse models of Alzheimer's disease. *J Neurosci* **24**, 6457-65 (2004).
239. Wiktor-Jedrzejczak, W. et al. Correction by CSF-1 of defects in the osteopetrotic op/op mouse suggests local, developmental, and humoral requirements for this growth factor. *Exp Hematol* **19**, 1049-54 (1991).
240. Rogove, A. D., Lu, W. & Tsirka, S. E. Microglial activation and recruitment, but not proliferation, suffice to mediate neurodegeneration. *Cell Death Differ* **9**, 801-6 (2002).
241. Wyss-Coray, T. et al. Amyloidogenic role of cytokine TGF-beta1 in transgenic mice and in Alzheimer's disease. *Nature* **389**, 603-6 (1997).
242. Lesne, S. et al. Transforming growth factor-beta 1 potentiates amyloid-beta generation in astrocytes and in transgenic mice. *J Biol Chem* **278**, 18408-18 (2003).
243. Naito, M. et al. Abnormal differentiation of tissue macrophage populations in 'osteopetrosis' (op) mice defective in the production of macrophage colony-stimulating factor. *Am J Pathol* **139**, 657-67 (1991).
244. Witmer-Pack, M. D. et al. Identification of macrophages and dendritic cells in the osteopetrotic (op/op) mouse. *J Cell Sci* **104 (Pt 4)**, 1021-9 (1993).

245. Raivich, G., Moreno-Flores, M. T., Moller, J. C. & Kreutzberg, G. W. Inhibition of posttraumatic microglial proliferation in a genetic model of macrophage colony-stimulating factor deficiency in the mouse. *Eur J Neurosci* **6**, 1615-8 (1994).
246. Bruccoleri, A. & Harry, G. J. Chemical-induced hippocampal neurodegeneration and elevations in TNFalpha, TNFbeta, IL-1alpha, IP-10, and MCP-1 mRNA in osteopetrotic (op/op) mice. *J Neurosci Res* **62**, 146-55 (2000).
247. Mucke, L. et al. High-level neuronal expression of abeta 1-42 in wild-type human amyloid protein precursor transgenic mice: synaptotoxicity without plaque formation. *J Neurosci* **20**, 4050-8 (2000).
248. Lehman, E. J. et al. Genetic background regulates beta-amyloid precursor protein processing and beta-amyloid deposition in the mouse. *Hum Mol Genet* **12**, 2949-56 (2003).
249. Masliah, E. et al. Comparison of neurodegenerative pathology in transgenic mice overexpressing V717F beta-amyloid precursor protein and Alzheimer's disease. *J Neurosci* **16**, 5795-811 (1996).
250. Mohajeri, M. H. et al. Passive immunization against beta-amyloid peptide protects central nervous system (CNS) neurons from increased vulnerability associated with an Alzheimer's disease-causing mutation. *J Biol Chem* **277**, 33012-7 (2002).
251. Lemere, C. A. et al. Amyloid-beta immunization in Alzheimer's disease transgenic mouse models and wildtype mice. *Neurochem Res* **28**, 1017-27 (2003).
252. Das, P., Murphy, M. P., Younkin, L. H., Younkin, S. G. & Golde, T. E. Reduced effectiveness of Abeta1-42 immunization in APP transgenic mice with significant amyloid deposition. *Neurobiol Aging* **22**, 721-7 (2001).
253. Dodart, J. C. et al. Immunization reverses memory deficits without reducing brain Abeta burden in Alzheimer's disease model. *Nat Neurosci* **5**, 452-7 (2002).
254. Hock, C. et al. Antibodies against beta-amyloid slow cognitive decline in Alzheimer's disease. *Neuron* **38**, 547-54 (2003).
255. Orgogozo, J. M. et al. Subacute meningoencephalitis in a subset of patients with AD after Abeta42 immunization. *Neurology* **61**, 46-54 (2003).
256. Check, E. Nerve inflammation halts trial for Alzheimer's drug. *Nature* **415**, 462 (2002).
257. Pfeifer, M. et al. Cerebral hemorrhage after passive anti-Abeta immunotherapy. *Science* **298**, 1379 (2002).
258. Poduslo, J. F. & Curran, G. L. Amyloid beta peptide as a vaccine for Alzheimer's disease involves receptor-mediated transport at the blood-brain barrier. *Neuroreport* **12**, 3197-200 (2001).
259. Bacskai, B. J. et al. Imaging of amyloid-beta deposits in brains of living mice permits direct observation of clearance of plaques with immunotherapy. *Nat Med* **7**, 369-72 (2001).
260. Solomon, B., Koppel, R., Hanan, E. & Katzav, T. Monoclonal antibodies inhibit in vitro fibrillar aggregation of the Alzheimer beta-amyloid peptide. *Proc Natl Acad Sci U S A* **93**, 452-5 (1996).
261. Solomon, B., Koppel, R., Frankel, D. & Hanan-Aharon, E. Disaggregation of Alzheimer beta-amyloid by site-directed mAb. *Proc Natl Acad Sci U S A* **94**, 4109-12 (1997).

262. Bacskai, B. J. et al. Non-Fc-mediated mechanisms are involved in clearance of amyloid-beta in vivo by immunotherapy. *J Neurosci* **22**, 7873-8 (2002).
263. Wilcock, D. M. et al. Intracranially administered anti-Abeta antibodies reduce beta-amyloid deposition by mechanisms both independent of and associated with microglial activation. *J Neurosci* **23**, 3745-51 (2003).
264. DeMattos, R. B., Bales, K. R., Cummins, D. J., Paul, S. M. & Holtzman, D. M. Brain to plasma amyloid-beta efflux: a measure of brain amyloid burden in a mouse model of Alzheimer's disease. *Science* **295**, 2264-7 (2002).
265. DeMattos, R. B. et al. Plaque-associated disruption of CSF and plasma amyloid-beta (Abeta) equilibrium in a mouse model of Alzheimer's disease. *J Neurochem* **81**, 229-36 (2002).
266. Pan, W., Solomon, B., Maness, L. M. & Kastin, A. J. Antibodies to beta-amyloid decrease the blood-to-brain transfer of beta-amyloid peptide. *Exp Biol Med (Maywood)* **227**, 609-15 (2002).
267. Games, D. et al. Prevention and reduction of AD-type pathology in PDAPP mice immunized with A beta 1-42. *Ann N Y Acad Sci* **920**, 274-84 (2000).
268. Austyn, J. M. & Gordon, S. F4/80, a monoclonal antibody directed specifically against the mouse macrophage. *Eur J Immunol* **11**, 805-15 (1981).
269. Uyama, O. et al. Quantitative evaluation of vascular permeability in the gerbil brain after transient ischemia using Evans blue fluorescence. *J Cereb Blood Flow Metab* **8**, 282-4 (1988).
270. Methia, N. et al. ApoE deficiency compromises the blood brain barrier especially after injury. *Mol Med* **7**, 810-5 (2001).
271. Blanc, E. M., Toborek, M., Mark, R. J., Hennig, B. & Mattson, M. P. Amyloid beta-peptide induces cell monolayer albumin permeability, impairs glucose transport, and induces apoptosis in vascular endothelial cells. *J Neurochem* **68**, 1870-81 (1997).
272. Thomas, T., Thomas, G., McLendon, C., Sutton, T. & Mullan, M. beta-Amyloid-mediated vasoactivity and vascular endothelial damage. *Nature* **380**, 168-71 (1996).
273. Mackic, J. B. et al. Human blood-brain barrier receptors for Alzheimer's amyloid-beta 1- 40. Asymmetrical binding, endocytosis, and transcytosis at the apical side of brain microvascular endothelial cell monolayer. *J Clin Invest* **102**, 734-43 (1998).
274. Poduslo, J. F., Curran, G. L., Sanyal, B. & Selkoe, D. J. Receptor-mediated transport of human amyloid beta-protein 1-40 and 1-42 at the blood-brain barrier. *Neurobiol Dis* **6**, 190-9 (1999).
275. Banks, W. A., Robinson, S. M., Verma, S. & Morley, J. E. Efflux of human and mouse amyloid beta proteins 1-40 and 1-42 from brain: impairment in a mouse model of Alzheimer's disease. *Neuroscience* **121**, 487-92 (2003).
276. Banks, W. A. et al. Passage of amyloid beta protein antibody across the blood-brain barrier in a mouse model of Alzheimer's disease. *Peptides* **23**, 2223-6 (2002).
277. Guo, J. T., Yu, J., Grass, D., de Beer, F. C. & Kindy, M. S. Inflammation-dependent cerebral deposition of serum amyloid a protein in a mouse model of amyloidosis. *J Neurosci* **22**, 5900-9 (2002).

278. Paris, D. et al. Soluble beta-amyloid peptides mediate vasoactivity via activation of a pro-inflammatory pathway. *Neurobiol Aging* **21**, 183-97 (2000).
279. Giri, R. et al. beta-amyloid-induced migration of monocytes across human brain endothelial cells involves RAGE and PECAM-1. *Am J Physiol Cell Physiol* **279**, C1772-81 (2000).
280. Suo, Z., Fang, C., Crawford, F. & Mullan, M. Superoxide free radical and intracellular calcium mediate A beta(1-42) induced endothelial toxicity. *Brain Res* **762**, 144-52 (1997).
281. Grammas, P. & Ovase, R. Inflammatory factors are elevated in brain microvessels in Alzheimer's disease. *Neurobiol Aging* **22**, 837-42 (2001).
282. Pogue, A. I. & Lukiw, W. J. Angiogenic signaling in Alzheimer's disease. *Neuroreport* **15**, 1507-1510 (2004).
283. Bamberger, M. E. & Landreth, G. E. Microglial interaction with beta-amyloid: implications for the pathogenesis of Alzheimer's disease. *Microsc Res Tech* **54**, 59-70 (2001).